AR-009-949

DSTO-TR-0459

Site Survey for an Ocean Engineering
Project West of Perth for July to
September 1992

Ian S.F. Jones, D.H Cato, L.J. Hamilton
and B.D. Scott

19970429 157

DEPARTMENT ◆ OF DEFENCE

DEFENCE SCIENCE AND TECHNOLOGY ORGANISATION
DTIC QUALITY INSPECTED 1

DISCLAIMER NOTICE
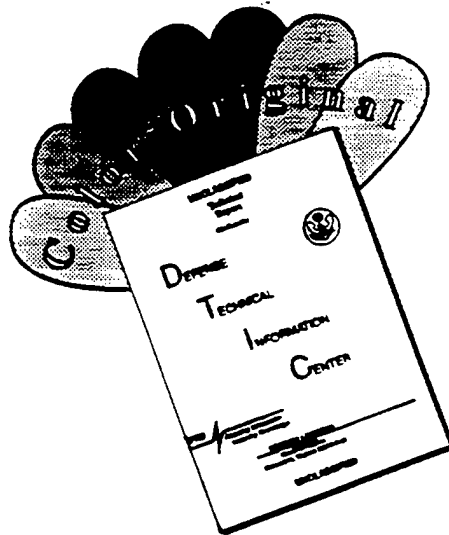
THIS DOCUMENT IS BEST QUALITY AVAILABLE. THE COPY FURNISHED TO DTIC CONTAINED A SIGNIFICANT NUMBER OF COLOR PAGES WHICH DO NOT REPRODUCE LEGIBLY ON BLACK AND WHITE MICROFICHE.

Site Survey for an Ocean Engineering Project West of Perth for July to September 1992

Ian S.F. Jones, D.H. Cato, L.J. Hamilton and B.D. Scott

Maritime Operations Division
Aeronautical and Maritime Research Laboratory

DSTO-TR-0459

ABSTRACT

Oceanic environmental surveys were made by DSTO off Perth, Western Australia over July to September 1992 to assess site suitability for an Underwater Radiated Noise Range for the Royal Australian Navy. Acoustic ranges are required to measure the noise radiated from ships and submarines. Salient factors for range design and performance include ambient noise, currents, topography and nature of the seafloor, water properties, wave, wind, and weather conditions. Measurements of these parameters indicate that the waters off Perth for bottom depths of 400 m are a difficult regime in which to construct and operate an acoustic range. High currents with strong vertical and horizontal shear were experienced, with directions varying through the water column, and with surface and bottom flows sometimes in opposite directions. Temperature micro-structure caused by meeting of warm, low salinity northern Leeuwin Current waters with cool, high salinity southern waters is predicted to cause fluctuations in intensity of acoustic signals. Ambient noise is significantly affected by rain, migrating whales, and shipping. Significant wave heights over 7 m were measured in August 1992. The environmental results are of general interest, and are presented for use by the wider scientific community.

RELEASE LIMITATION

Approved for public release

D E P A R T M E N T   O F   D E F E N C E

◆

DEFENCE SCIENCE AND TECHNOLOGY ORGANISATION

Contents

Site Survey for an Ocean Engineering Project West of Perth for July to September 1992

Executive Summary

On 1 July, 1992 the RAN requested that DSTO arrange for the collection and interpretation of data relevant to the design and installation of an acoustic range at a site about 70 km west of Fremantle, at location 32° 15'S, 115° 02' E. This site is on the continental slope in 400 m of water. An acoustic range is designed to measure the noise radiated from ships and submarines. The variables of importance to the ocean engineer were deemed to be the currents, the acoustic field, the topography and sea floor sediments, together with the wind, waves and rain. As well, the water properties were needed for the acoustic design of the noise range.

For design purposes we have presented the 10 year return period event as our criterion. Based on the measurements at the survey site, together with the historical data, one hour average design currents may be estimated as follows: surface current of 140 cm.s^{-1} (~3 knots), current at 125 m below the surface of 95 cm.s^{-1}, current at 200 m below the surface of 65 cm.s^{-1}, and current at 350 m below the surface of 35 cm.s^{-1}. The flow is typically along the isobaths and has a flow reversal near the sea floor. This enhances the current shear.

The temperature profile at this site exhibits spatial and temporal microstructure. Typical values that were observed are predicted to cause small fluctuation of acoustic intensity and phase at frequencies less than 2 kHz, but by 5 kHz the phase fluctuation, as a result of propagation over a 200 m path, can be expected to be 0.5 radians. Such a variation over an array would degrade its performance.

A significant wave height, averaged over 6 hours, of 9 m or higher is expected to be an appropriate 10 year return period design value. The number of rain free days is expected to be 240 per year. The wind speed is expected to be below 5 m.s^{-1} for 6 hour periods on 35% of the time during the months of May, June and July but in the summer months the 6 hour periods of calm occur less frequently.

Ambient noise at this site is significantly affected by rain, migrating whales and nearby shipping. The wind dependent noise was found to be consistent with Cato (1978a,b) but for low frequencies it is near the lower limit of the values presented in that reference. A summary of the acoustic results is shown in the report.

Authors

Ian S.F. Jones
Maritime Operations Division

Dr Ian Jones is a Principal Research Scientist in the Maritime Operations Division at AMRL Sydney. His research interests include ocean turbulence, satellite oceanography, air-sea interactions, and surface waves.

D.H. Cato
Maritime Operations Division

Dr Doug Cato is a Principal Research Scientist and Task Manager in the Maritime Operations Division at AMRL Sydney. His main research interest is the ambient noise in the ocean, including theoretical and experimental studies of sea surface noise and biological noise.

L.J. Hamilton
Maritime Operations Division

Mr Les Hamilton is a Senior Professional Officer Class C in the Maritime Operations Division at AMRL Sydney. With a background in physical oceanography his research interests include turbidity, ocean currents, surface waves, and satellite oceanography.

B.D. Scott
Maritime Operations Division

Mr Barry Scott is a Senior Professional Officer Class B in the Maritime Operations Division at AMRL Sydney. Originally from CSIRO he has a background in chemical oceanography and extensive experience in conducting oceanic surveys. Research interests include ocean eddies and productivity, and afternoon effect.

1. Introduction

The RAN requires an Underway Radiated Noise Range for their vessels. An acoustic range is designed to measure the noise radiated from ships and submarines. It must do this in the presence of background noise due to distant shipping, biological activity, seismic disturbances, and the ever present wind and waves. The design challenge is to produce a receiving array that can be installed and maintained in the presence of currents and at the same time be large enough to be able to 'image' a sound source against background noise. The problem has many analogies to a radio telescope which attempts to measure the strength of the signal from a target in the heavens.

DSTO were commissioned by the RAN to carry out a survey of a site chosen off Western Australia at 32°15'S, 115°02'E. The purpose of the survey was to provide some of the environmental data which would allow the more efficient design of the range. The following variables were assessed by DSTO as critical to range design and performance:

(a) **Ambient Noise.** This provides the main acoustic limit on system performance. Measurements need to be related to wind speed statistics and shipping movements to allow noise to be forecast.

(b) **Currents** limit the extent that acoustic arrays will maintain their geometry, and the accuracy that vessels can maintain the required path during the runs. They also influence factors such as design strength and configuration of hydrophone arrays, and flow noise generated at hydrophones.

(c) **Winds, weather, and rain** are important sources of ambient noise, and affect general sea conditions.

(d) **Waves and swell** affect the handling of vessels, as well as generating ambient noise through wave-breaking and other mechanisms.

(e) **Water Properties** such as temperature and salinity determine the sound speed profile and water density. A knowledge of sound speed profiles allows acoustic propagation predictions. Knowledge of water density is necessary for buoyancy calculations of array components.

(f) **Microstructure** or inhomogeneities in temperature and salinity may scatter acoustic energy and cause fluctuations in the received acoustic signal. It is predicted that these will occur because temperature and salinity of the major current in the area, the Leeuwin Current, is very different from the waters outside it. Such a situation can lead to intense fine-scale interleaving of the different water bodies.

(g) **Topography** of the bottom influences bottom bounce transmission paths, and possible routing for undersea cables. It may also influence directions of currents.

1

Details of the topography are described in Section 2; the currents are described in Section 3; water properties (temperature and salinity) are described in Section 4; microstructure of temperature and salinity in Section 5; wind, waves, and rain in Section 6; and ambient noise in Sections 7 to 10. A discussion is given in Section 11. The day to day details of the site survey are given in Appendix A.

Data were gathered from 15 July to 24 September 1992. As with almost all environmental questions, longer records are required to provide more definitive answers. However time was not available. A draft copy of this report was made available to the RAN and contractors in early September 1992. The present document is intended to allow a wider dissemination of results. Some typographical and factual errors in the draft are also corrected.
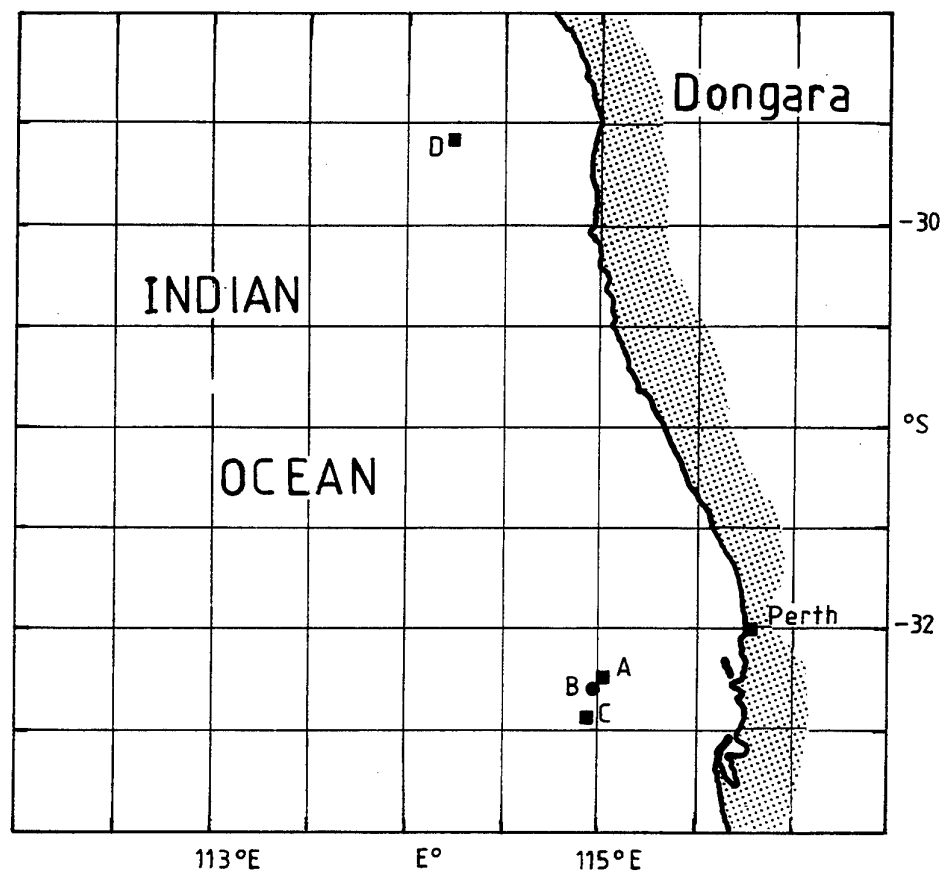
Fig 2.1 The site location A. Vertical current meter arrays were deployed at sites A, C and D (the Dongara site), but those at C were not recovered. Noise recordings were made at site B.

2. Topography and Site Location

The survey site lies on the north south oriented continental slope off Western Australia, at the position shown in Fig. 2.1. The topography influences that part of the acoustic propagation that involves bottom reflection and also the direction of currents. The profiles along three bearings through the survey site are shown in Figs 2.2 to 2.4, with bottom contours. (More detailed bottom contours are shown in the currents section e.g. Figs 3.4 and 3.22). Traversing southwestward from the shoreline along bearing 247.5° through the survey site the upper continental shelf lies between the 30 and 50 m isobaths, being about 12 nautical miles wide. The bottom slope then changes abruptly at 50 m to form the lower part of the continental shelf to about 200 m, below which the slope steepens. The site itself lies just shorewards of the 400 m isobath.

Extensions of the Perth submarine canyon are roughly 10 to 15 nautical miles distant from the site, encircling the site on the northwest quadrant. The influence of the canyon and its extensions on current flows and possible chanelling of sea noise are unknown. Currents in several submarine canyons worldwide are discussed by Shepard et al (1979). General findings were almost continuous flow up and down canyon axes at speeds up to 30 cm.s^{-1}, with tidal influences, internal waves, counter-currents, and turbidity currents. For some canyons, the fastest currents were normal to canyon axes.

ACOUSTIC RANGE SITE PROFILE
BEARING 292·5°
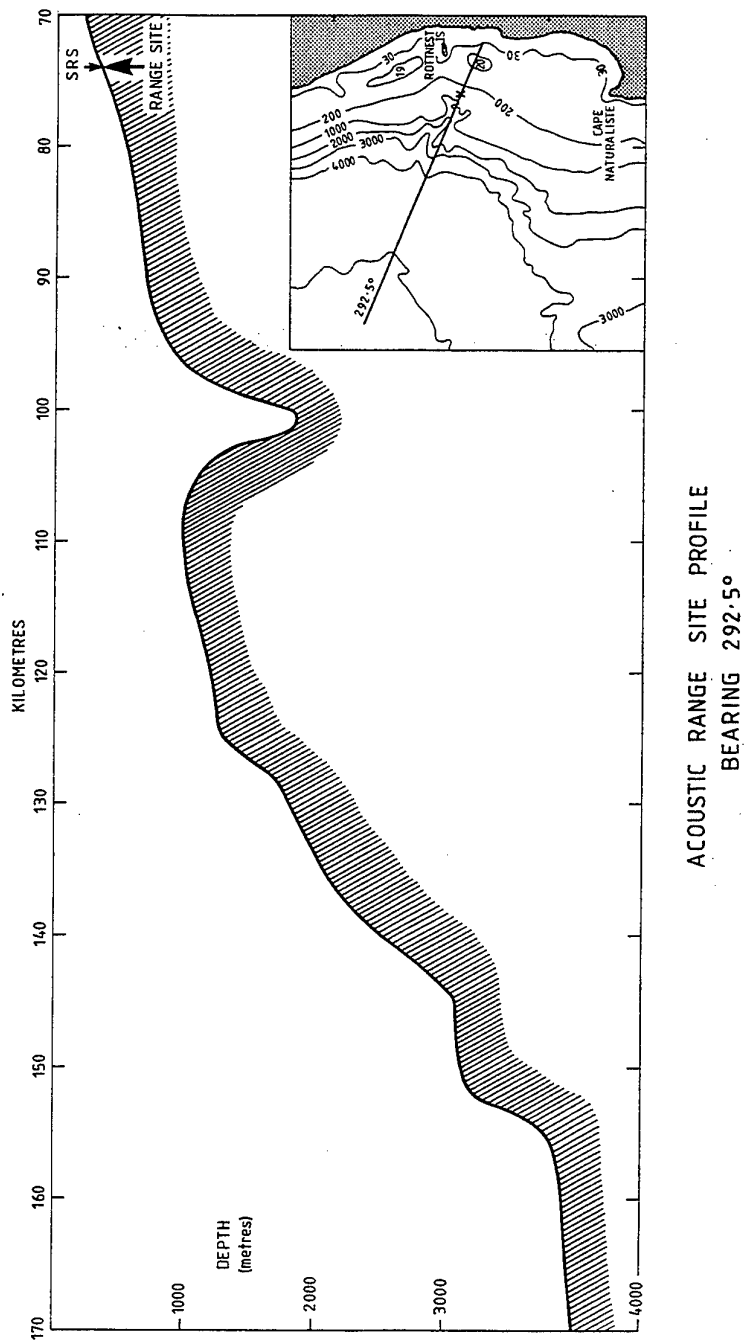
Fig 2.2 Bottom profile on an east-west line through site A.

ACOUSTIC   RANGE   SITE   PROFILE
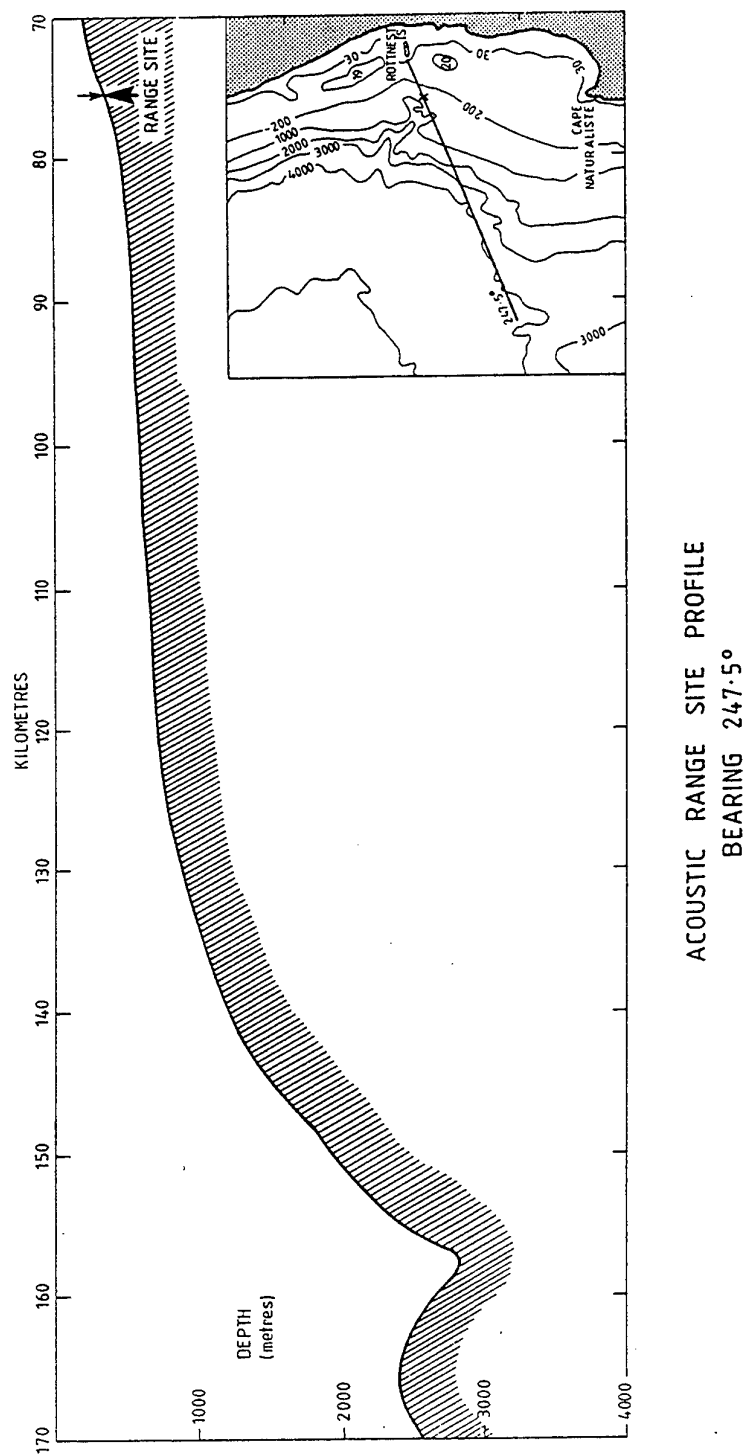
BEARING   247·5°

Fig 2.3 Bottom profile at bearing 247.5° through site A.

ACOUSTIC RANGE SITE PROFILE
BEARING 292·5°
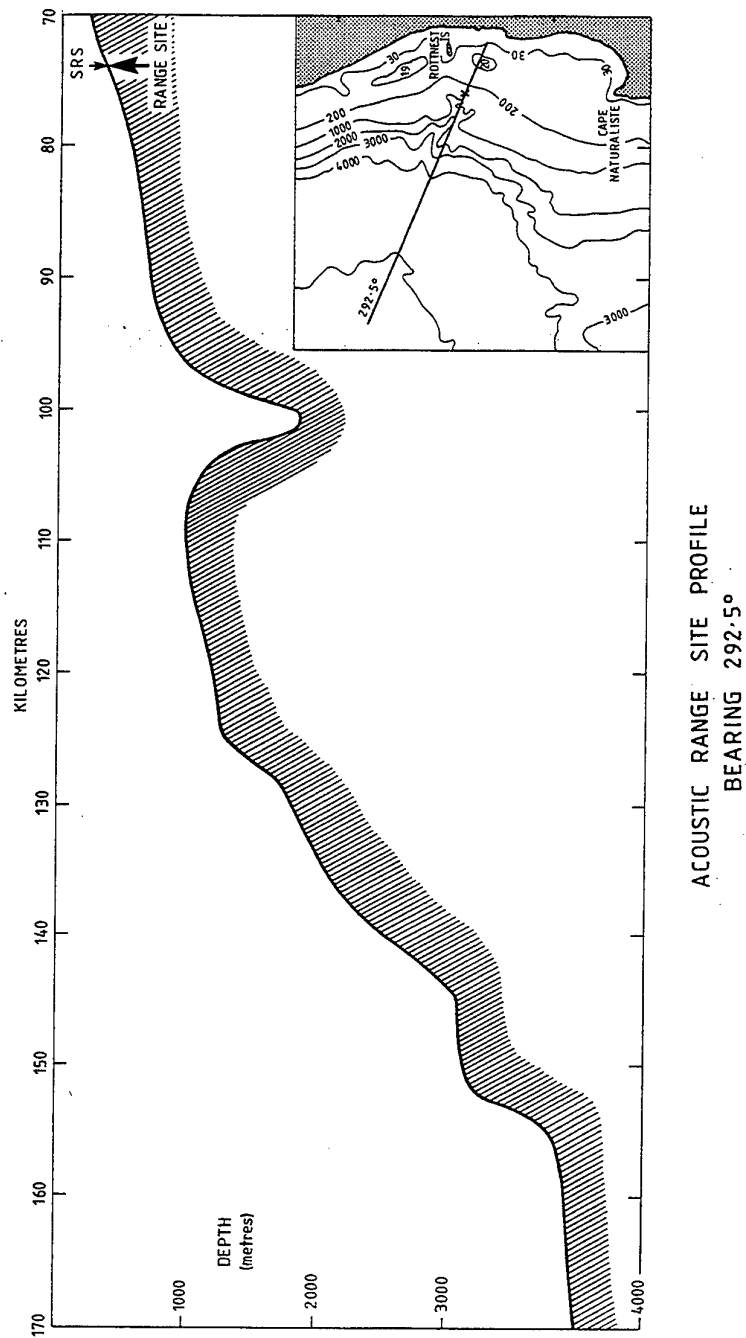
Fig 2.4 Bottom profile at bearing 292.5° through site A.

3. Currents off Western Australia

The types of information on the circulation of most importance to engineering for the site are considered to be current strengths, vertical and horizontal current shear, movements of oceanic fronts, persistency of flow features, seasonality, and temperature gradients associated with the currents. In view of the fact that two strong current systems having different water properties meet in this area, forming eddies and meanders of different size scales with clockwise or anti-clockwise circulations, **it is highly likely that currents will be critical to the design and construction of an acoustic range.** The currents are therefore described in some detail. Sections 3.1 to 3.4 describe features of the circulation described in the literature, and sections 3.5 to 3.8 describe results of measurements from the DSTO survey.

The physical oceanography of the site survey area is influenced by the large scale circulation features of the Indian Ocean, by local wind and shelf effects, and by the throughflow of warm Pacific Ocean waters into the eastern Indian Ocean through the Indonesian Archipelago. The general circulation features relevant to the site survey area are described, but in general the theory and driving mechanisms are not discussed.

3.1 Regional Circulation - Indian Ocean

The Ocean waters in the area of interest lie in the south-eastern portion of the Indian Ocean, being bounded eastwards from north to south by the Australian land mass, with no boundaries in other directions for some thousands of kilometres. *Wyrtki (1971, 1973)* describes three large scale surface circulation systems for the Indian Ocean which are shown schematically in Fig. 3.1.

I.   the seasonally changing monsoon gyre;
II. the south hemispheric subtropical anticyclonic (anticlockwise) gyre;
III. the Antarctic waters with the Circumpolar Current.

The subtropical gyre consists of the South Equatorial Current; the Agulhas current system flowing poleward along the southern portion of the east African south coast; eastward flow situated to the north of the Subtropical Convergence (roughly 41°S) driven by the prevailing westerly winds; with the system being closed by slow equatorward movements. All ocean basins have such a system which was first postulated by Tessan, as discussed in *Jones and Jones (1989)*. The three circulation systems are reflected in the distribution of chemical properties, especially phosphate content, with the subtropical gyre having very low values, and the monsoon gyre high values. Subtropical surface waters of high salinity (the South Indian Central water) form in the gyre from the excess of evaporation over precipitation. The highest surface salinities are found in a belt between 25-35°S, with the maximum occurring close to Australia, and approaching 36 practical salinity units (psu). An anomalous boundary current flows poleward along the southern portion of the Western Australian coast *(Andrews 1977; Cresswell and Golding 1980)*, at least one component of which is known
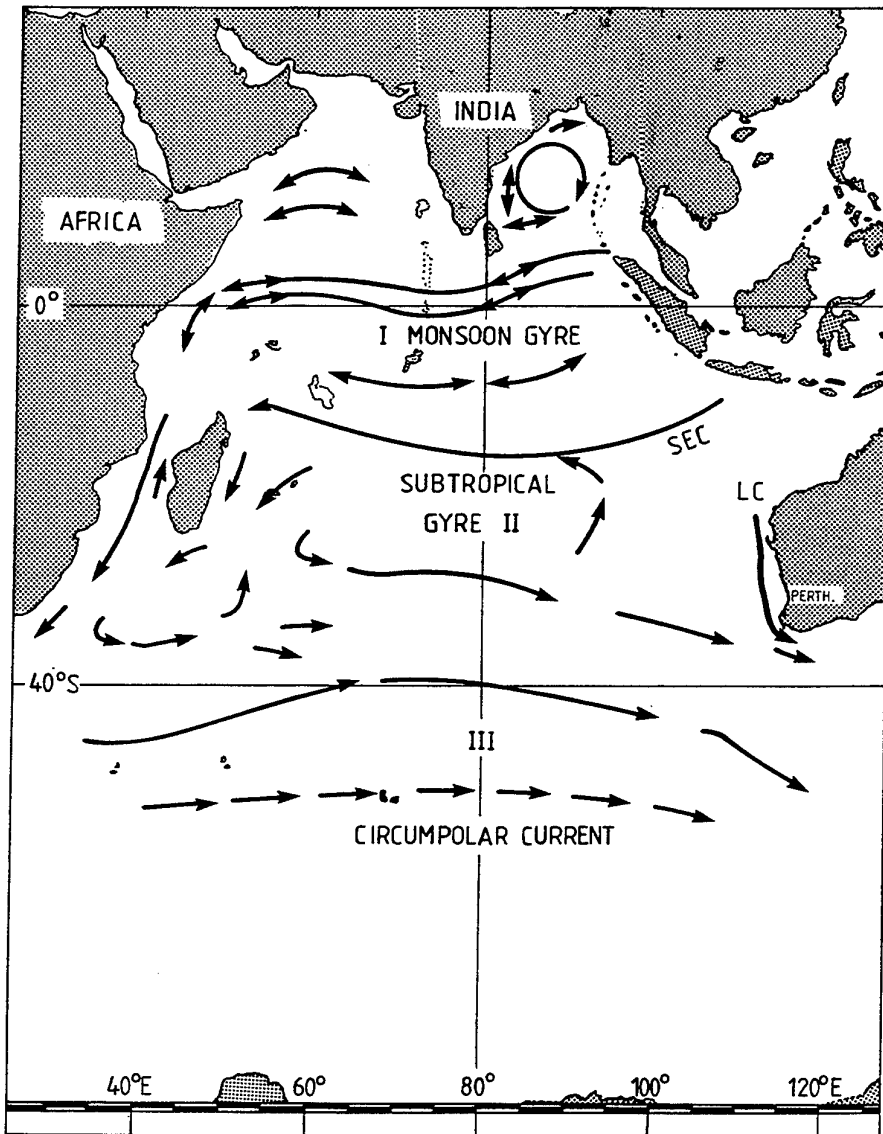
Fig 3.1 *Map showing area of interest in relation to the Indian Ocean and representation of principal circulation features in the south-east Indian Ocean (after Wyrtki 1973). LC = Leeuwin Current. SEC = South Equatorial Current.*
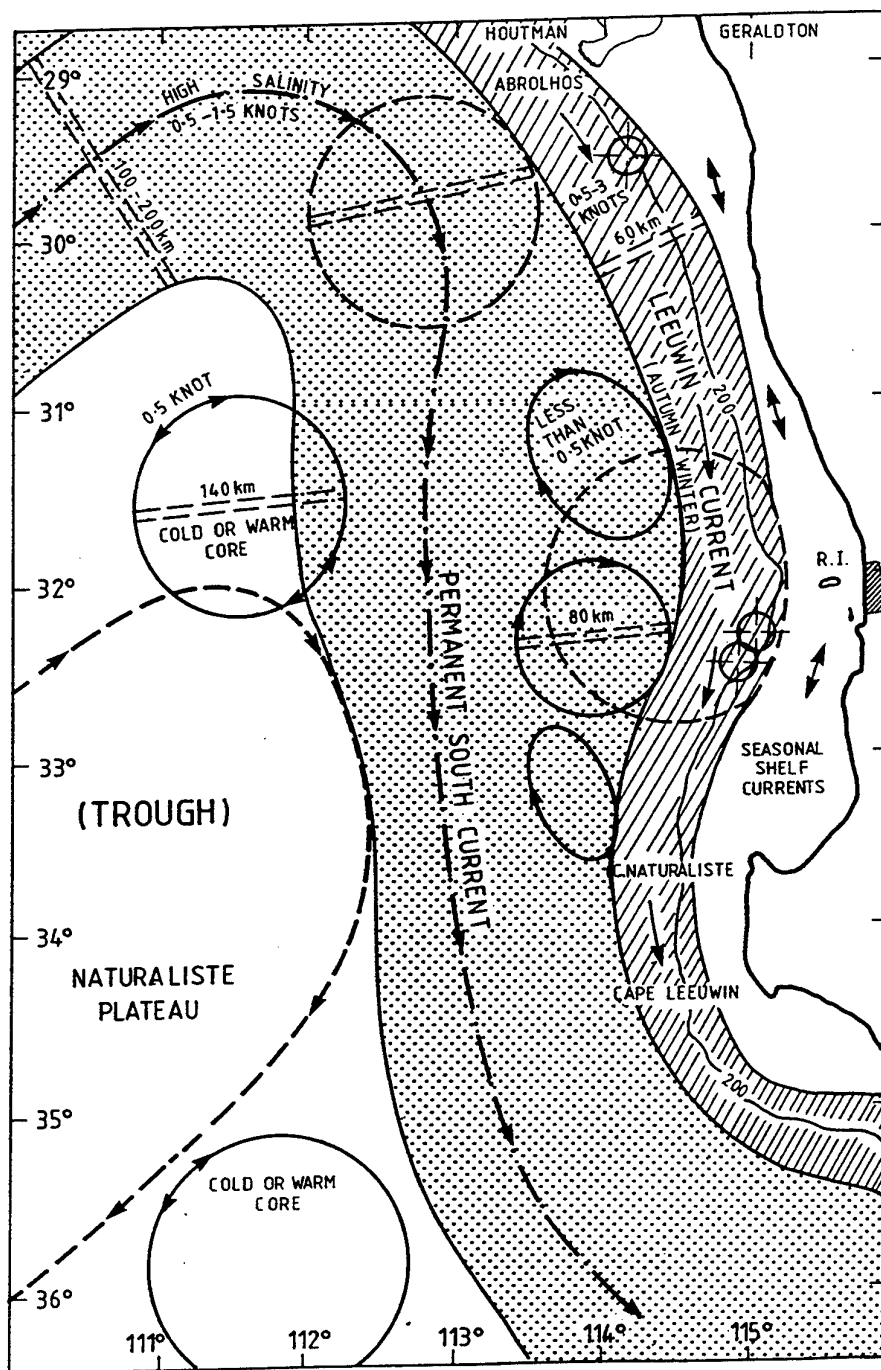
Fig 3.2 *Schematic representation of general circulation features in the south west Australian area (after Hamilton 1984). Two major current systems occur: the seasonal Leeuwin Current and a permanent southward current. Cold-core elliptical eddies flank the seawards side of the Leeuwin Current, with larger cold- and warm-core features seawards.*

as the Leeuwin current. The Current is different from other major eastern boundary currents, since it flows rapidly poleward, against the prevailing equatorward winds, rather than slowly equatorwards in a diffuse flow.

3.2 Circulation Patterns off South-West Australia

3.2.1 General

Pictorial representations of typical circulation patterns off south-western Australia are shown in Figures 3.2 and 3.3, with bottom topography in Fig. 3.4. The main circulation in the area is a warm southward flowing poleward boundary current system which flows down the shelf break along the 200 m contour. This flow turns at Cape Leeuwin (near 34°30'S, 115°E) to flow eastward across the Great Australian Bight. This circulation system is comprised of two currents. In winter the current originates largely from low salinity water from the North West Shelf area (17 to 20°S, Fig 3.3a) and in summer from an inflow of high salinity Indian Ocean water along 30-31°S, flowing east or north-east into the coast before turning south. Seasonal shelf currents are also seen which are influenced in direction by prevailing winds, with trends north in summer. Current strength for the high salinity water is halved at a depth of about 200 metres *(Webster, Golding, and Dyson 1979)*.

Both warm and cold-core eddies are associated with the currents. Warm-core rings are V-shaped in temperature cross-sections, with the V containing warmer water than the waters outside the eddy. The circulation of these features is anti-clockwise (anti-cyclonic) in the southern hemisphere. Cold-core eddies resemble upturned Vs in temperature cross-sections, and circulation about these features is clockwise (cyclonic) in the southern hemisphere. The upturned Vs contain cooler waters than outside the eddy. Over the slope on the seawards side the Leeuwin current is flanked by narrow, elliptical, cold-core rings of diameter typically 80 km *(Andrews 1983)*, which have clockwise circulation. Farther seawards of the slope the eddy pattern is more confused with length scales on average greater than 140 km, eddy circulations being both clockwise and anti-clockwise *(Andrews 1983)*.

Golding (1980), and Cresswell and Golding (1980) describe general circulation patterns for 29°S (Abrolhos Islands) to 33°30'S (Cape Naturaliste). Clear differences are seen between summer and winter patterns:

Normal summer: southward flow of high salinity water seawards of the slope from the inflow across 30 to 31°S, with meanders and eddies. Northward flow (wind driven) of high salinity water on the shelf from as far south as Cape Naturaliste.

Normal winter: southward flow of low salinity water of the Leeuwin Current along the slope with spreading onto the shelf; and southward shelf flow.

Late spring or early autumn: the low salinity Leeuwin Current flows southward along the slope; and shelf waters of high salinity flow northward in response to winds.
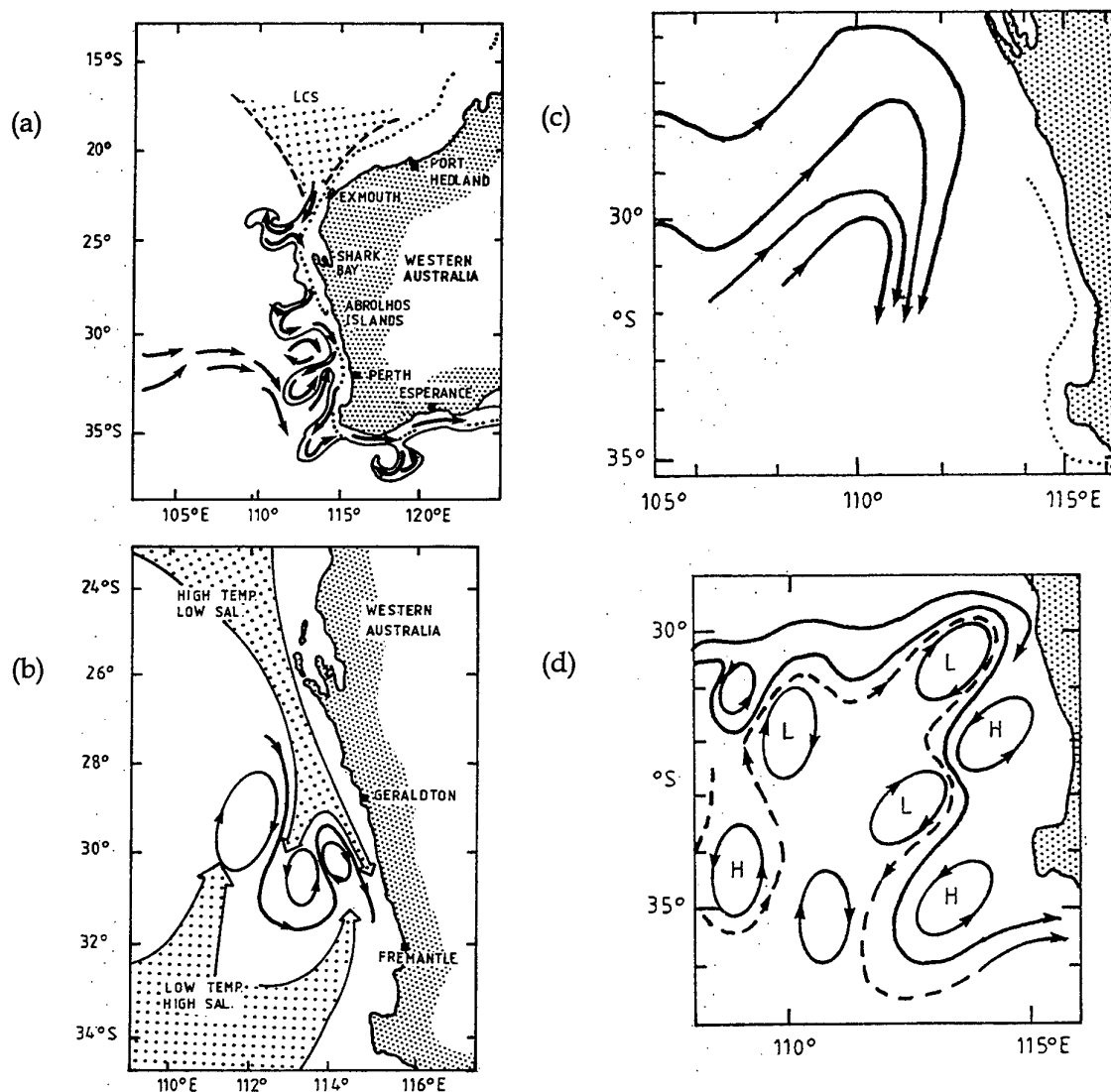
Fig 3.3 *Mesoscale features of the current systems off southwest Australia.*

(a) *Schematic diagram of the Leeuwin Current system, derived largely from satellite imagery (after Pearce 1991). The Leeuwin Current source is shaded, with the solid arrows indicating the flow in the warm surface meanders and jets as well as the currents in the cooler offshore waters,. The dotted line shows the 200 m contour. LCS = Leeuwin Current Source.*

(b) *Idealized representation of the two major water types found in the south-eastern Indian Ocean (after Kitani 1977).*

(c) *Inflow from the west along 30 °S (after Wyrtki 1971).*

(d) *The inflow from the west breaking into eddies and meanders (after Andrews 1977). H = high (warm feature); L= low (cold feature).*
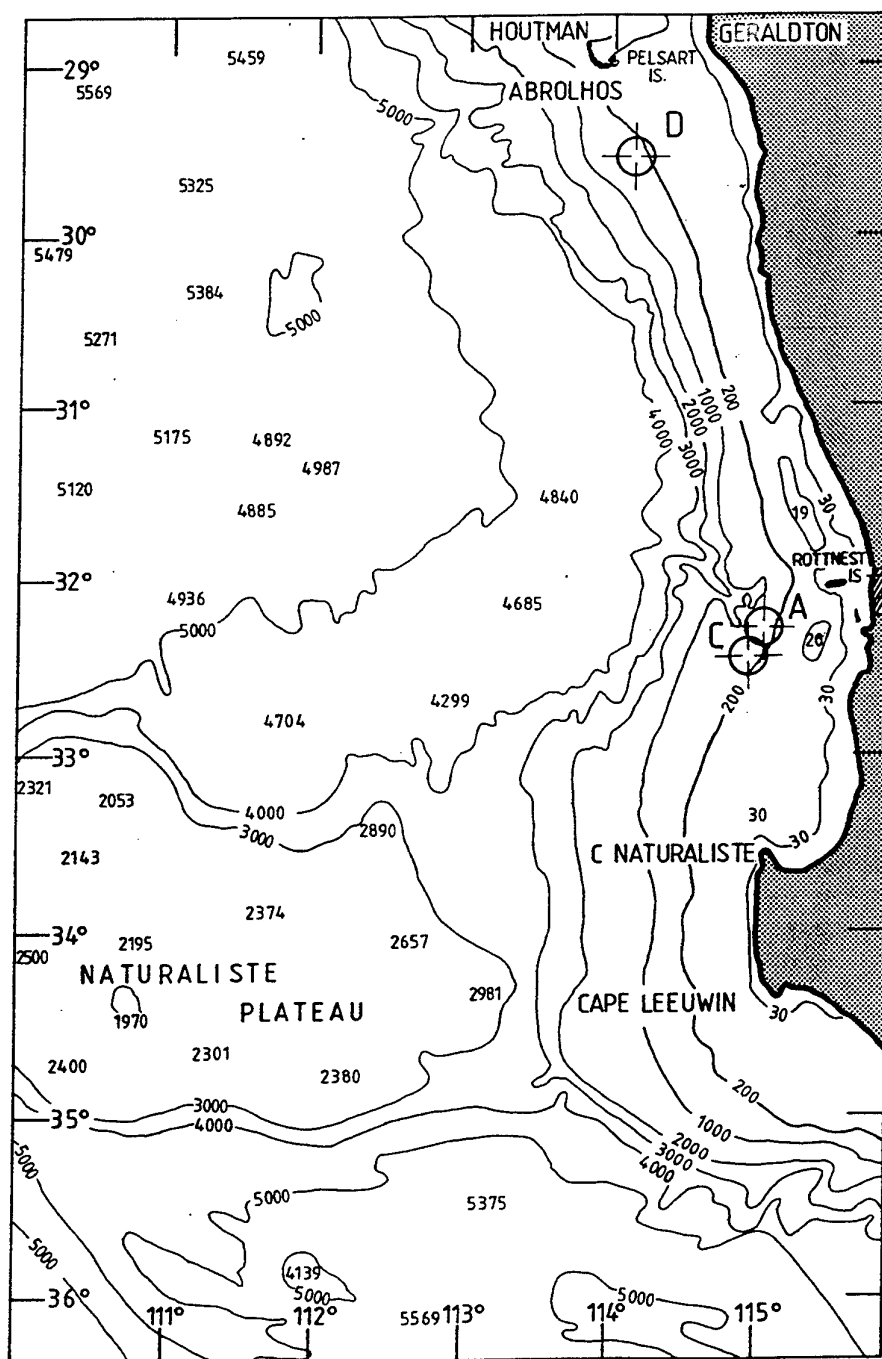
Fig 3.4 Bottom topography and major place names off south-west Australia. Current meter sites A, C and D were occupied from mid July to the end of August 1992. The current meters at site C were not recovered.

3.2.2 Leeuwin Current (a seasonal southward flowing current)

Relative to surrounding waters the Leeuwin Current is a high temperature and low salinity current (35.2 psu). The current originates from the North-West Shelf at 17 to 20°S (e.g. *Legeckis and Cresswell 1981*), usually flowing from late autumn to mid-winter and running along the continental shelf in a narrow stream between 22-27°S, and then above the slope to beyond 29°S. In spring the current may sometimes cease or flow only weakly from the north, with the south portion continuing on. The current intrudes between the coast and a southward flowing current farther offshore which is believed to be strongest in summer. Current speeds up to 1.5 m.s⁻¹ (~3 knots) have been reported, with the current accelerating southwards past Cape Naturaliste, and exhibiting faster speeds there on the landward side compared to offshore *(Cresswell and Golding 1980)*. Average speeds are probably of the order 50 cm.s⁻¹ (one knot), with width about 60 km. The current narrows from about 400 km at Shark Bay to be only about 20 - 100 km wide at the Capes. Its vertical extent deepens from 250 m at 29°S to 320 m at 34°S *(Smith et al 1991)*.

Near the Abrolhos Islands the current appears to move farther off the shelf, so that the eastern side interacts with the islands, leaving colder shelf waters *(Legeckis and Cresswell 1981)*.

3.2.3 The Leeuwin Current in Satellite Imagery

The Leeuwin Current is a warm water current from the north which flows southward in mid-year (autumn and winter) through surrounding waters which are cooling. It is therefore readily detectable by its sea surface temperature signature, and its surface expression can be monitored by infra-red (IR) imagery available from satellites. As seen in IR satellite imagery *(Legeckis and Cresswell 1981; Pearce and Griffiths 1991)* the seawards side of the current is subject to meandering and seawards offshoots. *Pearce and Griffiths (1991)* describe a series of wave-like meanders which transport Leeuwin Current water away from and back towards the coast, with meanders sometime developing into cyclonic-anticyclonic eddy pairs (Fig. 3.3a). The anticyclonic circulations were seen to grow offshore to a width of order 200 km, and may eventually "pinch-off" to form a free-standing eddy. Between the meanders the current tends to flow along the shelf-break and upper slope as a jet-like current towards the south, with cyclonic eddies on the seawards side. The meanders do not appear to propagate along the coast. Usually three to four co-existing meanders occurred at roughly equally spaced intervals between 26-34°S for 1984 and 1985, with no apparent preferred locations, and existing for 30 to 60 days. The subsurface structure and vertical extent of the offshoots is unknown. Data on the Leeuwin Current described in the next section found it to be often less than 250 m in vertical extent just off the shelf edge.

3.2.4 The Leeuwin Current Interdisciplinary Experiment (LUCIE)

Data for the LUCIE experiment were obtained from September 1986 to August 1987 by CSIRO and collaborators. Current meter arrays were placed out from the coast at 29.5°S and 34°S, and Conductivity-Temperature-Depth (CTD) profile data and meteorological observations were taken. The following description of the Leeuwin Current system found from the LUCIE experiment is extracted from *Smith et al (1991)*:

"The nearly year-long current meter measurements made across and along the shelf edge off Western Australia between September 1986 and August 1987, and the associated CTD surveys, showed poleward flow (the Leeuwin Current) above 250 m throughout the year. A narrow equatorward undercurrent along the continental slope was apparent in the current meter data between 250 and 450 m, but not clearly resolved in the CTD sections. Although there was seasonal variation, the poleward Leeuwin Current flowed during all seasons. Throughout the year, and along the entire Western Australian coast, there is a local temperature maximum at the core of the Leeuwin Current. At latitudes north of about 32°S, the core of the Leeuwin Current forms a salinity minimum. Between 29° and 34°S, the Leeuwin Current seems to entrain high-salinity subtropical waters from offshore. Farther poleward, offshore waters are relatively fresh and the core of the Leeuwin Current appears as a salinity maximum as well as a temperature maximum. The Leeuwin Current was strongest near the shelf edge in late summer and early autumn (March-May) and farther seaward in winter (June-August). It was weaker, and near the shelf edge, in spring (September-December) and almost vanished in early summer (January). The seasonal variation seems to be due to the seasonal variation in the wind stress, which is most strongly equatorward in spring and summer, rather than to any seasonal variation in the alongshore pressure gradient. The alongshore pressure gradient was nearly the same for the five CTD surveys (there was no cruise during spring, however) and agreed with Hamon's (1965) earlier "seasonal" study.

The strong, narrow Leeuwin Current depends on the alongshore pressure gradient of the Eastern Indian Ocean, which "drives" an onshore geostrophic transport in the upper 250-300 m, between about North West Cape (22°S) and Cape Leeuwin (35°S). Offshore of the upper continental slope, and offshore of the Leeuwin Current core, the onshore transport in the upper layer is balanced by offshore transport in a deeper layer; the vertically averaged geostrophic transport across the 2000 m isobath (relative to 1300 or 1750) is close to zero. Near the shelf break, the onshore geostrophic flow of the upper layer cannot be balanced by offshore geostrophic transport, and is greater than the offshore Ekman transport in the surface layer due the equatorward wind stress. Instead the onshore transport is balanced (or nearly balanced) by offshore Ekman transport in the bottom boundary layer under the poleward Leeuwin Current."

The LUCIE current meter arrays could not resolve eddies or offshore Leeuwin Current migrations because of their limited offshore extent.

3.2.5 Permanent Southward Current

For much of all of the year a current exists which appears to flow eastward or north-east along 30 to 31°S (Figs 3.2, 3.3) before turning southward (Wyrtki 1971; Andrews 1977). Andrews (1979) calls this the "West Australian Current", a term usually used for a

flow found farther north and east, and flowing to the north. *Pearce (1991)* suggests the name "West Australian Summer Current", but it is yet to be demonstrated that it is solely a summer feature. *Andrews (1979)* suggests that this current and general circulation are steered by the Naturaliste Plateau with a permanent gyre (a trough) situated over this plateau (see Fig. 3.2), and provides a diagram of bottom steering parameter for the area. The waters are subtropical in origin with high surface salinity (35.6 to 35.8 psu). Typical current values are probably about 1 to 1.5 knots with width of the current about 100 km.

3.2.6 Continental Shelf Currents

These are described in the general circulation remarks given earlier. *Cresswell and Golding (1980)* found buoy speeds up to 65 cm.s^{-1}. Buoys usually decelerated when moving onto the shelf. In the summary of *Pearce and Cresswell (1985)* currents on the inner continental shelf from Exmouth to Cape Leeuwin are described as *"a mean northward flow of order 10 to 20 cm.s^{-1} (1/5 to 2/5 knot) of high salinity water flow as far south as Cape Naturaliste driven by the dominant northward wind stress. However, currents fluctuate (and reverse) within a period of about a week due to variations in the wind stress."*

3.2.7 West Australian Current

This is a weak current found well seawards and north of the study area (e.g. Fig. 1a of *Cresswell and Golding 1980*). It is described here for completeness. The current seems to be composed of a weak, variable northward flow, and apparently represents the diffuse equatorward currents usually found in eastern boundary zones. *Hamon (1972)* found no evidence for a regular north-flowing current from dynamic topographies obtained from surveys with large station spacing. Most of the recent descriptions tend to emphasise the weak eastward flow from the central Indian Ocean towards Western Australia between about 15 to 35°S *e.g. Pearce and Cresswell (1985)*, (the permanent southward current described in section 3.2.5), rather than this current.

3.2.8 Eddies

Both warm and cold core eddies or rings are seen in the region, with possibly two size scales. The Leeuwin Current appears to be flanked by narrow elliptical cyclonic eddies over the slope on the seaward side with mean diameter suggested by buoys of 80 km *(Andrews 1983)*. See Fig 3.2.

Andrews (1983) describes two regimes with different dynamics, the flanking cyclonic rings (as above) over the slope, and a second regime seawards of the slope, where both mesoscale cyclonic and anti-cyclonic eddies are found, of length scale greater than 140 km. *Golding and Symonds (1978)* thought that mesoscale fields in summer and winter might be different, with more eddies in the summer months.

Kitani (1977) described two cyclonic and one anti-cyclonic eddy in November 1975 and shows a possible means of eddy formation with the interaction of high temperature

low salinity water from the north and low temperature higher salinity water from the south (Fig. 3.3b).

Webster, Golding and Dyson (1979) refer to both warm and cold core eddies of 100 nm diameter in the period November 1973 to December 1974, in the area 29 -32°S and 112 - 115°E. *Cresswell (1977)* found a diameter of 100 km from buoy data. Using infra-red imagery *Pearce and Griffiths (1991)* observed large meanders forming in the Leeuwin Current of diameter more than 200 km.

Eddy Current Speeds

Andrews (1983) gives maximum speeds of 1 m.s⁻¹ for the ring circulation about eddies. *Cresswell and Vaudrey (1977)* present diagrams of buoy speeds which can be interpreted as showing average ring speeds of 0.5 m.s⁻¹, with only a few cases over 1 m.s⁻¹ for buoys exhibiting loop patterns. *Cresswell (1977)* reports speeds of 0.2 to 1m.s⁻¹ for a buoy in an anti-cyclonic eddy, with the period between 4 and 7.5 days, and escape speed 1.25 ms⁻¹. The eddies flanking the Leeuwin current have been measured by buoys to have speeds 0.2 m.s⁻¹, compared to 0.5 m.s⁻¹ for the Leeuwin Current *(Cresswell and Golding 1980)*, with a temperature difference of 3°C from the Leeuwin Current. Period of rotation ranged from 3 to 12 days.

Eddy Translation

From drifting buoy data *Cresswell (1977)* describes one anti-cyclonic eddy of 100 km diameter between 32 -33°S, 112 - 114°E which was stationary for 30 days before moving NNE at 5 cm.s⁻¹. *Cresswell* also refers to a buoy in an anti-cyclonic eddy which moved WSW at 7.5 cm.s⁻¹ over a period of 12 days in January 1976, starting from 33°S, 113°E. South of Cape Leeuwin, *Cresswell and Golding (1980)* found westward drifts of between 6 to 7.4 km/day (about 7 to 8.5 cm.s⁻¹) for clockwise circulating features.

3.2.9 Deeper Flow and Undercurrents

In the area generally seawards of depths where the Leeuwin Current is found, the deeper flow, e.g. at 400 metres, may be opposite in direction to the surface flow, or bear little relation to the surface flow. *Webster et al (1979)* found that geostrophic currents calculated at 200 metres and deeper had a tendency to swing to the north. They also stated, however, that the dynamical condition which gave rise to stronger geostrophic currents in the middle of the year seemed to dominate current directions all the way to 1000 metres and so sometimes reversed the currents at 200 metres and deeper.

Andrews (1979) found a change of regime from 250 to 400 metres depth in the vertical, although the temperature fields shown by *Andrews* at 250 and 400 metres show many broadly similar features. *Andrews (1983)* presents a temperature-depth cross-section (his Fig. 7c) where isotherms are depressed at depths above 250 m (implying anti-clockwise circulation) and sharply uplifted at depths greater than 250 m (implying

clockwise circulation). In a contour diagram of temperature at 250 m the feature appears as a warm-core ring, but in the temperature field at 400 m as a cold-core ring *(near 29°45'S, 111°E in Andrews' Fig. 2)*.

Thompson and Cresswell (1983) refer to an undercurrent where cool, high salinity, high oxygen water is being advected northward and downward underneath the Leeuwin Current in May 1982. They reported an equatorward current of 32 cm.s⁻¹ at 300 metres depth (near bottom) off North-west Cape and Shark Bay (near 25°S in Fig 3.3a).

Current meter data from the LUCIE project *(Boland et al 1988; Smith et al 1991)* at 29.5°S and 34°S showed an equatorward undercurrent below 250 m and 320 m respectively. At 29°S the undercurrent had a maximum speed of 15 cm.s⁻¹ over November 1986 to January 1987, coinciding with strongest equatorward winds. At 34°S the undercurrent was not observed for March to May 1987.

In an unrelated mechanism, calculated onshore geostrophic transport exceeded offshore Ekman transport induced by equatorward wind stress, and was presumably balanced over the upper slope and outer shelf at depths less than about 250 m by the offshore Ekman transport near the bottom under the Leeuwin Current. The offshore flow may occur in a bottom boundary layer 15 to 33 m thick for water depths of 85 to 108 m *(Smith et al 1991)*. This offshore flow at Dongara (29.5°S) was stronger for May to July 87 than March to May 1987.

3.3 Current Shear

Current shear is important to the design of an acoustic range, because it can affect hydrophone array or cable geometry e.g. by bending the array or distorting its shape. Shear places additional stresses and tensions on ocean structures which can potentially cause damage or failure.

3.3.1 Vertical Current Shear

For the CSIRO LUCIE experiment in 1986-87 described earlier in section 3.2.4, vertical strings of current meters were deployed across the shelf off Dongara (29.5°S) and the Capes (34°S). An examination of current meter measurements from the CSIRO LUCIE project shown in *Boland et al (1988)* shows high current shear sometimes occurs at both Dongara and near the Capes. At Dongara a southward surface current of 2 knots overlay a northward current of 1.2 knots at 250 m and deeper. At the Capes similar circumstances occurred, but with both current strengths about 35 cm.s⁻¹. The reversals in current direction occurred somewhere between 120 to 230 m. Further details are given in the following paragraphs. Alongshore current averages over 72-day periods for Dongara in a bottom depth of 107 m were 18 cm.s⁻¹ at 92 m below the surface, and 8 cm.s⁻¹ at 102 m below the surface *(Smith et al 1991)*.

The LUCIE Dongara array had vertical current meter strings in bottom depths of 53, 85, 108, 305, and 700 m. Closest current meter depths to the DSTO survey site A depth of 400 m were 250 m below the surface in 305 m water depth, and 246, 254, 446, and 454 m below the surface in 700 m water depth.

The LUCIE array at 34°S had vertical current meter strings in bottom depths 116, 200, 186, and 720 m. Closest current meter depths to 400 m were 230 and 320 m below the surface in 720 m water depth. Some details of the measured CSIRO currents are shown in the following table.

Peak of hourly averaged currents (knots) at selected depths at Dongara and the Capes for the CSIRO LUCIE study. Constructed from data shown in Boland et al (1988).

Depth of current meter below the surface (m)	Dongara Speed (knots)	The Capes Speed (knots)	Bottom Depth (m)
0	1.7	-	300
0	2.0	1.6	700-720
320	-	1.0	720

At Dongara (LUCIE Period 1 September 1986 to February 1987) maximum currents of 85 cm.s $^{-1}$ were measured at 75 and 125 m below the surface for 300 m bottom depth. The currents 250 m below the surface for bottom depth 300 m had a maximum of 30 cm.s $^{-1}$. and current directions showed only occasional correlation with the upper levels, sometimes being in the opposite direction. The currents at 75 and 125 m below the surface were strongly in phase.

At Dongara (LUCIE Period 2 - February to August 1987) for a bottom depth of 308 m a peak current of 105 cm.s $^{-1}$ at 83 m below the surface was seen in April. Current meters at 83 and 133 m below the surface showed high correspondence in current speeds and directions. Currents at 258 m below the surface had speeds less than 15 cm.s $^{-1}$ and the speeds and directions showed little if any correlation with upper levels.

At Dongara (LUCIE Period 1 - September 1986 to February 1987) for a bottom depth of 704 m, the currents at 79 and 129 m below the surface were strongly correlated. The currents at 254 and 454 m below the surface were strongly correlated, and were correlated with the upper level currents in periods of strong (45 cm.s $^{-1}$) northward flowing currents. When this latter situation occurred the northward currents were seen first at 454 m with a phase lag upwards to the 79 m current. Otherwise, deeper currents could be opposite in direction to upper level currents.

At Dongara (LUCIE Period 2 - February to August 1987) for a bottom depth of 696 m, currents at 71 m below the surface were as high as 120 cm.s $^{-1}$ and were well correlated

with currents 121 m below the surface. Currents at 246 and 446 m below the surface were well correlated with each other, but not with the currents at upper levels. Northward flowing deeper currents were seen in May to June 1987 (0.60 m.s^{-1}) when currents at the upper levels were southward and at their peak values (over 2 knots). At other times, e.g. mid-April 1987, currents were correlated throughout the column.

At Cape Mentelle (34°S), the currents at 90, 160, 230, and 320 m below the surface in a bottom depth of 720 m were well correlated for much of February 87 to August 87, with peak speeds at 90 m of 80 cm.s^{-1}. Peak speeds at 320 m below the surface were just over 0.5 m.s^{-1}. However in June 1987 northward currents of 0.35 m.s^{-1} were seen at 320 m below the surface when surface currents were at about the same strength southward. In July 1987 currents reversed from southward to northward with a phase lag upwards from 320 m below the surface to 90 m below the surface. The reversals in current directions occurred somewhere between 160 and 230 m below the surface.

In summary, at 29°30'S and 34°S the current speeds and directions from the surface to 130 m below the surface can be decorrelated with those from 250 m to 450 m. The currents in these two depth regimes can be opposite in direction. At both Dongara and the Capes current reversals from southward to northward flow occurred, which were seen first at the deepest current meter of a particular site. Such high currents and current shears, with currents in different (and opposite) directions could cause problems in acoustic array performance.

3.3.2 Horizontal Current Shear

In summer there is a region of strong shear on the outer shelf between the northgoing shelf waters and the southgoing waters farther out to sea (30°30' to 32°00'S) *(Cresswell and Golding 1980 - their Fig. 7)*. Buoys carried from cyclonic features on the seawards side of the Leeuwin current into the Leeuwin Current were accelerated and encountered higher surface temperatures (e.g. from 0.2 to 0.5 m.s^{-1} with a 3°C temperature increase). Conversely buoys leaving the Leeuwin Current on the seawards side decelerated and encountered lower temperatures on entering a cyclonic feature. Buoy data also suggested that the Leeuwin Current accelerates southward as it nears the continental slope off Cape Naturaliste and that it is faster the nearer it is to the shelf edge. A buoy on the shelf accelerated from 0.4 to 0.65 m.s^{-1} from December 17 to 19 from Cape Naturaliste to Cape Leeuwin.

3.4 Current Variability

At all times of the year the mid-shelf currents were strongly influenced by passing weather patterns, which resulted in current variations of up to 0.5 m.s^{-1} and sea level changes of about 30 cm *(Cresswell 1991 - his Fig. 12)*. (The data is for 10 m above a 44 m bottom near the Abrolhos Islands - near 29°S, see Fig 3.2). Northward winds of several days duration were required to affect the current. *"In summer, atmospheric troughs from the north interrupted the northward wind stress and allowed the shelf waters to move south. In*

winter, the passage of lows near and south of Cape Leeuwin gave rise to strong north-westerly winds that augmented the southward Leeuwin Current flow on the shelf."

During LUCIE current variability was stronger over the upper slope and shelf-break than on the midshelf. Current variability at 29.5°S led that at 34°S by about 1.5 days. The currents inshore of the shelf-edge were forced directly by the coastal wind with Carnarvon winds leading the Dongara site by about one day. Carnarvon winds had a "seasonal" band of variability of 60 to 325 days and a "synoptic" band of 6 to 12 days, coherent with similar bands for currents *(Smith et al 1991)*. Weather systems (highs) move from west to east along 30°S at the rate of about one per week (Australia Pilot 1972), with intervening cold fronts.

As mentioned in the section on infra-red imagery, the seaward side of the Leeuwin Current experiences large seaward offshoots. The speed at which these features form is unknown, but such formations could perhaps cause increased surface currents at a site.

3.5 Location of Current Meters for the DSTO survey July to September 1992

Steedman Science and Engineering were contracted by DSTO to deploy vertical current meter arrays at sites A, C, and D shown in Fig. 3.4. Details of the arrays are as follows:

Site Location		Depth (m)	Current Meter Depths from Surface (m)	Period (1992)
(A) 32°16.98'	115°01.71'	400	125, 175, 200, 350	21 Jul to 03 Aug
(C) 32°27.27'	114°56.88'	300	50, 125, 200, 250	NO DATA
(D) 29°32.60'	114°09.45'	300	125, 250	16 Jul to 01 Sep

In view of the strong currents and shears expected, DSTO requested the contractors to deploy two current meter arrays (A and C) near the survey site to maximize the chances of a data return for the once only deployment. Array C was lost, showing the soundness of this decision. Loss of array C meant that estimates of horizontal shear and current variability about the site could not be obtained. Five days data near the site were also lost, because the array at site A was not able to be deployed at the planned time because of rough weather.

Array site D was previously occupied by a LUCIE current meter array for September 1986 to August 1987 (the Dongara site). This site was reoccupied by DSTO to see if statistical relations could be established between the short term DSTO data at sites A and D, and the longer term LUCIE data at site D. Such relations could allow potentially more viable statistical current parameters of e.g. the maximum expected current speed at site A to be derived from the year's worth of LUCIE data.

Fig 3.5 Time series plots of current meter speed, direction (north = 0°) and temperature for site A for 21 July to 30 August 1992. Water depth 400 m. Figures supplied by Steedman Science and Engineering.

(a) for the current meter 125 m below the surface.

Fig 3.5 *Time series plots of current meter speed, direction (north = 0°) and temperature for site A for 21 July to 30 August 1992. Water depth 400 m. Figures supplied by Steedman Science and Engineering.*

(b) for the current meter 175 m below the surface.

Fig 3.5   Time series plots of current meter speed, direction (north = 0°) and temperature for site A for 21 July to 30 August 1992. Water depth 400 m. Figures supplied by Steedman Science and Engineering.

(c) for the current meter 200 m below the surface.

Fig 3.5 Time series plots of current meter speed, direction (north = 0°) and temperature for site A for 21 July to 30 August 1992. Water depth 400 m. Figures supplied by Steedman Science and Engineering.

(d) for the current meter 350 m below the surface.

3.6 Currents and Temperatures Observed during the DSTO Survey at Site A

Current meters were deployed at site A from 1130 hours 21 July 1992 to 1050 hours 30 August 1992 (Western Australian time), at depths of 125, 175, 200, and 350 m below the surface in 400 m water depth. Data are available as 10 minute averages. Time series plots of current meter speed, direction and temperature are shown in Fig. 3.5, and Figure 3.6 shows the associated current roses.

Currents from 125 to 200 m below the surface flowed southward for much of the deployment, overlying a northward flowing counter current at the current meter 350 m below the surface, which measured a maximum northward speed of 27 cm.s^{-1} (half a knot). The maximum speed recorded by the array was about 60 cm.s^{-1} at 125 m below the surface, with maxima of 40, 44, and 27 cm.s^{-1} at 175, 200, and 350 m below the surface. Set and drift from GPS navigation indicated a surface speed of 1.6 knots (about 82 cm.s^{-1}) at the start of the current meter record, with variable direction to between 135 and 188 degrees south. Current meter speeds at 125, 175, and 200 m below the surface were about 50, 37, and 30 cm.s^{-1} at that time, flowing to 182, 190, and 200 degrees respectively, indicating a current turning with depth to align with the bathymetry.

Percentage exceedence histogrammes for the current meter speeds at site A are shown in Fig 3.7, for ten minute averages, and speed increments of 2 cm.s^{-1}. Exceedence curves for hourly averages and 10 cm.s^{-1} bins for site A and site D are shown in Figs 3.8 and 3.9. Note that Fig 3.8 plots the log of speed versus percent probability of exceedence, and Fig 3.9 plots speed. Wave heights for example often show a log-normal distribution when plotted as in Fig 3.8 i.e. log(height) vs percent probability of exceedence. The type of distribution for current speeds at the sites is unknown, and so the two types of plots were made. The distribution of Fig 3.9 i.e. linear speed vs percent probability appeared to give more realistic (lower) values for 10 year return currents than log(speed) vs percent probability, and this is the only reason for it being preferred over the other distribution. The distribution of Fig 3.8 indicated ten year expected maxima for the currents at 125, 175, 200, and 350 m below the surface at site A of 95, 65, 65, and 35 cm.s^{-1}, respectively. The ten year return speed for the hourly averaged speed is the hourly averaged speed expected to be exceeded only once in 10 years, which equates to a probability of 0.001% exceedence in 10 years. Similar curves constructed for the LUCIE data (not shown) indicated a ten year surface maximum current of 3 knots. This figure is likely to be an underestimate for reasons described next.

At the Dongara site the short term currents measured by DSTO are consistently higher than the LUCIE currents measured at the same column depth or shallower over September 1986, but the trends for both sets of exceedence data are similar (Fig 3.9). While somewhat tenuous, the similar distributions for the DSTO and LUCIE data at the same location indicate that the longer term CSIRO data can be used to indicate return speeds for depths not sampled by DSTO at Dongara, but that such estimates

must be adjusted upwards. The shallowest DSTO current meter was 125 m below the surface, whereas upper CSIRO current meters were close to the surface.

Comparison of site A current meter data to 250 m below the surface in 400 m water depth were made with LUCIE data 250 m below the surface at the Capes in 700 m water depth. The DSTO and CSIRO distributions were similar for the CSIRO period 01 July to 08 August 1987, and DSTO currents were higher by 10cm.s^{-1} than for the CSIRO period 18-30 September 1986.

Temperatures for 125 to 200 m below the surface were usually within one degree C of each other, but dropped by 5 to 7°C in going from 200 to 350 m depth below the surface. Similar behaviour is seen in average temperature profiles for the area 32 to 33°S, 114 to 115°E for this season (Table 4.1). In summer a drop of 3 to 4°C may also be seen in going from 125 to 200 m below the surface.
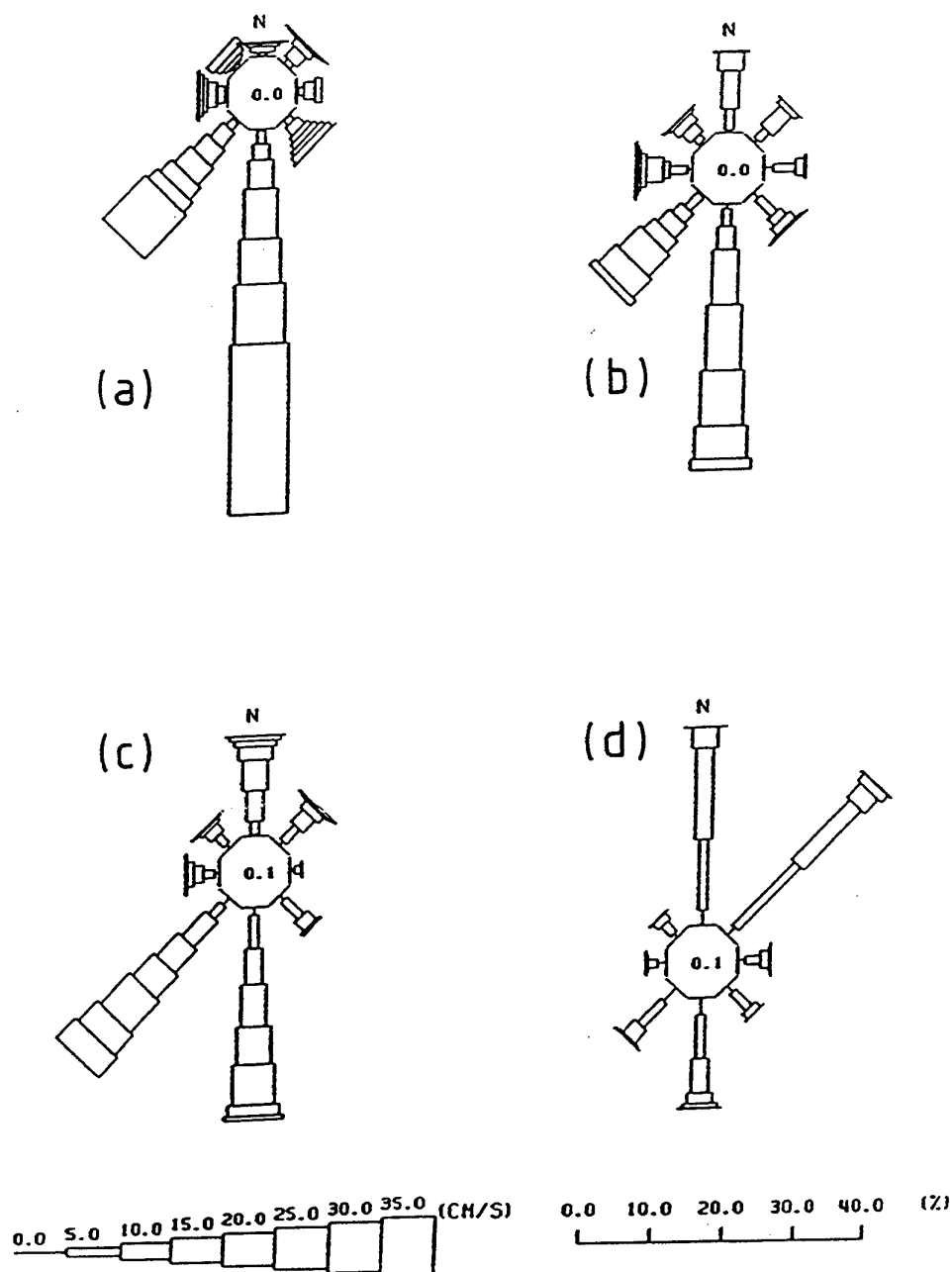
Fig 3.6 Current roses for the four current meters at site A for 21 July to 30 August 1992.
Water depth 400 m. Figures supplied by Steedman Science and Engineering.

(a) for the current meter 125 m below the surface.
(b) for the current meter 175 m below the surface.
(c) for the current meter 200 m below the surface.
(d) for the current meter 350 m below the surface.

STEEDMAN SCIENCE & ENGINEERING
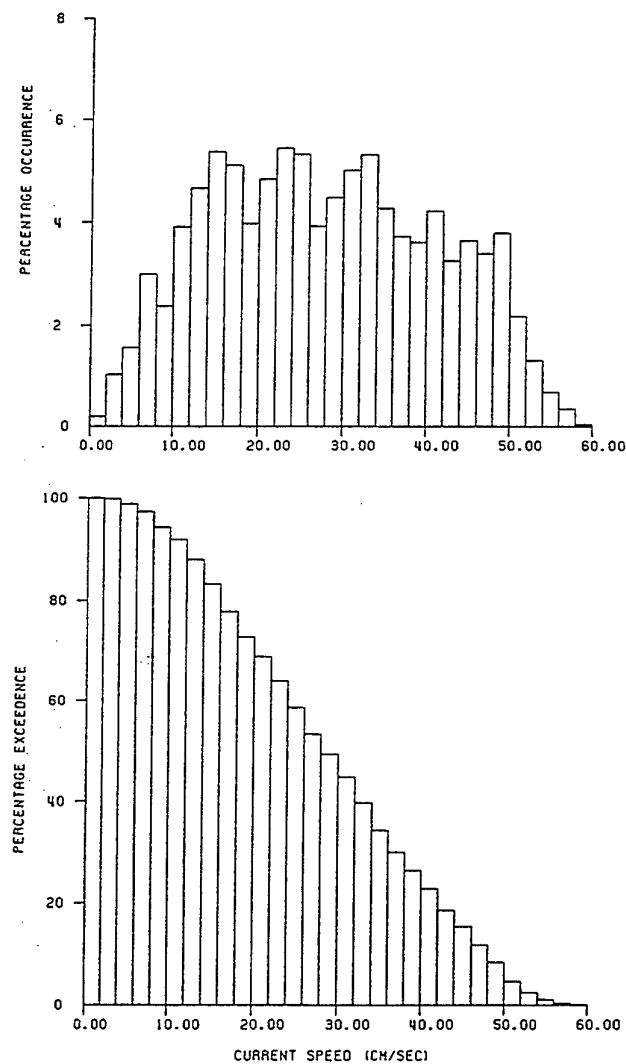
LOCATION A - CURRENT SPEED AT 275 M ASB

Fig 3.7 *Histogrammes of percentage occurrence and percentage exceedence of 10 minute current speed averages at site A for 21 July to 30 August 1992. Water depth 400 m. Figures supplied by Steedman Science and Engineering.*

(a) *for the current meter 125 m below the surface.*

STEEDMAN SCIENCE & ENGINEERING
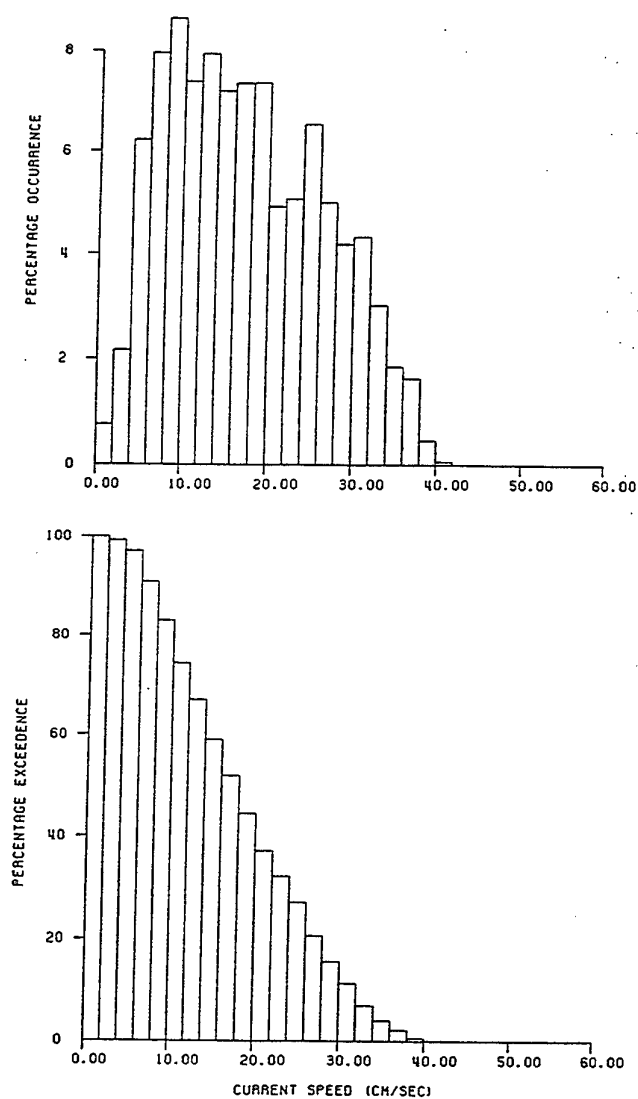
LOCATION A - CURRENT SPEED AT 225 M ASB

Fig 3.7 *Histogrammes of percentage occurrence and percentage exceedence of 10 minute current speed averages at site A for 21 July to 30 August 1992. Water depth 400 m. Figures supplied by Steedman Science and Engineering.*

(b) for the current meter 175 m below the surface.

30

STEEDMAN SCIENCE & ENGINEERING
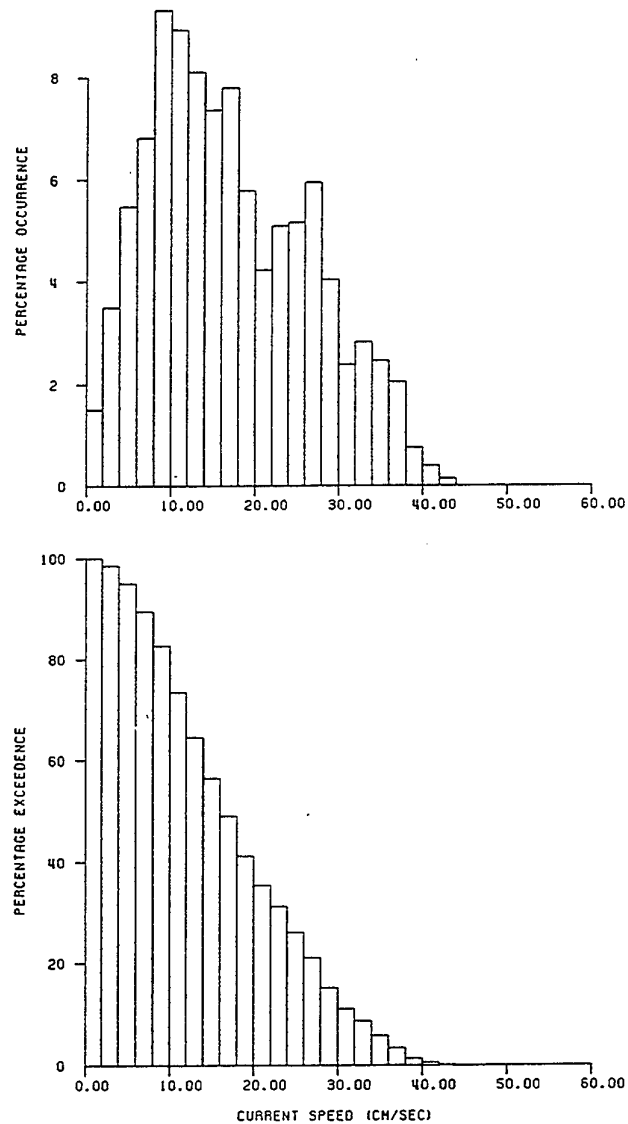
LOCATION A - CURRENT SPEED AT 200 M ASB

Fig 3.7 Histogrammes of percentage occurrence and percentage exceedence of 10 minute current speed averages at site A for 21 July to 30 August 1992. Water depth 400 m. Figures supplied by Steedman Science and Engineering.

(c) for the current meter 200 m below the surface.

STEEDMAN SCIENCE & ENGINEERING
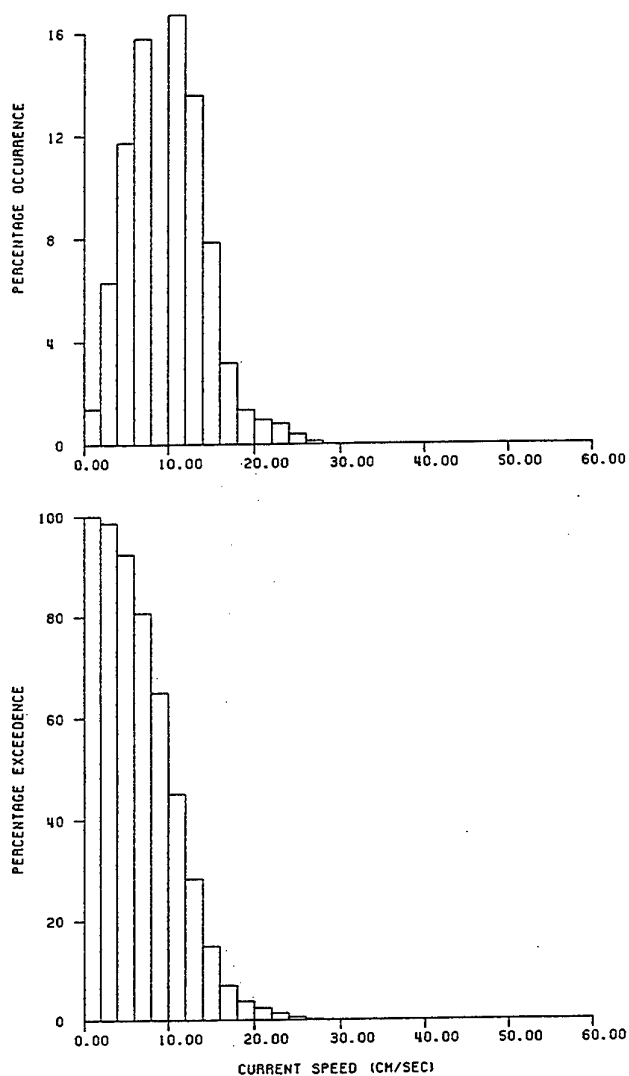
LOCATION A - CURRENT SPEED AT 50 M ASB

Fig 3.7 *Histogrammes of percentage occurrence and percentage exceedence of 10 minute current speed averages at site A for 21 July to 30 August 1992. Water depth 400 m. Figures supplied by Steedman Science and Engineering.*

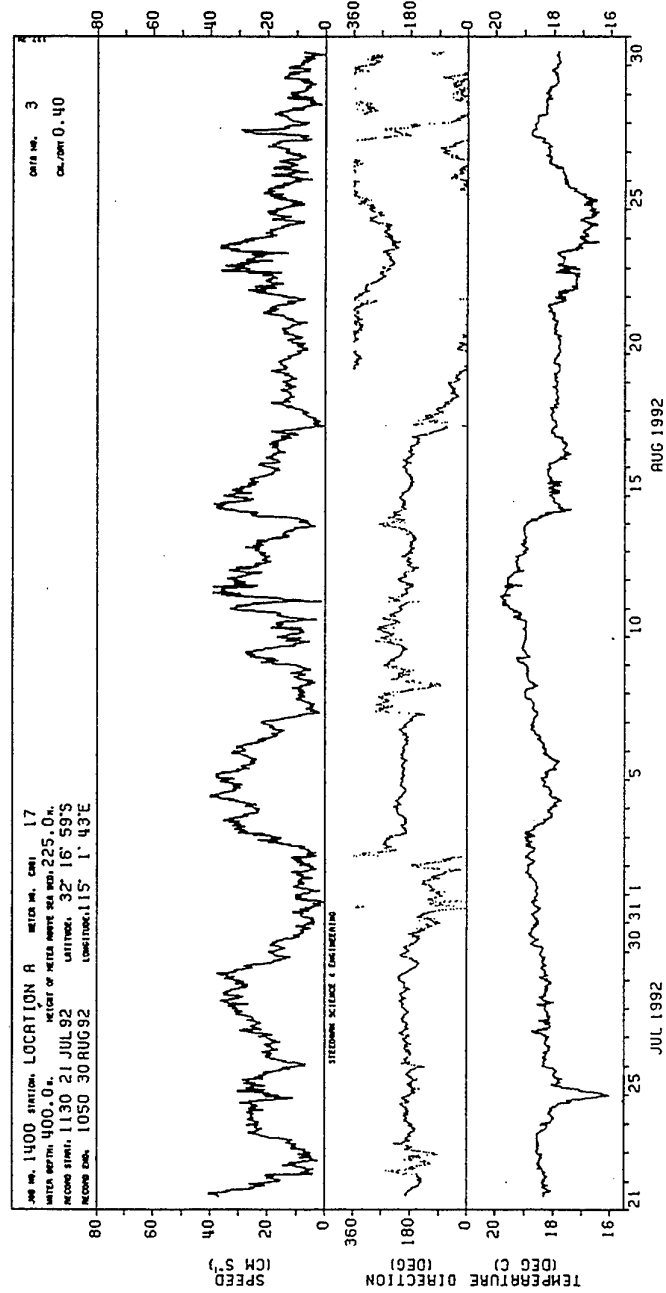*(d) for the current meter 350 m below the surface.*
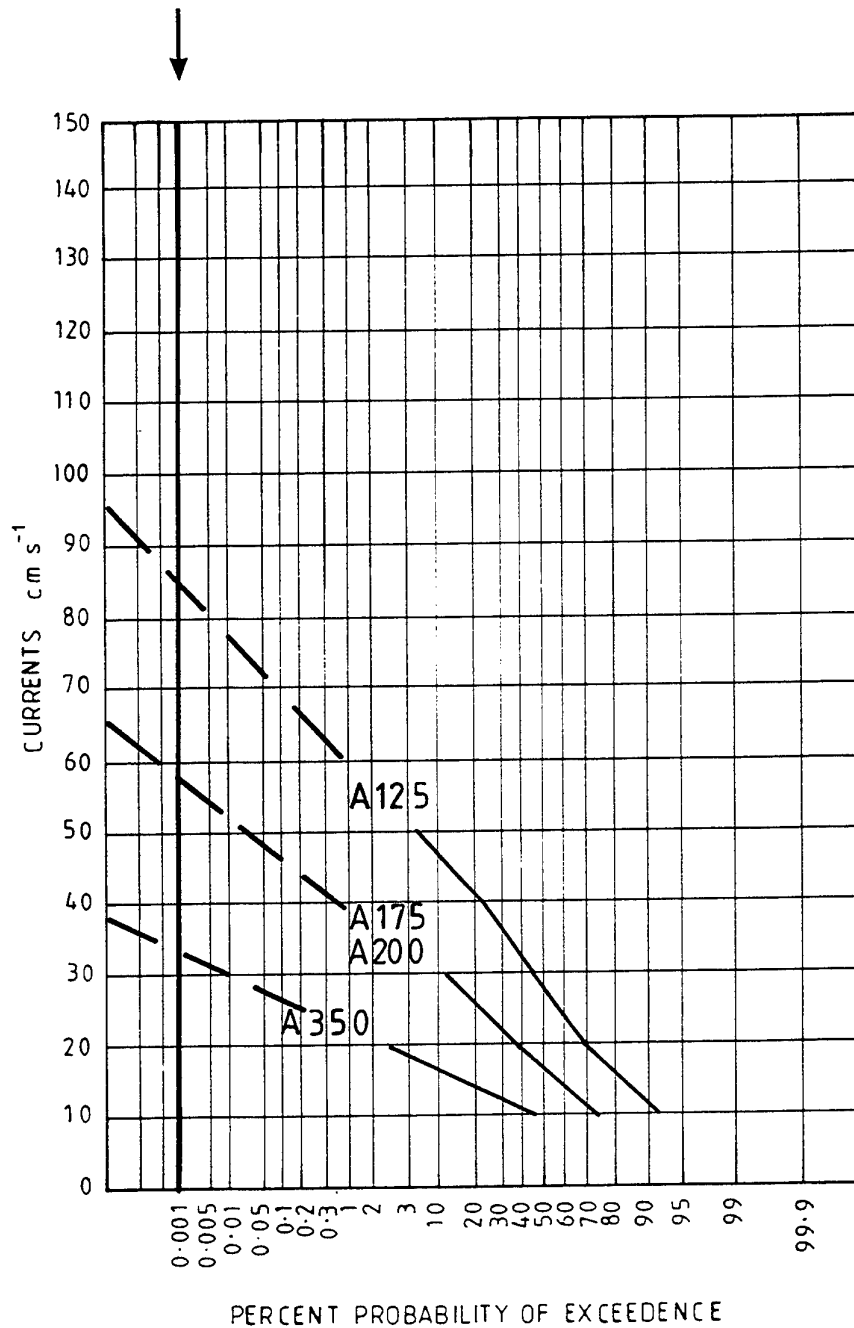
Fig 3.8   Exceedence curves for hourly current meter speeds at site A in 10 cm.s^{-1} bins, as log (speed) vs percent probability of exceedence. A straight line plot indicates a lognormal type distribution. The arrow shows ten-year return probability. Numerals with the curves indicate depth below the surface.
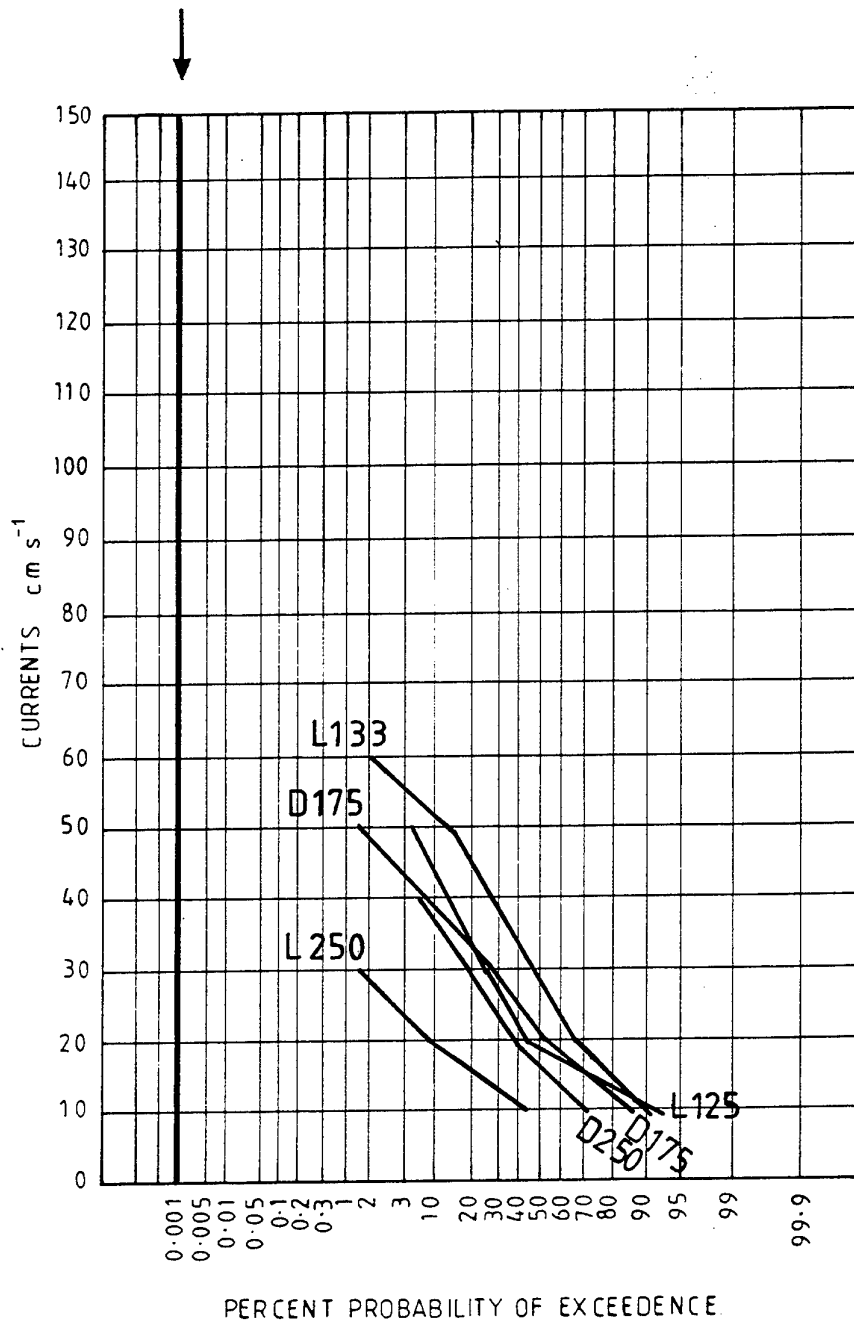
Fig 3.9 Exceedence curves for hourly current meter speeds at site D in 10 cm.s^{-1} bins, as linear speed vs percent probability of exceedence. The arrow shows ten-year return probability. Numerals with the curves indicate depth below the surface. D = DSTO data for July to August 1992. L = LUCIE data for September 1986 to February 1987, supplied by CSIRO Marine Laboratories, Hobart.

3.6.1 Variability of Currents at Site A

The variability of current speeds within an hour (gustiness) was determined using standard deviations, and the range in the maximum speed difference of the 10 minute samples within an hour (the difference between the minimum and maximum speeds in any hour). Gustiness can introduce sudden changes in tensions and stresses including torsions on ocean structures, as well as causing distortions of shape. Gustiness is essentially an estimate of the steadiness (or non-steadiness) of the current. Little to no trend with increasing speed was observed in the standard deviation of the currents in any hour for any current meter (Fig. 3.10). The average standard deviations within an hour were almost the same for each current meter, being 1 cm.s^{-1}. Plotting the difference between the minimum and maximum speeds in an hour versus the average hourly speed showed a few differences of 12 to 18 cm.s^{-1} (4 in 5757), but most differences were than 8 cm.s^{-1}. Ranges for the current meters 200 and 350 m below the surface were all less than 12 cm.s^{-1}, with maximum hourly average speed for these current meters of 42 cm.s^{-1} and 25 cm.s^{-1} respectively. The current speeds in any one hour therefore tended to be constant.

For 21 July to 18 August currents from 125 to 175 m below the surface were southward and generally decreased with depth, but the currents at 175 m below the surface were sporadically higher than those at 125 m below the surface by up to almost 20 cm.s^{-1}. This was accompanied by a decrease in the 125 m current to near zero, and a swing in the currents from south to north in an anti-clockwise direction, over about 5 and a half days (see Fig 3.5). The strongest northward current at 125 m below the surface was about 37 cm.s^{-1}. Currents at 175 and 200 m below the surface were very close in strength during the deployment, but the 200 m speeds were often slightly higher than at 175 m.

On 18 August the flow at 125 m below the surface swung anti-clockwise from south to north-east, then swung a full circle clockwise from north-east to east from 19 to 26 August. A peak speed of almost 40 cm.s^{-1} then dropped to zero in about half a day and a southward current resumed which reached over 35 cm.s^{-1} in about 14 hours. The current directions at 175 and 200 m below the surface swung anti-clockwise from south to north (rather than to north-east as for the current at 125 m below the surface), then continued northward for two and a half days before swinging clockwise to be the same as those at 125 m below the surface. This behaviour could be explained by various eddy translations. From 28 to 31 August directions at 175 and 200 m below the surface were northward when directions at 125 m below the surface were southward.

On 0720 hours 11 August, the current speed at 125 m below the surface rose from zero to a peak deployment speed of 58.5 cm.s^{-1} in 8 hours. Similar behaviour was seen at 175 m below the surface, with a speed increase of 37 cm.s^{-1} in 5 hours, but at 200 m below the surface, speeds remained near constant at 30 cm.s^{-1}. About one day before this occurrence, the bottom undercurrent began reversing to the south.

The current flow at 350 m below the surface was northward from 21 July to 10 August but then changed, with southward flow at all depths from 10 to 16 August. Southward flow at all depths also occurred from 20-25 August and 28-31 August. After the first occurrence of southward flow throughout the column, the flow at 350 m below the surface tended to be in the same direction as the current meter at 125 m below the surface, with only one occurrence (over 27 to 28 August) of a northward bottom current and a coincident southward current at 125 m below the surface.

3.6.2 Vertical Shear at Site A

A rough measure of the vertical shear was obtained by plotting current meter speeds through the column against each other, and estimating a linear fit of the form: Speed at current meter 1 = m * Speed at current meter 2. North-south components and east-west components were also analysed. Graphical results are shown in Fig. 3.11 to 3.13 and Tables 3.1 to 3.3 (page 39) show the regression coefficients. The east-west components tended to have more directional correlation than the north-south components.

The DSTO survey has no current meter data from the surface to 125 m below the surface. Linear regression coefficients, correlation coefficients, and scatter plots formed in the present analysis from the LUCIE current meter speeds indicated reasonable linear relations between speeds from 50 to 125 m below the surface. These data are not shown, but indicated that simple estimates of average vertical shear could also be got from the LUCIE data.
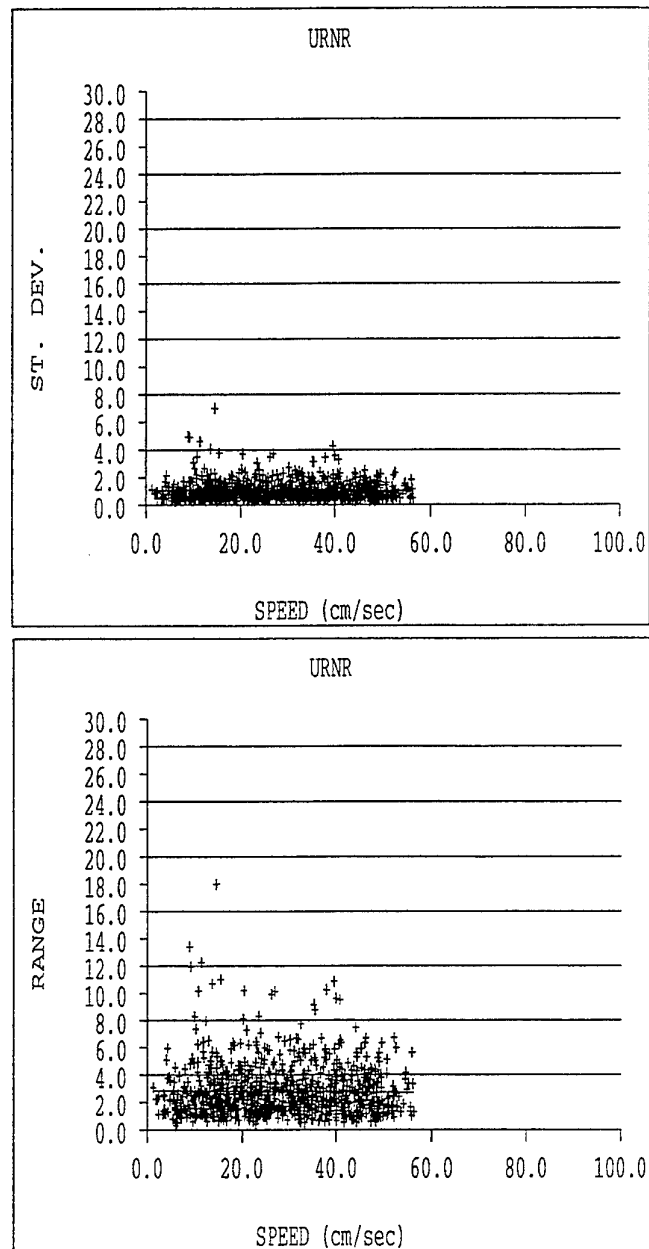
Fig 3.10 Current variability within an hour as a function of average hourly speed at site A.

(a)   standard deviation of 10 minute averaged speeds within an hour vs average hourly speed for the current meter 125 m below the surface.

(b)   maximum difference between any two 10 minute averaged speeds within an hour vs average hourly speed for the current meter 125 m below the surface.
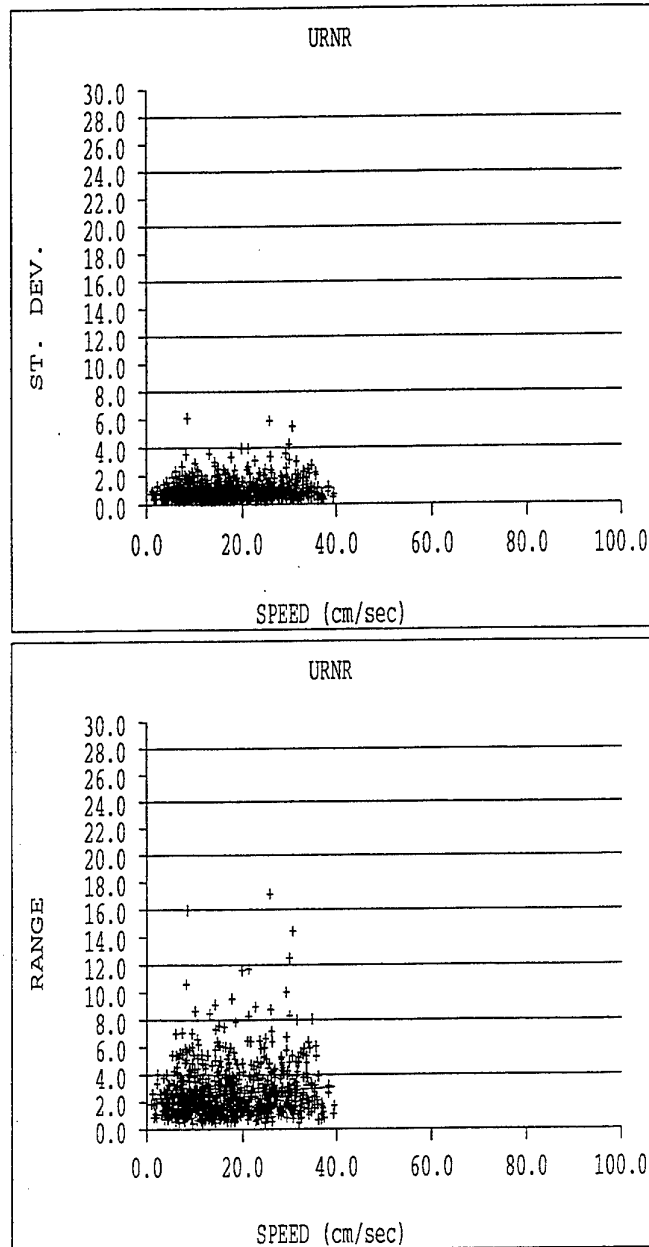
Fig 3.10 Current variability within an hour as a function of average hourly speed at site A.

    (c)   standard deviation of 10 minute averaged speeds within an hour vs average hourly speed for the current meter 175 m below the surface.

    (d)   maximum difference between any two 10 minute averaged speeds within an hour vs average hourly speed for the current meter 175 m below the surface.

Table 3.1 Linear regression coefficients for current meter speeds at site A. E.G. Speed at current meter 1 (at depth 200 m below the surface) = 0.94 * Speed at current meter 2 175 m below the surface.

| | | Depth of current meter 2 (m) | | | |
		125	175	200	350
Depth of	125	1			
current	175	0.58	1		
meter 1	200	0.56	0.94	1	
(m)	350				1

Table 3.2 Linear regression coefficients for north-south component of current meter speeds at site A

| | | Depth of current meter 2 (m) | | | |
		125	175	200	350
Depth of	125	1			
current	175	0.49	1		
meter 1	200	0.55	0.099	1	
(m)	350				1

Table 3.3 Linear regression coefficients for east-west component of current meter speeds at site A　﹅

| | | Depth of current meter 2 (m) | | | |
		125	175	200	350
Depth of	125	1			
current	175	0.56	1		
meter 1	200	0.55	0.36	1	
(m)	350				1

```
          .+....+....+....+....+....+....+....+....+....+....+.
   50.00++                                                    +
        ..                                                    .
        ..                                                    .
        ..                                                    .
        ..                                                    .
   45.00++                                                    +
        ..                                                    .
        ..                                                    .
        ..                                                    .
        ..                                                    .
   40.00++                                    1152            +
        ..                                  1 11234           .
        ..                                 11341 322          .
        ..                                 7849464421         .
        ..         16  2              1 75329D3 23            .
   35.00++     1 11   22    1      11  63538732421            +
        ..     11423                 21347537865451           .
        ..     1 132 1     141  1 433445A84BB231              .
        ..     11 12           65 12223ED9696A74              .
        ..     1 13512 1   24524248D96E5ED22141               .
   30.00++     223312 1   11575579A7F89228632111              +
        ..     13 1 211   11 6887119BA9787332                 .
        ..     2212 121   3546B5666BG5649B4211                .
        ..     1361 12232 415A521379B77BI742                  .
        ..     14313111 11 46A5434B9AAAFN97831                .
   25.00++     421 1 3226 13639552CHDALGTH323                 +
        ..      23423  761 514565945A7B89J763 3               .
        ..      1521412 29443353584339GAHDC4831               .
        ..     2 1132221 6D78361557C343652346 1               .
        ..      51252624 1164E46758C5795337421                .
   20.00++ 115636547254342C568A7A4A664414    1                +
        ..12288 D56H42436686AAIGC99A7512 1                    .
        .1211562CCFB9157249B67QOQAFA77434   12                .
        ..1255 8515B421141B566NEMC7C95 211                    .
        .. 1325ABCCCA31643B76BG98BC74511                      .
   15.00++ 225AEE6AAA61364CB7CD576G31212                      +
        .1155FHFB65HSD946FA42A74558321                        .
        .2244LH5D7CIGE69GB8577883 721                         .
        ..1467DE9LBTCB679BN414664451                          .
        .. 69F567EFBEB8EMDE46624222222                        .
   10.00++ 655836697F96CCRA9286313  1222                      +
        ..1568733A78NOBDHDJFE94912324323                      .
        ..45243227CDTVGMGZJAEA63665832                        .
        ..  2262DC6F5HFNOBBF2DA72511                          .
        .. 1232989777DJB4H5H33A681                            .
    5.00++  21 6EA57BIHDAHB9A47756                            +
        ..    4656896I9E7687856422                            .
        ..    1453652343431212221                             .
        ..     341221132 3431 2                               .
        ..      11  221  192                                  .
    0.00+1....+....+...1+...1+..1.+....+....+....+....+....++
         .+....+....+....+....+....+....+....+....+....+....+.
       0.00    15.00    30.00    45.00    60.00    75.00
           7.50     22.50    37.50    52.50    67.50
```

Fig 3.11 Scatter plots of current meter speeds at site A vs the speed at a current meter higher in the water column. Numerals and letters indicate number of counts in a bin with 1 ... 9, A=10, B=11, ... Z=26. Units are $cm.s^{-1}$.

(a) speed at 175 m below the surface vs speed at 125 m below the surface.

```
      .+....+...+....+....+....+....+....+....+....+....+.
  50.00++                                                    +
   ..                                                        .
   ..                                                        .
   ..                                                        .
   ..                                                        .
   ..                                                        .
  45.00++                                                    +
   ..                  1                                     .
   ..                              1                         .
   ..               2 11          31 1  1                   .
   ..               1 1            2 1 21                    .
  40.00++              11          12141223                  +
   ..                  1             213 1636 1 1            .
   .. .                1             1254 61116312           .
   ..                  1            11136556659A231          .
   ..                2   11         12985773462             .
  35.00++          11      2   2  3 466B9933572             +
   ..                  1 21242 1 3574HE7631                 .
   ..                22   123252 13334185834482232          .
   ..                14    2 2433  5444454334112113         .
   ..                14 11336411143437473 2211 2            .
  30.00++           111 11312385556924812114152             +
   ..                1 3532   1197B767A87A783343441         .
   ..                12131 221119F69BFE8F857441             .
   ..                  11   75516EC7AALA87478434            .
   ..              1  21   549642AQH5EB8658A21812           .
  25.00++           2 132 2265A9479DELF83315141 1           +
   ..                1 2414669B648B89KA65114  2             .
   ..              13 2611444B47AB6D7LC9B43212              .
   .. 1             11221492775796DC68CA412221 1            .
   ..               42313261373953475B51124253             .
  20.00++          1464443A5997EA98612451442313             +
   ..             4697656989787FHA9 222421425               .
   .. 1 312AA877GJHH84FB5723211232222     1                .
   .. 17BE7B73CGVXD8EB443373341131412       1              .
   .. 2543862AIBGA45B6A679665744741                        .
  15.00++   2158C67PEB97CB977744IG552321                    +
   .. 11 45999F6CB7DGIKE3876DE551 1 1                       .
   ..1142228BD6QH6D7CFOC75266C642    1                     .
   .. 11358CGBLJF7BHBEG585 44524 1   11 1                  .
   .. 115A5DOYFJFGF7Q9B9B2113  32      1                   .
  10.00++ 246BHOXMNQ7HCAC6DJ632  2  21  1                   +
   ..  167GRZLJFAGJCD787211   13  32 1  1                  .
   ..  5CHLNPP7BJBF7CBC611 1  11121  1                     .
   .. 2BFQEICB78963A84B53    11211    11                   .
   ..158TFK7FC78464948652    211 1 11                      .
   5.00+1563CLDBLH8784354  123 111   1                      +
   ..843BKC9F76534251  332  2 1      1                      .
   ..2449H16986544333 12222 2  11      3                    .
   .113357657473 31 1 2 21   3 1                            .
   .1 14A327142  12    2      3                             .
   0.00+1...3221221....+....+....+....+....+....+....+....++
      .+....+....+....+....+....+....+....+....+....+....+.
     0.00    10.00    20.00    30.00    40.00    50.00
        5.00    15.00    25.00    35.00    45.00
```

Fig 3.11 Scatter plots of current meter speeds at site A vs the speed at a current meter higher in the water column. Numerals and letters indicate number of counts in a bin with 1 ... 9, A=10, B=11, ... Z=26. Units are $cm.s^{-1}$.

(b) speed at 200 m below the surface vs speed at 175 m below the surface.

```
        .+....+....+....+....+....+....+....+....+....+....+.
50.00++                                                      +
   ..
   ..
   ..
   ..
 . ..
45.00++                                                      +
   ..                              1
  . ..                            1
   ..          1            71              1                .
   ..          1            31             12                .
40.00++          3            15          12 51               +
   ..                        1   11 22374 22                 .
   ..          2            22 111 21343 173 1               .
   ..         23            2312111 6254585653               .
   ..     2    5           3 33 2411457324243                .
35.00++   1    151        11    23411949E5353 1               +
   ..         42   111  1  1    1 249885524C423              .
   .. 3   351 21    31  1     1157352C2854 71                .
   .. 23 21121     51 11  1 323115294463121                  .
   .. 211112234    21 3  2   422  649527 111                 .
30.00++ 21    32263 11312 1 2   522167A54162 1                +
   . .111   414    61 2115 12622  49B995CB855411             .
   .11  1 11113412241 1 4421 33AI9H58HC512                   .
   .1 1 3   1    1 112 44415B4374HIC36HB6214                 .
   ..131323532 1121422346A6A322FB8BCF92 111                  .
25.00++34 52 841313 53 2344775645B76B4F71       1             +
   .12136216112516242222147638726648995                     .
   .. 531214   13137521357ACBAAB8C665311                     .
   .. 262 43 5532341228874AA6A99462 1                        .
   .. 232   2 B6621112 274384479524   111 1                  .
20.00++ 227 2 13DA3127353336697B984511 5   1                  +
   ..    A32189B722B86932158B4EB53232 1 2                    .
   .. 69D887494249D6HE615663875112 142                       .
   .. 17DCF37CDDC64CIEEB54336F4 14421221                     .
   ..13177317HC74658DD988847743 116 D21                      .
15.00++2218B678I856368D9468853867 642AG312                    +
   .. 3 37556E37B56JAKD974AE447738225B322                    .
   .. 1 5454E6CGA6EAEB1447GB45986231955 1                    .
   ..   145E7BB7BBCGECF3E22343A66B42 4121                    .
   ..1423546FBFACJFGGB6BHD25386514821  2                     .
10.00++144383E9GJA57NS*ABB8I552552 11     2                   +
   .. 15248EBGECB8FHNO99E74862 1611    1                     .
   .. 12696CJFAIGAH97S5C2HA4321 242                          .
   .. 11221CN88EEA76848BDAA33321  33                         .
   ..    123886DI99323BCEAJG45112  11                        .
 5.00++  1 23689H8953237CCABC7732                             +
   .. 131 1556B3H562469A638A5                                .
   ..   2 32644C88446817C364                                 .
   ..   1 1 315 134555463982                                 .
   ..       364 12223615611                                  .
 0.00+1....+....+2..21.1.1+231.+....+....+....+....+....++
    .+....+....+....+....+....+....+....+....+....+....+.
    0.00     15.00     30.00     45.00     60.00     75.00
        7.50     22.50     37.50     52.50     67.50
```
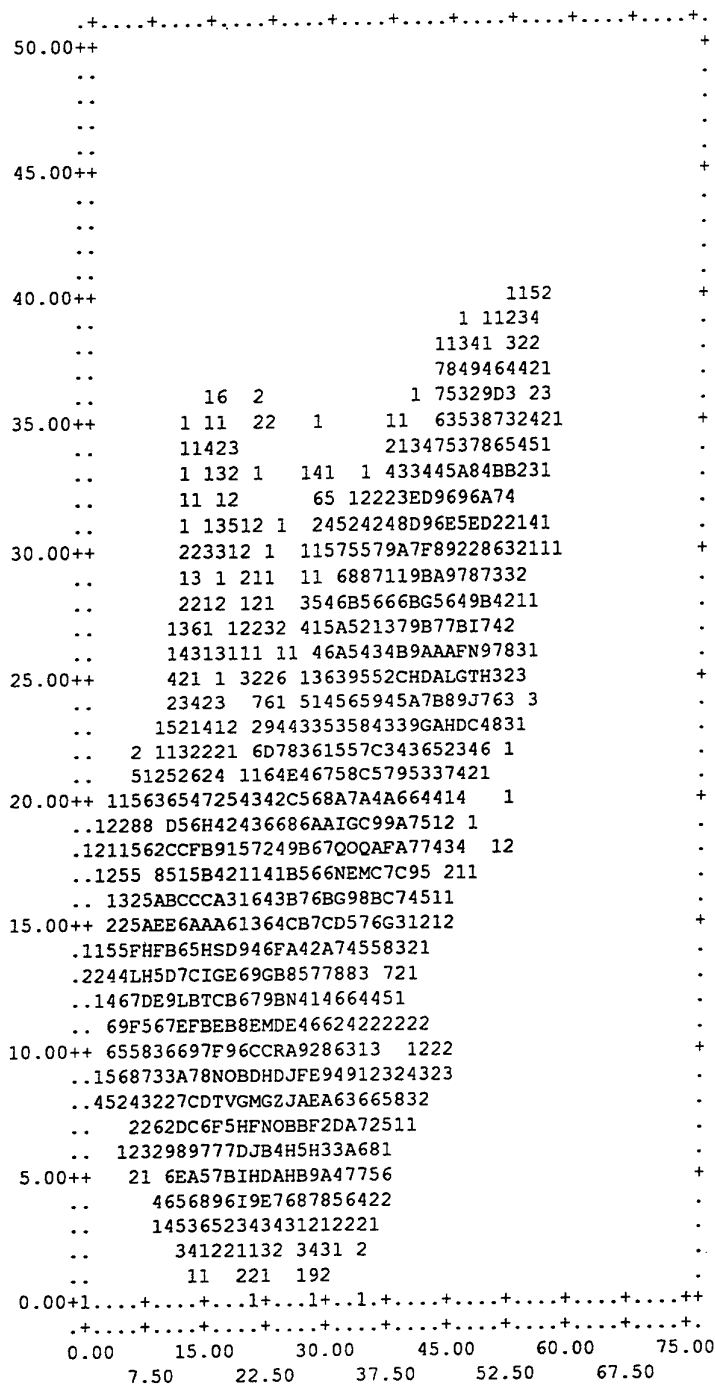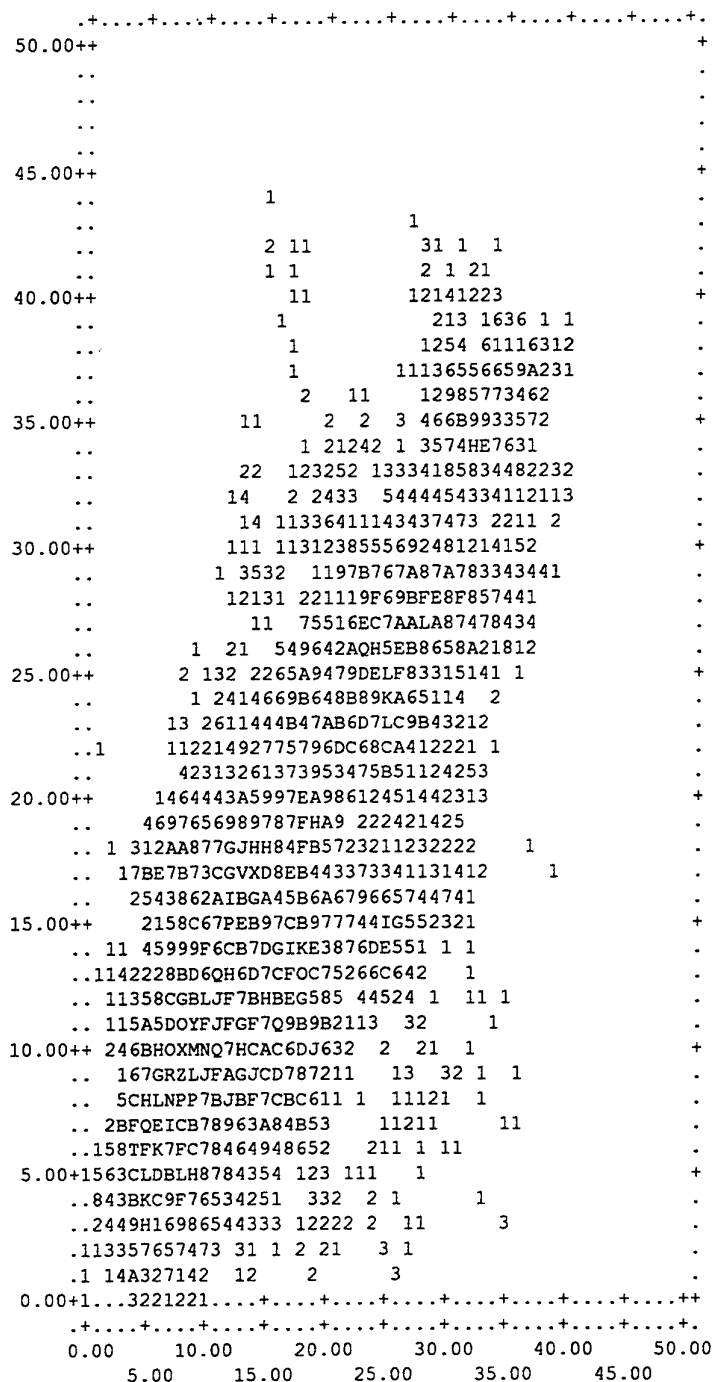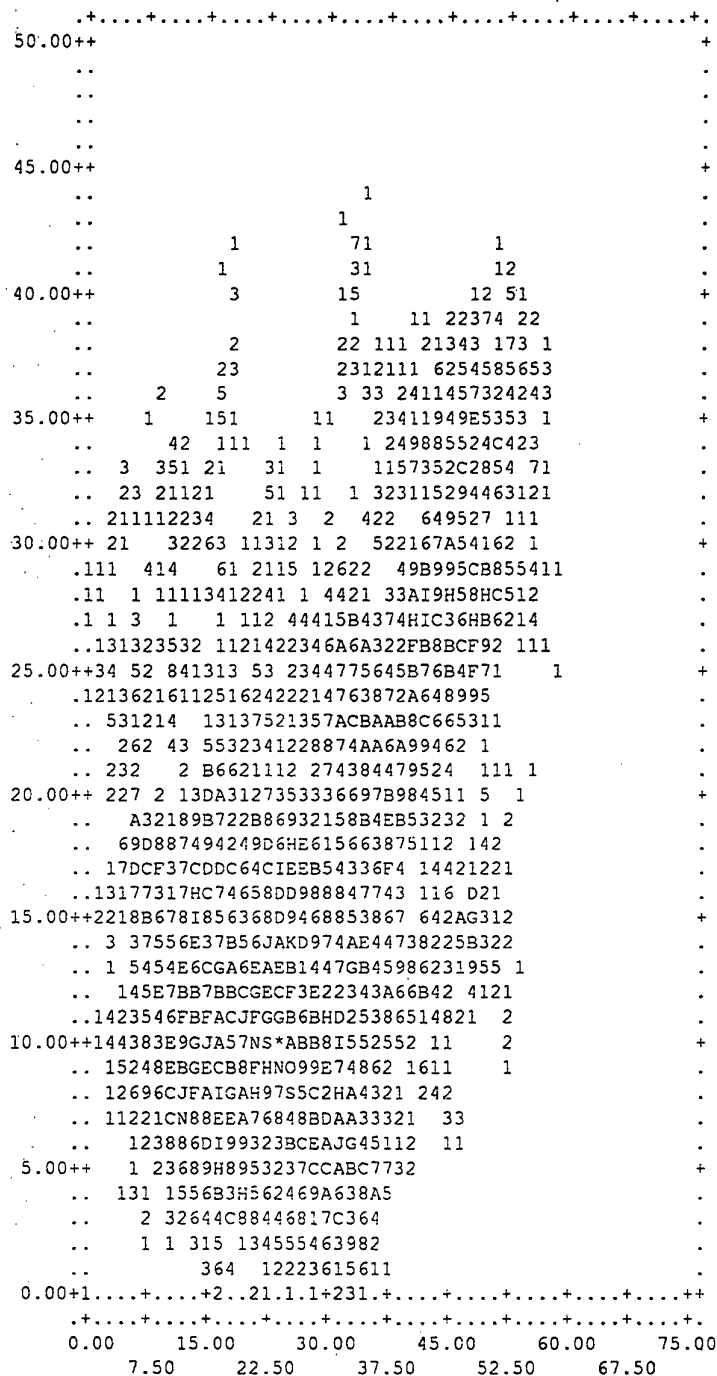
Fig 3.11 Scatter plots of current meter speeds at site A vs the speed at a current meter higher in the water column. Numerals and letters indicate number of counts in a bin with 1 ... 9, A=10, B=11, ... Z=26. Units are cm.s^{-1}.

(c) speed at 200 m below the surface vs speed at 125 m below the surface.

```
        +....+....+....+....+....+...:+....+....+....+....+....+.
        .                        .                    .
        .                        .                    .
        .                        .                    .
 30.00+                          . +2                 +
        .                        .                    .
        .                        .8                   .
        .                        .31                  .
        .                        231     1            .
 22.50+                          1261    51           +
        .                    ·  2631    23            .
        .                        113    5       2     .
        .                        1113   41 1    21    .
        .                    · 13 2   24 221 22 2     .
 15.00+                        2331   B 72 1 433      +
        .                1       43152313331 252      .
        .               41    112113322  57 1 11      .
        · .          2 26      13.22 23 288 213       .
        .            22  44   ·48.42 2 48E6512        .
  7.50+            455191    155421  112DC411         +
        .          5938A    128334432 12B341          .
        .        11864922   1385.  1 2164332          .
        .      1  6A 8321 32162.    172 122           .
        .     1 112725A41158425 .1 3367 133           .
  0.00+....+....+.1..2832E421347311.1.44623.2.1....+....++
        .        . 41272639827697432 .2355 3 22       .
        .        1  7A6263446684892.41H7946           .
        .        1287AB86832343639A1317BJG22          .
        .        263889A553994495CF434.AFAB2 1        .
 -7.50+        13A1J7597763497447J71E55MIBA           +
        .      1AF9C4B5C96B663A1DMACE5O865611          .
        .      325GFH9MEJH74937H6IG53EGF2628           .
        .      15AJOF*ERWJ736D5KD8776BIA35A731         .
        .      195RGKBDMVI7C6BJM7876BE8444641          .
-15.00+     3568MFSXUFL*LG4DOQD85576D472A41           +
        . 7156FHRNMBBKVG83KFH57A937H42141             .
        . 1988C7AXASGNA78AAKOHOH6DBD1 1               .
        . 13B7HRVFCZN3957DGIK8MEA6BZ 1.               .
        . 13975ZOPJRG2 7E8TTCCG41C9F 1.               .
-22.50+ 1275NRI7EGD  CJBUFAC511I352 +                 +
        . 456BHA1B9252GFDI4553651436 .                .
        .  56G3135B31939EG2632158212 .                .
        . 11 561552 7558A1254 414531  .               .
        . 2221 41147548C42  121322  · .               .
-30.00+   1 721335694855  23225   .+                  +
        .  2    45BC4B662211221 1   ·.                .
        .  1   27336897  2521       .                 .
        .  2  142114A73 442        · .                .
        .  2 42   25 1 1            .                 .
-37.50+  1 1      31                +                 +
        .  21                       .                 .
        .                           .                 .
        +....+....+....+....+....+...·.+....+....+....+....+.
     -60.00   -40.00   -20.00    0.00    20.00   40.00
         -50.00   -30.00   -10.00   10.00    30.00
```
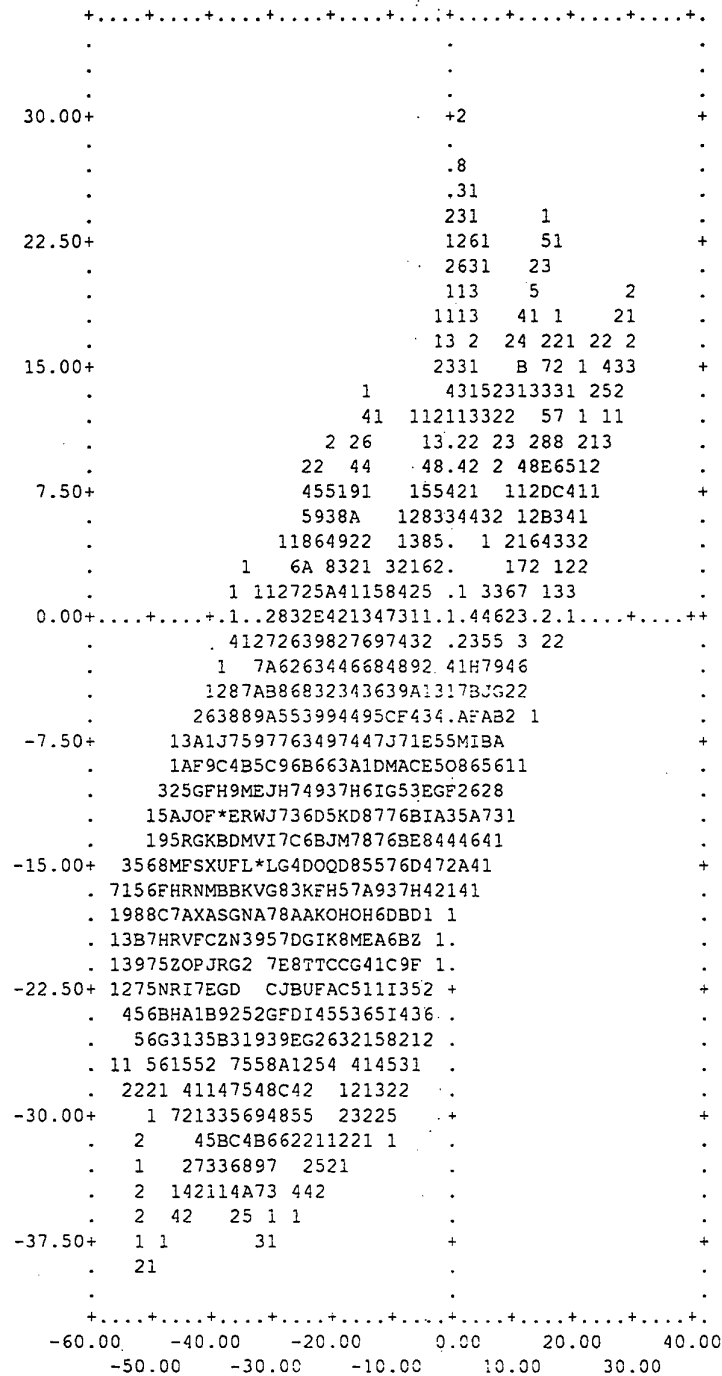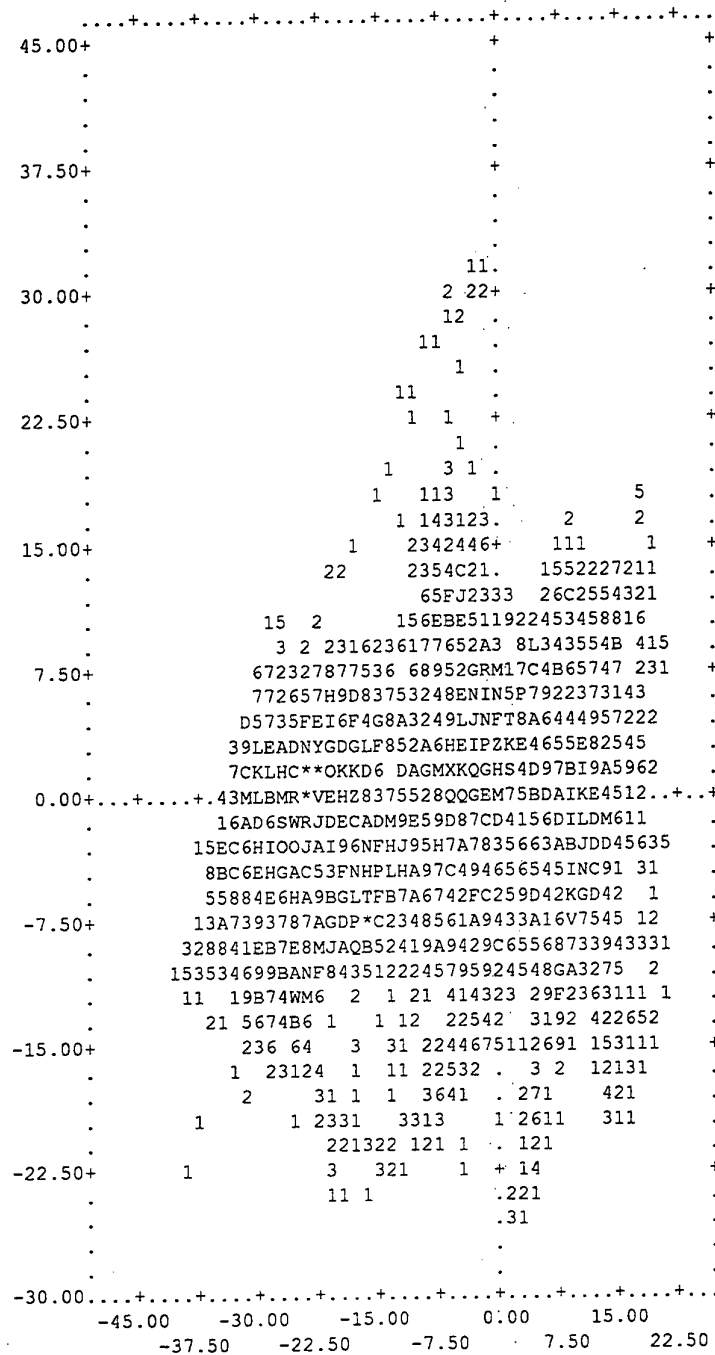
Fig 3.12 Scatter plots of north-south current meter speed components at site A vs the north-south speed components at a current meter higher in the water column. Units are cm.s^{-1}.
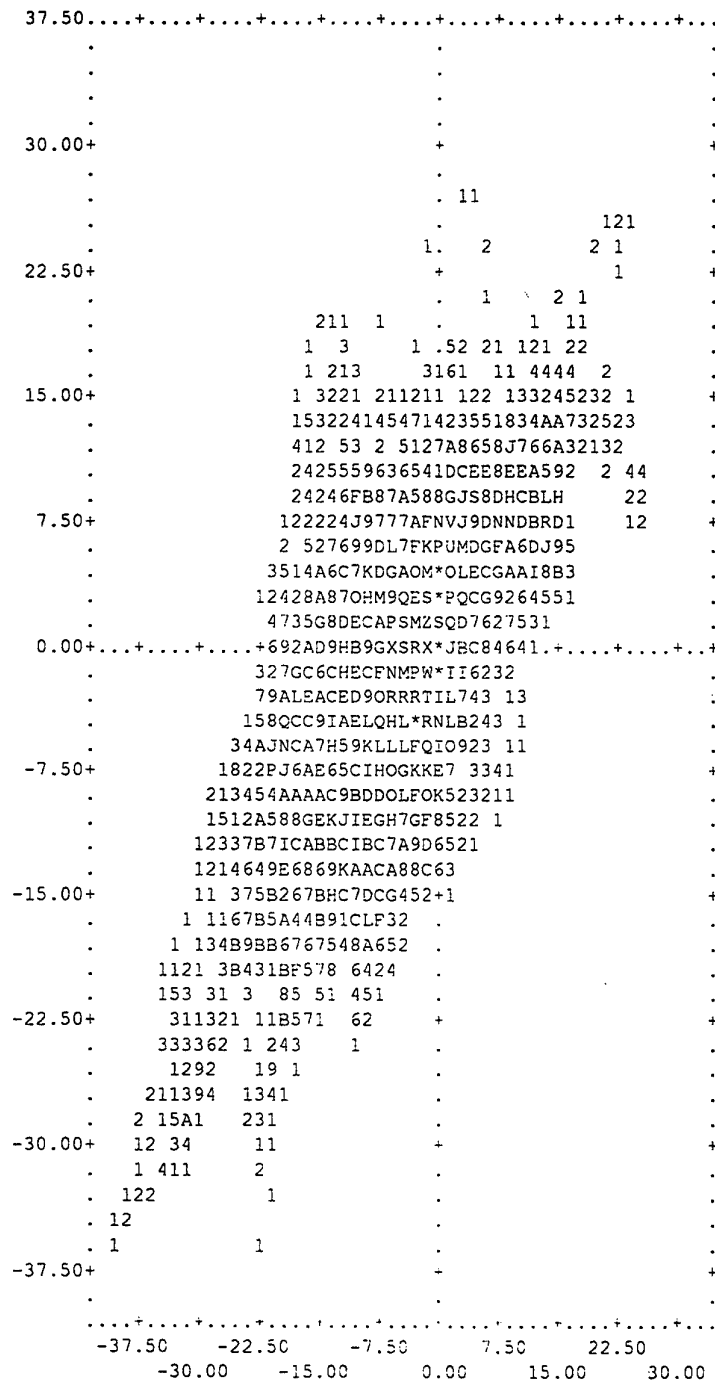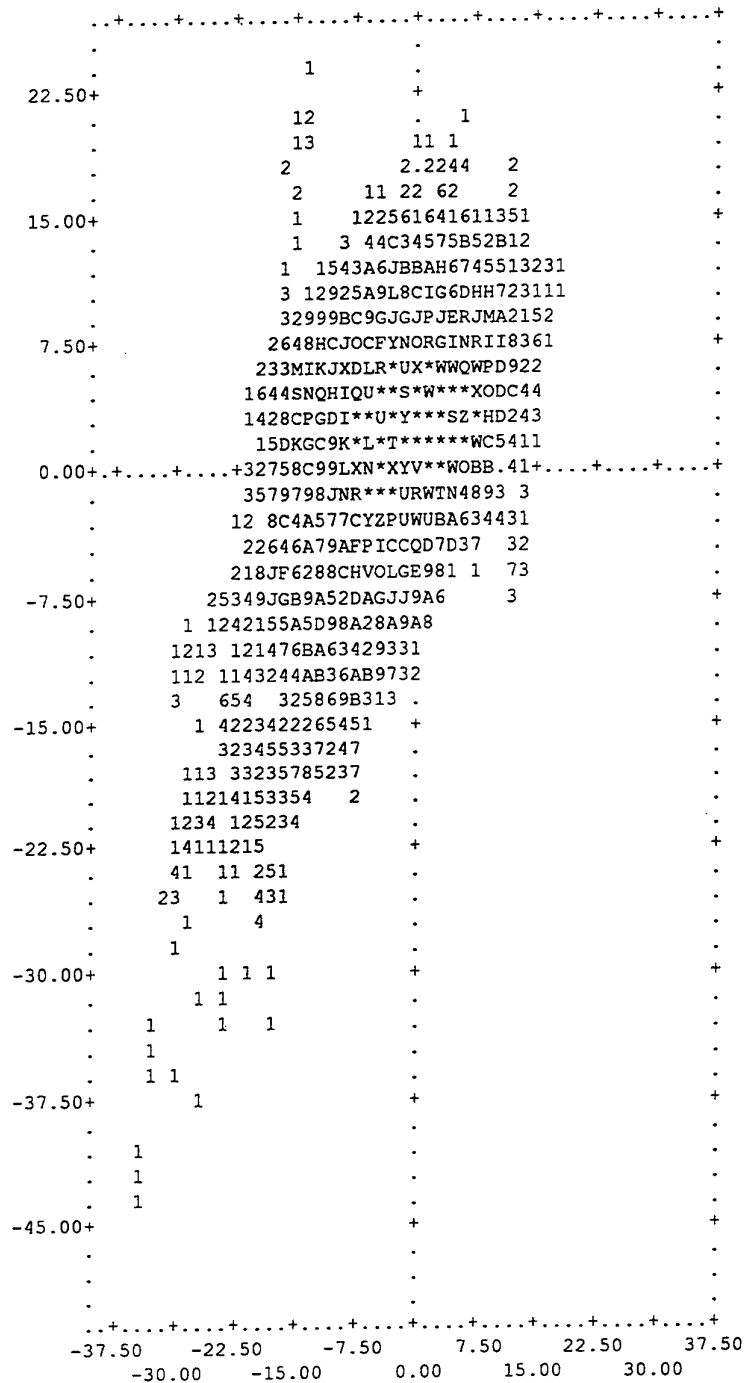
(a) 175 m below the surface vs 125 m below the surface.

```
         ....+....+....+....+....+....+....+....+....+....+...
   45.00+                                     +               +
       .                                       .               .
       .                                       .               .
       .                                       .               .
       .                                       .               .
   37.50+                                      +               +
       .                                       .               .
       .                                       .               .
       .                                       .               .
       .                                     11.               .
   30.00+                                 2 22+  .             +
       .                                 12    .               .
       .                               11     .                .
       .                                1     .                .
       .                            11       .                .
   22.50+                           1   1   + .               +
       .                                1    .                .
       .                         1    3 1 .  .                .
       .                      1   113  1        5             .
       .                    1 143123.    2     2              .
   15.00+               1      2342446+   111     1           +
       .               22     2354C21.  1552227211            .
       .                     65FJ2333  26C2554321             .
       .          15   2     156EBE511922453458816            .
       .          3  2 2316236177652A3 8L343554B 415          .
    7.50+       672327877536 68952GRM17C4B65747 231          +
       .        772657H9D83753248ENIN5P7922373143             .
       .       D5735FEI6F4G8A3249LJNFT8A6444957222            .
       .      39LEADNYGDGLF852A6HEIPZKE4655E82545             .
       .       7CKLHC**OKKD6 DAGMXKQGHS4D97BI9A5962           .
    0.00+...+....+.43MLBMR*VEHZ8375528QQGEM75BDAIKE4512..+..+
       .       16AD6SWRJDECADM9E59D87CD4156DILDM611           .
       .      15EC6HIOOJAI96NFHJ95H7A7835663ABJDD45635        .
       .       8BC6EHGAC53FNHPLHA97C494656545INC91 31         .
       .       55884E6HA9BGLTFB7A6742FC259D42KGD42  1         .
   -7.50+     13A7393787AGDP*C2348561A9433A16V7545 12        +
       .     328841EB7E8MJAQB52419A9429C65568733943331        .
       .    153534699BANF8435122245795924548GA3275  2         .
       .     11  19B74WM6  2  1 21 414323 29F2363111 1        .
       .      21 5674B6 1   1 12  22542  3192 422652          .
  -15.00+        236 64    3  31 2244675112691 153111        +
       .       1  23124  1  11 22532 .  3 2  12131            .
       .         2     31 1  1  3641  . 271     421           .
       .      1       1 2331   3313    1 2611    311          .
       .              221322 121 1  .. 121                    .
  -22.50+     1            3  321    1  + 14                  +
       .                  11 1          .221                  .
       .                               .31                    .
       .                                .                     .
       .                                .                     .
  -30.00....+....+....+....+....+....+....+....+....+....+...
       -45.00    -30.00    -15.00    0.00     15.00
           -37.50    -22.50    -7.50    7.50    22.50
```

Fig 3.12 Scatter plots of north-south current meter speed components at site A vs the north-south speed components at a current meter higher in the water column. Units are cm.s^{-1}.

(b) 200 m below the surface vs 175 m below the surface.

44

```
37.50....+....+....+....+....+....+....+....+....+....+...
     .                        .                    .
     .                        .                    .
     .                        .                    .
     .                        .                    .
30.00+                        +                    +
     .                        .                    .
     .                        . 11                 .
     .                        .            121      .
     .                    1.    2        2 1        .
22.50+                        +              1      +
     .                        .  1    2 1           .
     .              211  1    .        1  11        .
     .              1  3     1 .52 21 121 22        .
     .              1 213      3161  11 4444  2     .
15.00+            1 3221 211211 122 133245232 1     +
     .            15322414547142355183 4AA732523    .
     .            412 53 2 5127A8658J766A32132      .
     .            2425559636541DCEE8EEA592  2 44    .
     .            24246FB87A588GJS8DHCBLH      22   .
7.50+             122224J9777AFNVJ9DNNDBRD1    12   +
     .            2 527699DL7FKPUMDGFA6DJ95         .
     .            3514A6C7KDGAOM*OLECGAAI8B3        .
     .            12428A87OHM9QES*PQCG9264551       .
     .            4735G8DECAPSMZSQD7627531          .
0.00+...+....+....+692AD9HB9GXSRX*JBC84641.+....+....+..+
     .            327GC6CHECFNMPW*II6232            .
     .            79ALEACED9ORRRTIL743 13           .
     .            158QCC9IAELQHL*RNLB243 1          .
     .            34AJNCA7H59KLLLFQIO923 11         .
-7.50+            1822PJ6AE65CIHOGKKE7 3341         +
     .            213454AAAAC9BDDOLFOK523211        .
     .            1512A588GEKJIEGH7GF8522 1         .
     .            12337B7ICABBCIBC7A9D6521          .
     .            1214649E6869KAACA88C63            .
-15.00+           11 375B267BHC7DCG452+1            +
     .            1 1167B5A44B91CLF32  .            .
     .            1 134B9BB6767548A652 .            .
     .            1121 3B431BF578 6424  .           .
     .            153 31 3  85 51 451   .           .
-22.50+           311321 11B571  62     +           +
     .            333362 1 243    1     .           .
     .            1292   19 1           .           .
     .           211394  1341           .           .
     .          2 15A1    231           .           .
-30.00+          12 34    11            +           +
     .          1 411     2             .           .
     .         122        1             .           .
     .        12                        .           .
     .        1           1             .           .
-37.50+                                 +           +
     .                        .                     .
     ....+....+....+....+....+....+....+....+....+....+...
     -37.50    -22.50    -7.50     7.50     22.50
          -30.00    -15.00    0.00     15.00     30.00
```

Fig 3.13 Scatter plots of east-west current meter speed components at site A vs the east-west speed components at a current meter higher in the water column. Units are cm.s^{-1}.

   (a)   175 m below the surface vs 125 m below the surface.

```
           ..+....+....+....+....+....+....+....+....+....+....+
           .            .        .                        .
           .            1        .                        .
    22.50+               +       .                        +
           .           12        .  1                     .
           .           13          11 1                   .
           .            2          2.2244    2            .
           .            2       11 22 62     2            .
    15.00+              1     122561641611351             +
           .            1   3 44C34575B52B12              .
           .            1  1543A6JBBAH6745513231           .
           .            3 12925A9L8CIG6DHH723111           .
           .            32999BC9GJGJPJERJMA2152            .
     7.50+             2648HCJOCFYNORGINRII8361            +
           .           233MIKJXDLR*UX*WWQWPD922            .
           .           1644SNQHIQU**S*W***XODC44           .
           .           1428CPGDI**U*Y***SZ*HD243           .
           .           15DKGC9K*L*T*****WC5411             .
     0.00+.+....+....+....+32758C99LXN*XYV**WOBB.41+....+....+....+
           .           3579798JNR***URWTN4893 3            .
           .           12 8C4A577CYZPUWUBA634431           .
           .           22646A79AFPICCQD7D37   32           .
           .           218JF6288CHVOLGE981 1  73           .
    -7.50+            25349JGB9A52DAGJJ9A6    3            +
           .         1 1242155A5D98A28A9A8                 .
           .         1213 121476BA63429331                 .
           .         112 1143244AB36AB9732                 .
           .         3   654  325869B313 .                 .
   -15.00+           1 4223422265451    +                  +
           .           323455337247     .                 .
           .         113 33235785237    .                 .
           .         11214153354   2    .                 .
           .         1234 125234        .                 .
   -22.50+         14111215             +                  +
           .         41  11 251         .                 .
           .         23  1  431         .                 .
           .          1     4           .                 .
           .          1                 .                 .
   -30.00+            1 1 1             +                  +
           .           1 1              .                 .
           .        1     1   1         .                 .
           .        1                   .                 .
           .        1 1                 .                 .
   -37.50+          1                   +                  +
           .                            .                 .
           .       1                    .                 .
           .       1                    .                 .
           .       1                    .                 .
   -45.00+                              +                  +
           .                            .                 .
           .                            .                 .
           .                            .                 .
           ..+....+....+....+....+....+....+....+....+....+....+
         -37.50   -22.50   -7.50    7.50    22.50    37.50
            -30.00    -15.00    0.00    15.00    30.00
```

Fig 3.13 Scatter plots of east-west current meter speed components at site A vs the east-west speed components at a current meter higher in the water column. Units are cm.s^{-1}.

(b)   200 m below the surface vs 175 m below the surface.

46

3.7 Ancillary Oceanographic Data

Several types of data other than current meter data were obtained to aid the interpretation of the current meter measurements. These were:

(i) infra-red satellite imagery from 15 July 1992 onwards.

(ii) one CTD (Conductivity-Temperature-Depth) section to 100 m below the surface from west of the site to inshore waters on 21 July 1992.

(iii) XBT (eXpendable Bathy-Thermograph) temperature profiles

It was intended to correlate changes in direction of currents measured at the site with changes in surface features indicated by the satellite imagery, and to use the imagery and XBT temperature sections to estimate widths and vertical extents of features. Also of interest is the degree to which subsurface features could be inferred from surface features indicated by the infra-red imagery. This could be of benefit in planning any operations at the range site. However as explained in the following section not enough data were gathered for definitive analyses to be made.

3.7.1 Infra-red Imagery for the Site Survey

For reasons mentioned earlier in section 3.2.3, the surface expression of the Leeuwin Current in midyear is readily detectable in satellite infra-red imagery. Infra-red (IR) imagery of sea surface temperature patterns derived from NOAA satellite data were obtained under contract from CSIRO Marine Laboratories Western Australia. These were intended to be used to monitor shifts in the current, and to see how representative the IR surface patterns were of subsurface flow patterns. Twelve images were received, for 15, 21, 22, 23, 26, 30, 31 July, 16, 18, 19, 21, 22 August. Of these, only the images for 15, 21, 22 July, and 22 August showed useful information for site A, the others being obscured by cloud. Previous investigations by DSTO and more recent investigations by CSIRO have shown that heavy cloud cover is a major limitation in the use of IR imagery for August and September near Perth. Colour coded imagery for selected days is reproduced in Figs 3.14 to 3.17.

The IR imagery has been enhanced to show up the warm Leeuwin Current waters, not absolute temperature values. Colour boundaries do not necessarily show surface temperature isotherms. However colour for a particular range of temperatures is approximately consistent from image to image.

According to the imagery for July the current meters at site A lay close to the western edge of the core of the Leeuwin Current, where flow is expected to be predominantly near southward along isobaths. In the July 21 image (Fig 3.15) site A lies just north of a small south-westwards projection of warmer waters from the western edge of the core. The image for 22 July (Fig 3.16) indicates the same southward flow conditions as for 21 July, but from north of the site warm Leeuwin Current waters appear to have spread to

Geraldton

Jurien

Perth

N11/19610
15 July 92
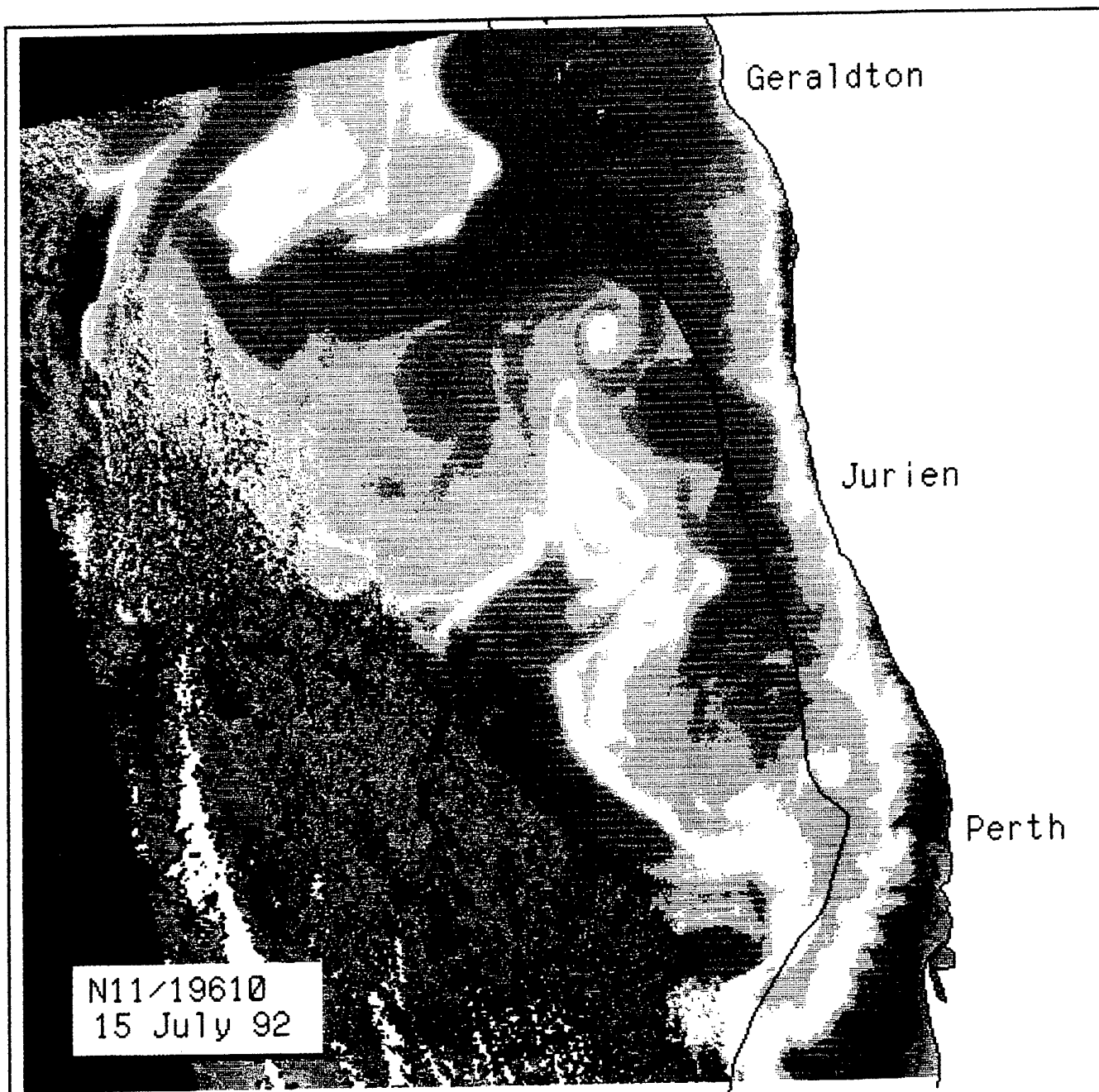
Fig 3.14 Infra-red image of the Leeuwin Current for 15th July 1992 derived from NOAA satellite data. In the image, the continental shelfbreak (200 m) isobath is shown in black, and clouds offshore are mottled blue/white. The Leeuwin Current is the band of warm (brown/red) water streaming down the shelfbreak, with periodic meanders offshore into deeper waters. Cooler waters are shown in green and blue. DSTO current meter sites (+). Image supplied under contract by CSIRO Marine Laboratories, Perth.
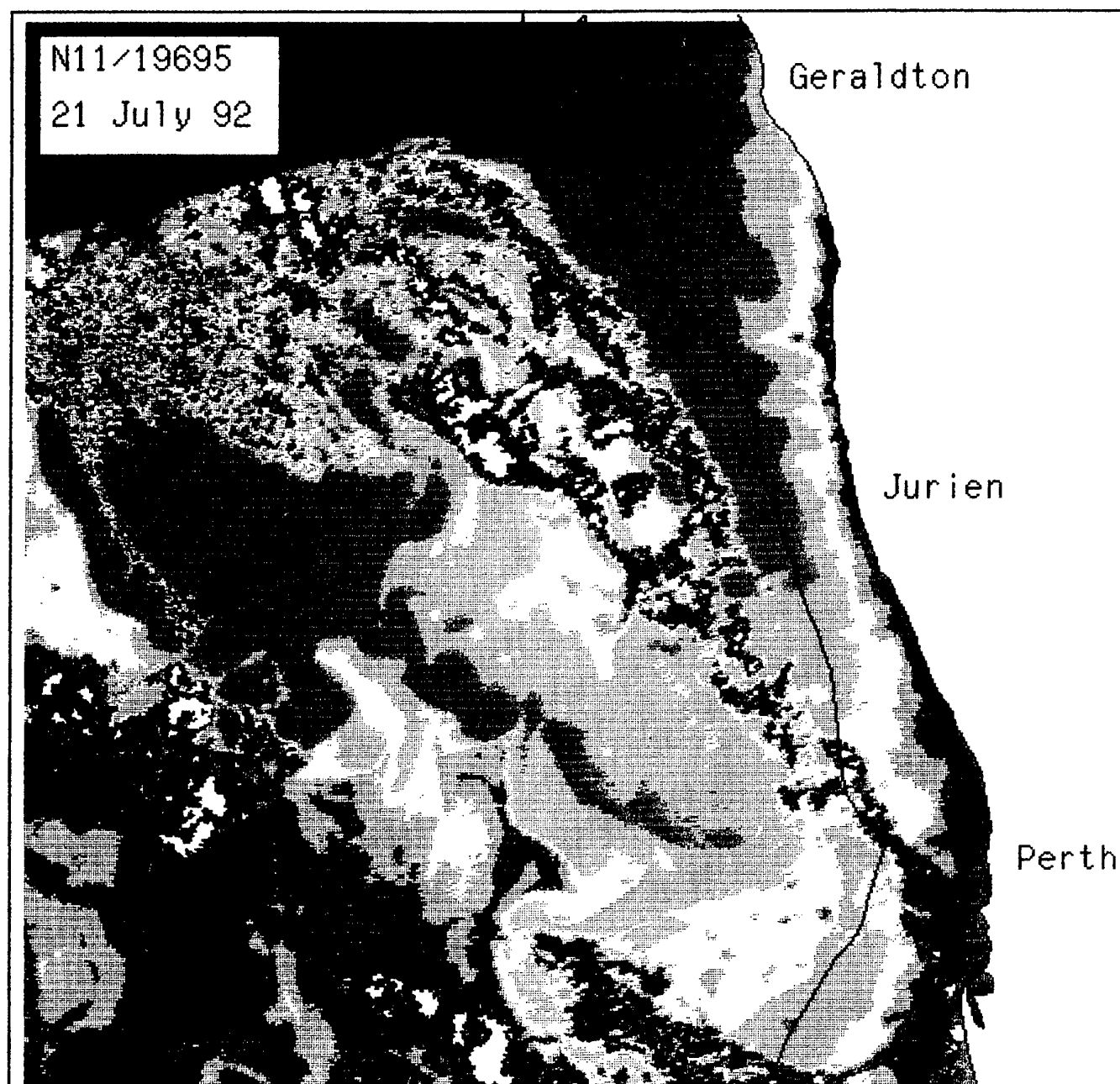
Fig 3.15 Infra-red satellite image of sea surface temperature patterns off south-western Australia for 21 July 1992. See Fig 3.14 for an explanation of major features. Image supplied under contract by CSIRO Marine Laboratories, Perth.
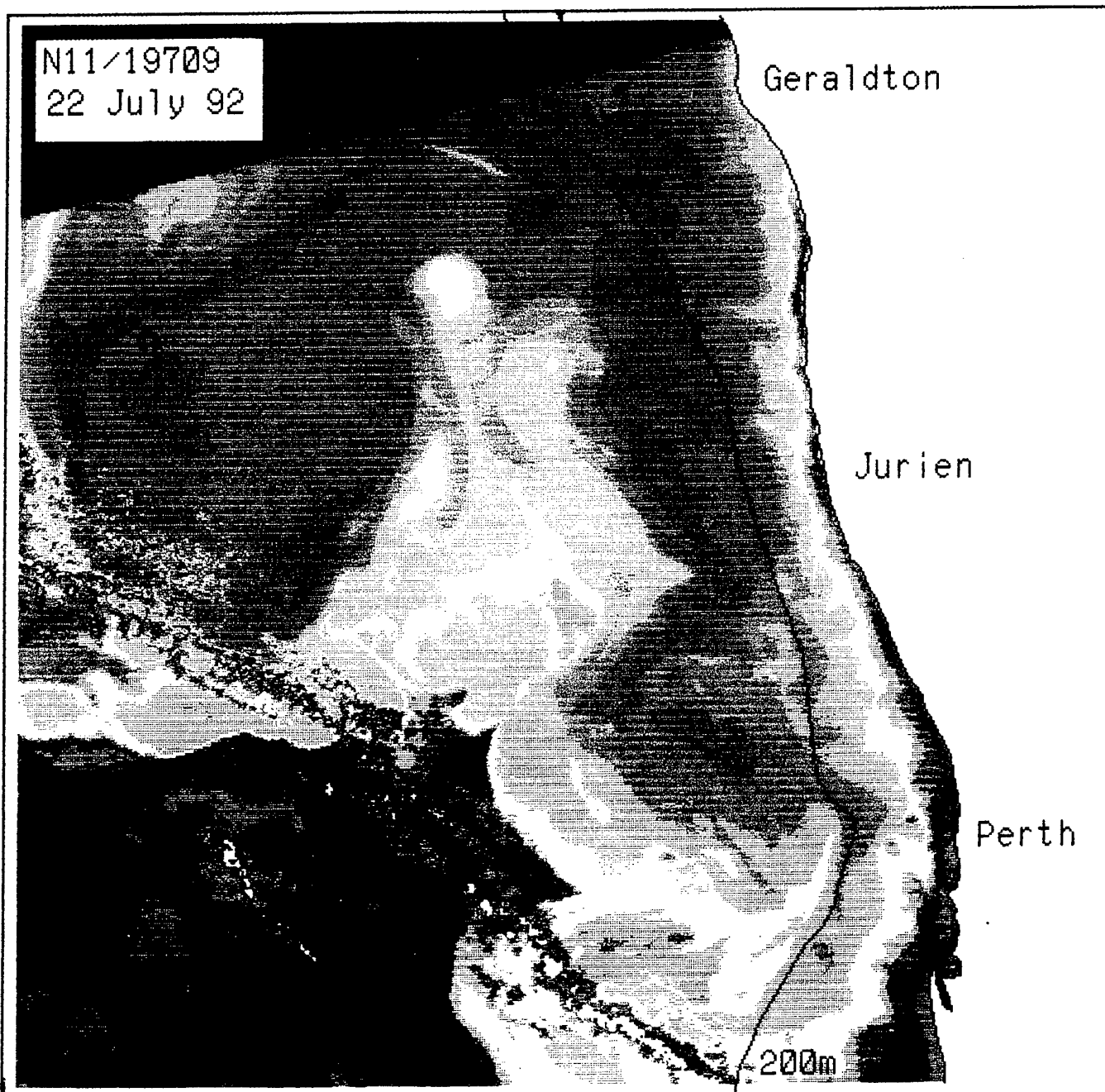
Fig 3.16 Infra-red satellite image of sea surface temperature patterns off south-western Australia for 22 July 1992. See Fig 3.14 for an explanation of major features. Image supplied under contract by CSIRO Marine Laboratories, Perth.
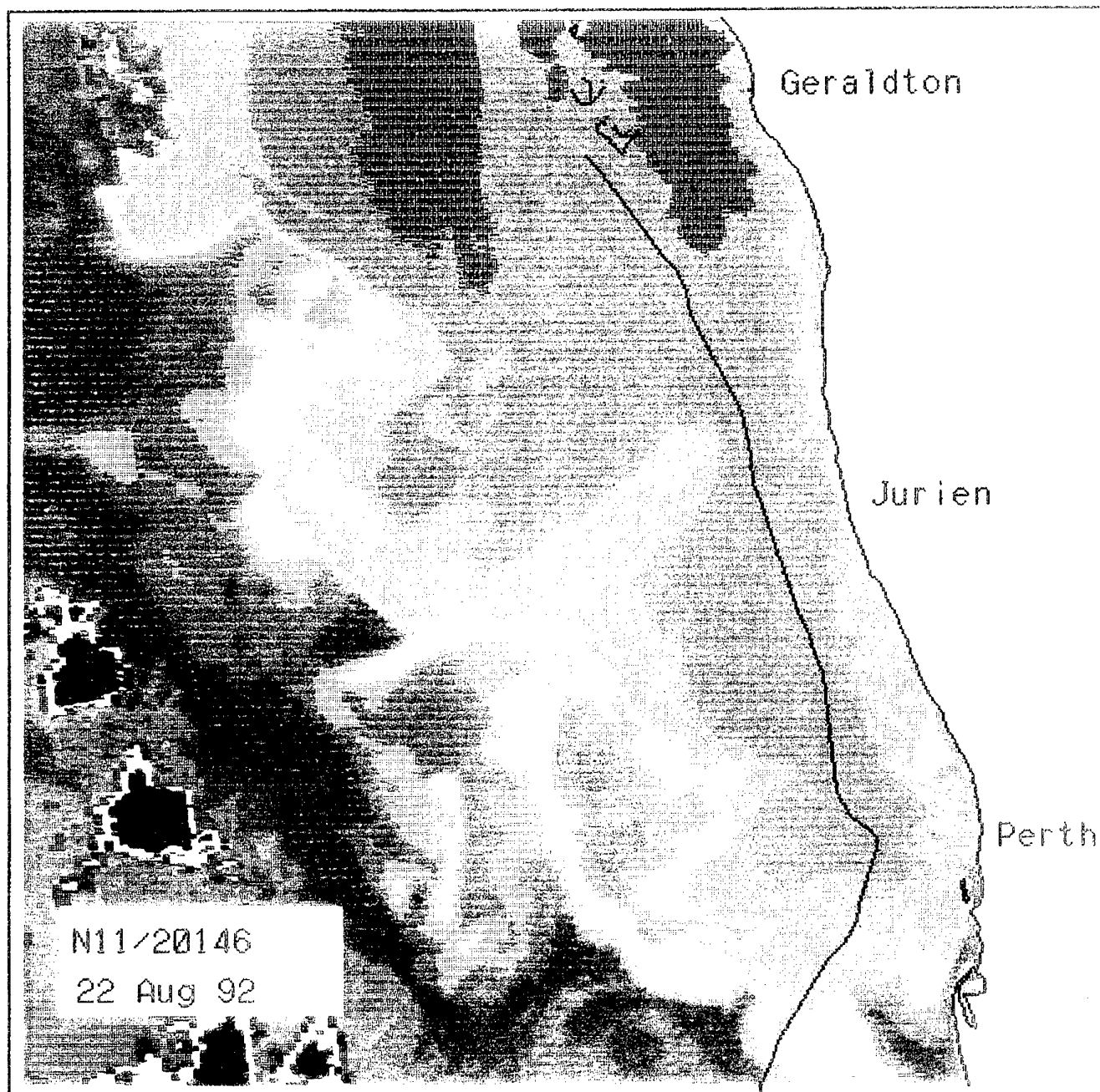
Fig 3.17 Infra-red satellite image of sea surface temperature patterns off south-western Australia for 22 August 1992. See Fig 3.14 for an explanation of major features. Image supplied under contract by CSIRO Marine Laboratories, Perth.

the southwest, with a thin lead of cooler waters lying between this spread and site A. The image of 21 July, which is possibly affected by cloud, places site A directly in the surface core.

The image for 22 August (Fig 3.17) shows roughly the same conditions as for 21 July, but flow appears to be to the southwest rather than the south, if the warm tongue at the site is caused by advection along the current core. This is the direction measured by the current meter at 125 m below the surface at the start of 22 August local time, indicating that this interpretation is correct. **The satellite imagery indicate that the survey site lies close to the core of the Leeuwin Current, where maximum near surface currents and maximum vertical shear can be expected.**

The Dongara current meter is northeast of a cyclonic feature, and east of a seawards moving offshoot. The site is just to the north of the bifurcation of westward and southward flow seen in Fig 14. The surface current at the current meter site appears to be to the south and southwest.

Apart from the very limited comparisons with the current meter data, the only other subsurface data available for verification of features inferred from the surface IR imagery is one shallow CTD (Conductivity-Temperature-Depth) section taken on the 21 July 1992. The position of this section is shown in Fig 3.18, and cross-sections drawn from the data are shown in Figs 3.19 to 3.21. Although it is difficult to see, the 22 July image (Fig 3.16) shows a thin ribbon of warmer water along the 200 m contour which is seen in the temperature section of Fig. 3.19 at stations 6 and 7. Figs 3.20 and 3.21 show that the high temperature waters of the Leeuwin Current are characterised by lower salinities and densities, as discussed in earlier sections. The supposition that station 1 is on the western surface edge of the Leeuwin Current is supported, but the images do not show the warmer waters in the CTD section at station 1. The eastern boundary between warmer Leeuwin Current waters and cooler inshore waters seen in the CTD section is seen in the 22 July image.

Scattered XBT data taken by RAN vessels are known to be available from signal reports (Fig. 3.22), which could aid further analyses. HMAS Brisbane had earlier offered to take digital XBT sections for the survey, but advised that they could not be taken due to extremely rough weather. If the Fleet XBT are in digital format, they could be useful for examining fine-structure, which causes fluctuations in acoustic signals. See section 5. The fleet XBT have not been used for this report.

It appears that infra-red imagery does reflect subsurface features at the site, but the limited data set does not allow quantitative rules relating to depths of features or relations of surface features to current strengths. The variability discussed in section 3.6.1 shows that surface currents sometimes extended to more than 250 m but to less than 350 m below the surface at site A (in a water depth 400 m), at which time the bottom current was sometimes opposite in direction to the surface current. At other times the surface current extended to 350 m. The IR imagery cannot be used to infer current directions for depths more than about 250 m below the surface at the site.
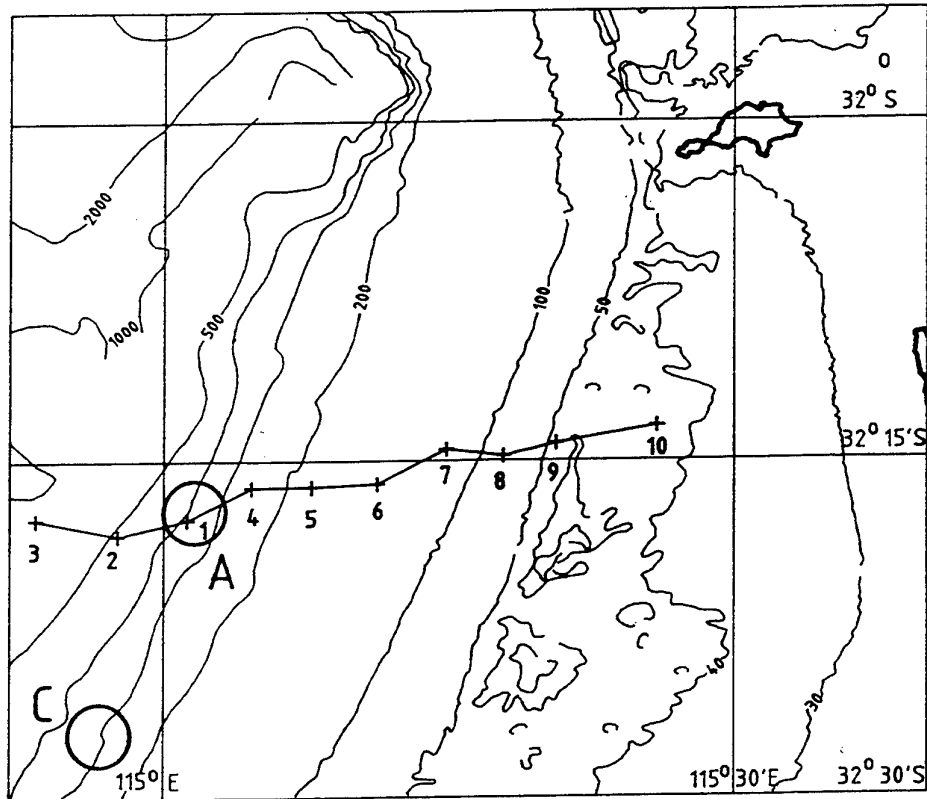
Fig 3.18 Station positions for a CTD survey taken on 21 July 1992. Current meter sites A and C are also shown.
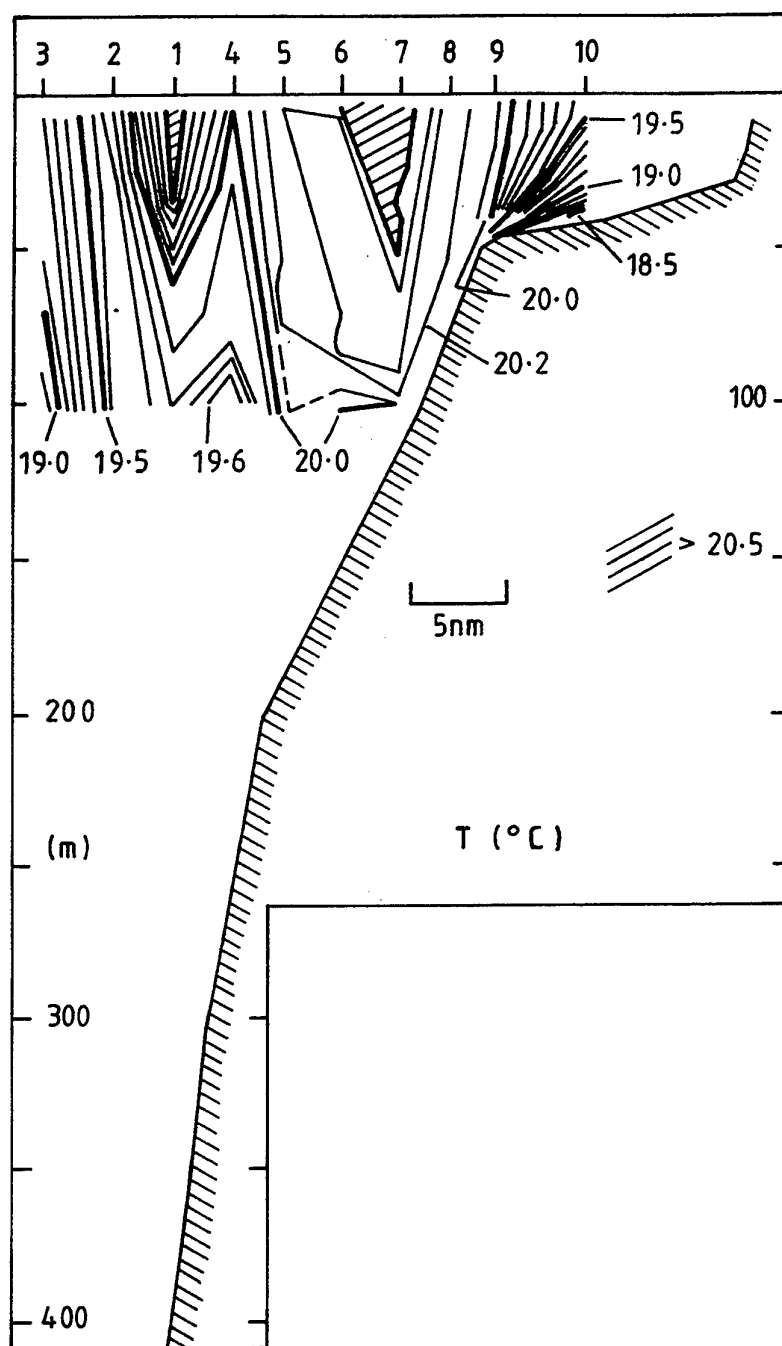
Fig 3.19 Temperature cross-section through site A taken on 21 July 1992 by DSTO. Site A is at station 1. See Fig 3.18 for station positions. Note the down-welling cooler shelf waters, and warm features at stations 1 and 7.
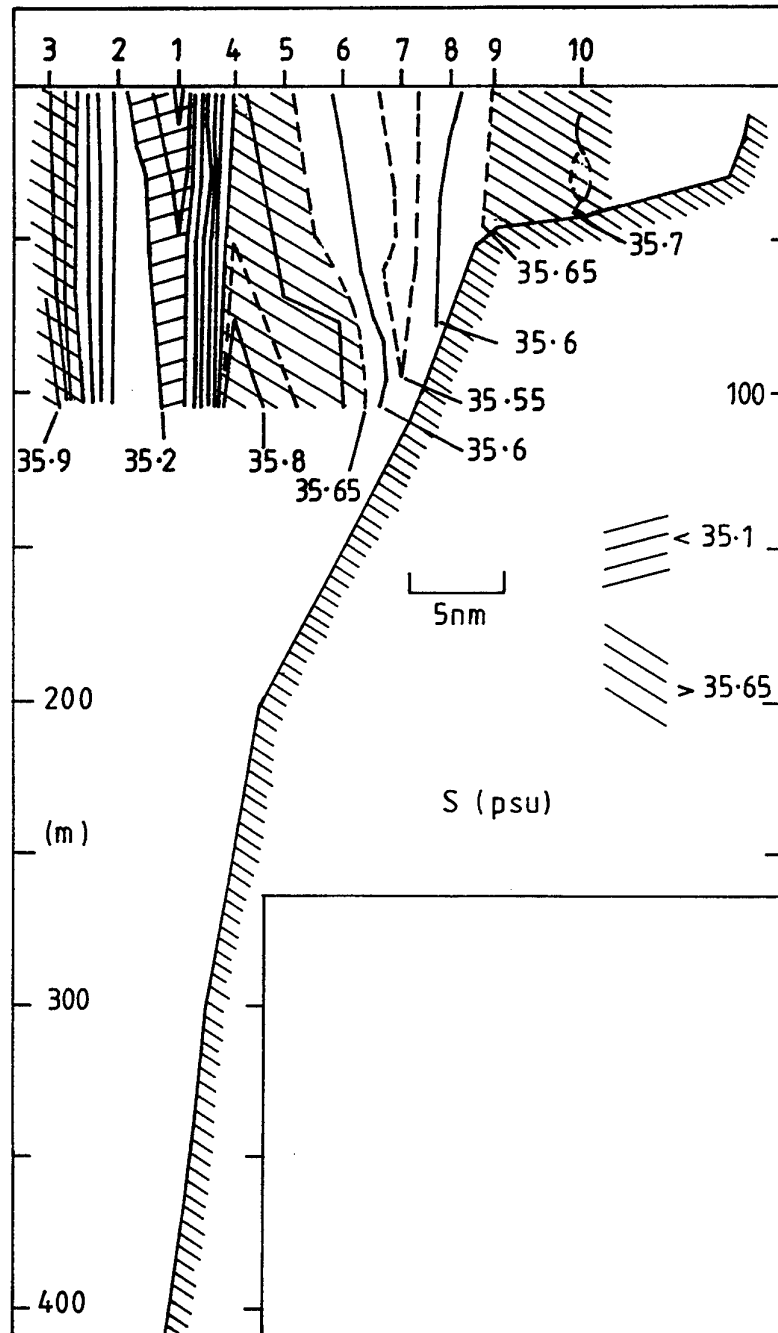
Fig 3.20 Salinity cross-section through site A taken on 21 July 1992 by DSTO. Site A is at station 1. See Fig 3.18 for station positions.
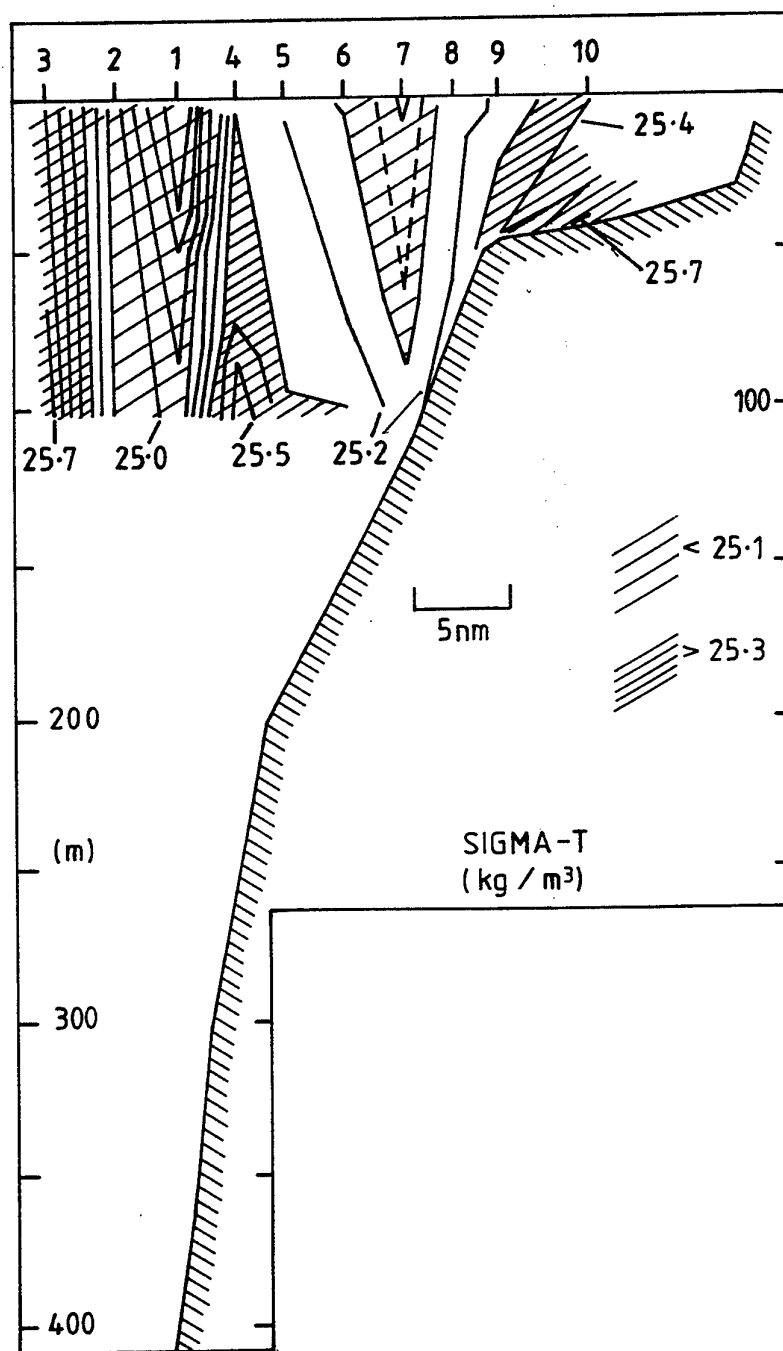
Fig 3.21 *Density (sigma-t) cross-section through site A taken on 21 July 1992 by DSTO. Units of sigma-t are density ((kg/m³)-1000). Warm features at stations 1 (site A) and 7 appear as lower density V or cone shapes.*
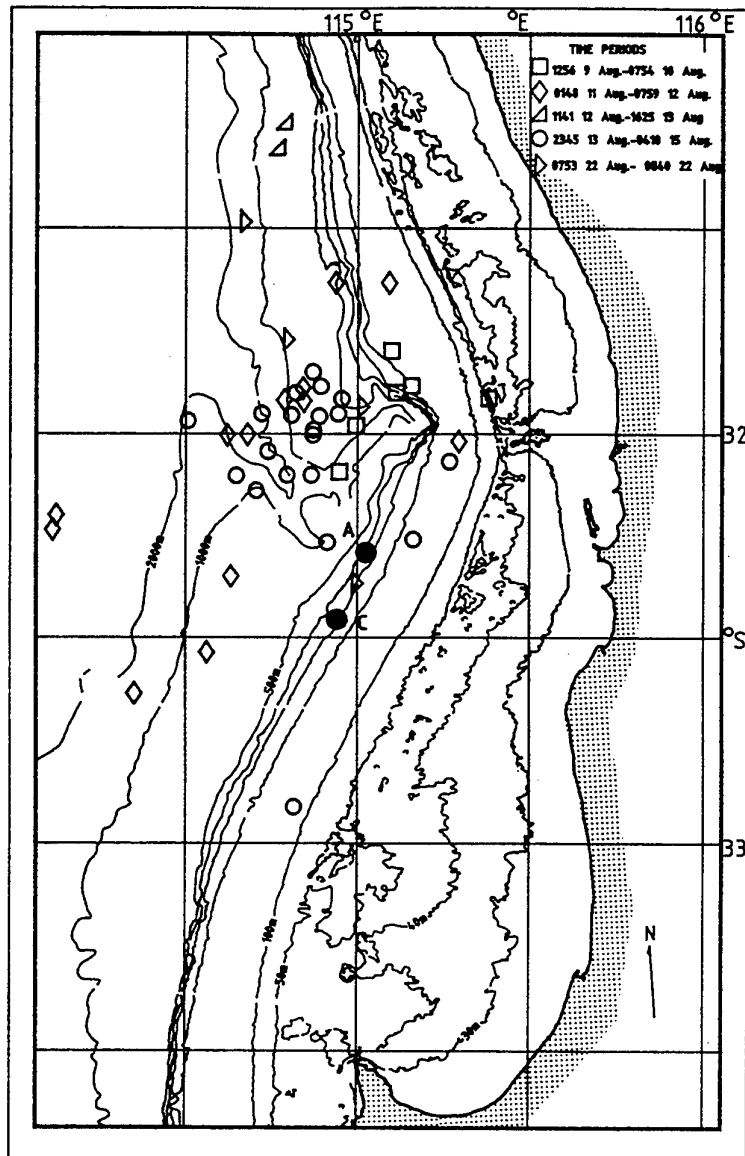
Fig 3.22 Sites of XBT profiles taken by RAN vessels near sites A and C for 9-22 August 1992.

3.8 Overview Of Currents at Site A

Site A appeared to lie in or west of the surface core of the Leeuwin Current. This is expected to lead to strong southward surface currents at site A, of more than 2 knots. The current meter data show that near surface currents often trended parallel to isobaths i.e. south to south south west. The predominantly southward surface currents were usually found in occurrence with a north to north-north-eastward bottom counter current. Episodes occurred when the currents at all depths through the column were in the same direction, while at other times the current directions varied through the column. **Episodes were seen when the surface currents were northward, but the bottom currents were southward, a complete opposite of the usual flow pattern.** Subsurface current speeds at 200 m below the surface were sometimes slightly higher than speeds 175 m below the surface. Subsurface current speeds at 175 m below the surface were sometimes up to 20 cm.s^{-1} higher than speeds 125 m below the surface.

It is possible that some of this behaviour is caused by east-west Leeuwin Current frontal movements, and by seaward offshoots of the Leeuwin Current, in conjunction with vertically sloping fronts. These combine to cause a complicated subsurface current regime which is difficult to predict from surface data alone. However the gustiness of currents within an hour was usually low. The current regime at site A is similar to that shown by the LUCIE current meter data for sites near Dongara at 29.5°S and Cape Mentelle at 34°S, with an occasional bottom undercurrent and flow reversals through the column.

High variability in horizontal and vertical shear can be expected at the survey site and at Dongara. Current speeds can be expected to be steady in any one hour, but to vary as the result of seaward offshoots of the Leeuwin Current, transverse frontal movements, and the movements and formations of clockwise and anti-clockwise circulating eddies and meanders (see Figs 3.14 to 3.17). The high current speeds and shears can be expected to cause flow noise at hydrophones, and to distort hydrophone array shape, while subjecting horizontal or vertical arrays to high stresses and torsions.

Table 4.1 *Average yearly and monthly temperature profiles (°C) for 32-33°S, 114-115°E formed from BT data for 1960 to 1980. Month 1 is January.*

DEPTH (M)	YEAR AVERAGE	1	2	3	4	5	6	7	8	9	10	11	12
0	21.0	21.1	21.7	22.0	22.1	22.6		18.9	17.5	19.3	19.7	19.7	22.0
10	20.9	20.9	21.7	22.0	22.0	22.6		18.9	17.7	19.3	19.6	19.7	22.0
20	20.9	20.7	21.7	22.0	21.9	22.6		18.9	17.7	19.3	19.6	19.6	22.0
30	20.9	20.6	21.6	22.0	21.8	22.6		18.8	17.7	19.3	19.5	19.6	21.7
40	20.8	19.9	21.5	21.9	21.7	22.6		18.7	17.7	19.1	19.4	19.5	20.7
50	20.6	19.4	21.3	21.6	21.1	22.6		18.5	17.7	19.0	18.9	19.4	19.3
60	20.5	18.9	20.8	21.1	20.7	22.9		18.3	17.7	18.9	18.7	19.2	18.0
70	20.2	18.4	20.1	20.0	20.1	22.8		18.1	17.7	18.8	18.1	19.0	17.2
80	19.9	18.1	19.4	19.1	19.5	22.7		17.8	17.7	18.8	18.1	18.8	16.6
90	19.6	17.5	19.0	18.4	18.6	22.6		17.5	17.7	18.6	17.8	18.6	16.1
100	19.5	17.1	18.7	17.9	17.9	22.4		17.5	17.7	18.7	17.6	18.4	15.7
110	19.3	16.7	18.4	17.2	17.3	22.6		17.3	17.7	18.5	17.6	18.1	15.4
120	19.0	16.3	18.0	16.7	16.7	22.4		17.0	17.6	18.5	17.5	17.9	15.1
130	18.7	15.9	17.7	16.0	15.7	22.2		16.9	17.5	18.3	17.3	17.3	14.9
140	18.5	15.6	17.4	14.9	15.3	21.9		16.7	17.4	18.0		17.0	14.8
150	18.3	15.4	17.0	14.6	15.0	21.7		16.6	17.3	17.9		16.8	14.6
160	18.0	15.2	16.4	14.4	14.5	21.4		16.3	17.1	17.7		16.6	14.4
170	17.7	14.9	16.0	14.2	13.9	21.3		16.0	16.9	17.6		16.4	14.3
180	17.5	12.6	15.7	13.9	13.6	21.0		15.7	16.6	17.3		16.2	14.1
190	17.2	12.5	15.3	13.6	13.6	20.5		15.6	16.4	17.1		16.0	13.9
200	16.9	12.2	14.9	13.4	13.5	20.0		15.5	16.4	16.9		15.8	13.7
210	16.5	12.0	14.6	13.1	13.4	19.4		15.2	16.4	16.6		16.1	13.4
220	16.2	11.6	14.2	12.9	13.2	19.0		14.9	15.8	16.3		15.2	13.2
230	15.9	11.4	13.7	12.7	13.0	18.4		14.6	15.6	16.0		15.0	13.0
240	15.6	11.2	13.5	12.4	12.8	17.9		14.8	15.3	15.7		13.7	12.7
250	15.5	11.1	13.2	11.8	12.7	17.4			14.7	15.5		14.0	12.5
260	15.2	11.0	12.9	11.6	12.4	16.9			14.1	15.3		13.7	12.3
270	14.9	10.8	12.0	11.4	12.1	16.4			13.8	15.0		13.3	
280	14.5	10.6	11.9	11.2	11.9	15.9			13.5	14.6		13.0	
290	14.2	10.5	11.8	11.0	11.6	15.4			13.1	14.4		12.7	
300	13.8	10.4	11.6	10.8	11.4	14.9			12.9	14.1		12.4	
310	13.4	10.3	11.4	10.6	11.2	14.5			12.8	13.8		12.2	
320	13.1	10.2	11.1	10.5	11.0	14.2			12.4	13.5		11.9	
330	12.8	10.1	10.9	10.3	11.0	13.8			12.1	13.2		11.7	
340	12.5	10.0	10.8	10.2	10.7	13.4			11.7	12.9		11.4	
350	12.2	9.9	10.6	10.1	10.6	13.0			11.5	12.6		11.3	
360	11.9	9.8	10.5	10.0	10.5	12.7			11.4	12.3		11.0	
370	11.6	9.7	10.3	9.9	10.5	12.4			11.3	11.0		10.8	
380	11.3	9.5	10.2	9.9	10.3	12.0			11.1	10.7		10.5	
390	11.1	9.5	10.1	9.8	10.2	11.7			10.9	10.6		10.3	
400	10.9	9.4	10.0	9.7	10.1	11.4			10.8	10.4		10.1	
410	10.6	9.3	9.9	9.7	10.1	11.2			10.6	10.1		9.9	
420	10.5	9.2	9.9	9.6	10.1	11.2			10.4	9.9		9.8	
430	10.4	9.1	9.6	9.6	10.0	11.2				9.8		9.8	
440	10.3			9.5		10.4				9.7			
450	9.6			9.4		10.2				9.5			
460	9.4									9.4			
470	9.3									9.3			
480	9.2									9.2			
490	9.1									9.1			
500	9.0									9.0			

4. Water Properties

4.1 Importance of Water Properties to the Acoustic Range

The sound-speed profiles about a site must be known before acoustic propagation can be satisfactorily modelled. Density profiles can be used to determine buoyancy of objects in the water column. From density profiles the amount of flotation necessary to keep an instrument moored in a vertical position in the presence of currents of varying strengths can be estimated. Sound-speed and density profiles for the water column are determined by the water temperature, salinity, and pressure (depth). The temperature usually has the dominant effect in determining the sound-speed, with salinity having a second-order effect. Water properties vary with location and season, and sometimes daily in response to local heating and cooling effects.

4.2 Temperature and Salinity Data

Average bathy-thermograph temperature profiles for 114 to 115° E in 1° latitude bands from 30 to 35°S are shown in *Hamilton (1984), (his Fig. 7)* with tables of monthly averages for the surface to a depth of 250 m in 50 m depth increments. Data for 32 to 33°S, 114 to 115°E are closest to the survey site. Table 4.1 shows average monthly temperatures for this area (unpublished data from Hamilton 1984). The number of BT profiles for each month is low, yielding some poor average profile shapes. "*The behaviour of sea surface temperature (SST) and temperature of waters to between 50 and 100 m is strongly seasonal, but does not follow a classic sinusoidal variation, being upheld from summer to autumn. Highest SST is seen for April and May. Temperatures from 50 to 200 m have two yearly maxima, with highest values to 150 m and deeper seen over autumn and winter, and not summer*" *(Hamilton 1986)*. This behaviour is caused by the unseasonally warm waters of the Leeuwin Current arriving at this area in the middle of the year (austral winter).

Ridgway (1982) provides non-seasonal average curves of temperature vs salinity for the two areas 30 to 32.5°S, 32.5 to 35°S; 110 to 115°E. These very broad non-seasonal averages could be used to synthesize salinity profiles from temperature profiles, allowing both temperature and salinity to be used in calculations of sound-speed from the XBT data. However because the averages are so broad, using a constant salinity of about 35.5 psu is recommended as a more economical method. A subsurface salinity maximum is expected below the Leeuwin Current, since it has relatively lower salinity overlying South Indian Central water of high salinity. This subsurface maximum does not appear in Ridgway's broad curves, where the maximum is seen at the surface. This subsurface salinity maximum could lead to a deeper local sound-speed maximum than that predicted from only a temperature profile, depending on the sign and strength of the temperature gradient below the temperature mixed layer, thus changing the expected propagation conditions.

It is apparent that seasonal temperature-salinity (or soundspeed) curves are required for the Leeuwin Current and surrounding waters before propagation can be satisfactorily modelled.

4.3 Effect of Waters with Different Properties

Compared to local waters, the Leeuwin Current has much higher temperatures, and much lower salinities. It is known that intense interleaving of water masses with different properties can occur at thickness scales of centimetres and smaller, and with some larger effects for thickness of the order of metres. This condition is known as micro-structure or fine structure. Micro-structure can affect acoustic propagation by causing fluctuations in intensity of the signal received at a hydrophone. Micro-structure can be expected at the site area, because two water bodies with very different properties meet in this area (the South Indian Central water, and Leeuwin Current water, as discussed in section 3). The effects of micro-structure are discussed in the following section 5.

5. Microstructure

The waters of the ocean are not well mixed but rather contain many inhomogeneities as a result of the interposing of different water masses and varying surface heating. This results in 'microstructure' in properties such as the temperature and speed of sound. As noted in the last section the speed of sound depends strongly on the temperature.

5.1 Effect of Microstructure on Sound Propagation

Acoustic energy is scattered by inhomogeneities such as temperature microstructure. Such scattering results in fading between a source and receiver. As the water moves past the receiver, the acoustic path crosses a different combination of inhomogeneities and the energy arriving at a point fluctuates, making e.g. estimates of the range of a sound source uncertain.

5.2 Microstructure near the Perth Site

The temperature profile in a water depth of 580 m at 31°58.82'S, 115°11.42'E obtained using a CTD (Conductivity Temperature Depth) probe is shown in Fig 5.1. The profile was obtained from experiments carried out by the CSIRO on RV Franklin from 1st October to 5th November 1985. The temperature profile shown is for data averaged over uniform depth intervals of 2 m. The average temperature in the 0-200 m segment was 20.19°C, in the 200-400 m segment 15.10°C, and in the 400-600 m segment 8.92°C.

The temperature gradient profile for 0 to 580 m is shown in Fig 5.2, and exhibits a great deal of structure. The magnitude of the temperature gradients are of the same order as that observed in the western North Atlantic region of 28°N, 70°W (see Hayes et al 1975; Joyce and Desaubies 1976), and also that in the central North Pacific 27°N, 155°W (see Gregg, Cox and Hacker 1973). The normalised gradient temperature variance (identical to the Temperature Cox number C^2), defined as the ratio of the variance of the temperature gradient to the square of the mean temperature gradient (see Osborn and Cox 1975), is related to the ratio of the actual rate of vertical diffusion of heat to that which would occur due to diffusion along the mean gradients. If there are no net lateral transports of temperature fluctuations, then the coefficient of vertical diffusion (K_z) is equal to kC^2, where k is the molecular coefficient of heat diffusion. The Cox numbers for the three depth intervals 0-200 m, 200-400 m, and 400-600 m were 1.10, 0.852, and 1.5 respectively. The average temperature gradients for these three segments in °C.m^{-1} were 2.38×10^{-2}, 3.30×10^{-2} and 2.07×10^{-2} respectively. In the Western North Atlantic region for the interval 600-800 m the average Cox numbers computed with 1 m segments were 0.36 and 0.71 at two nearby locations. At the central North Pacific region the Cox numbers varied from 1.3 to 2.2 for various depth intervals in the upper

TEMPERATURE VS DEPTH; 31 58.82'S 115 11.42'E; STN=14
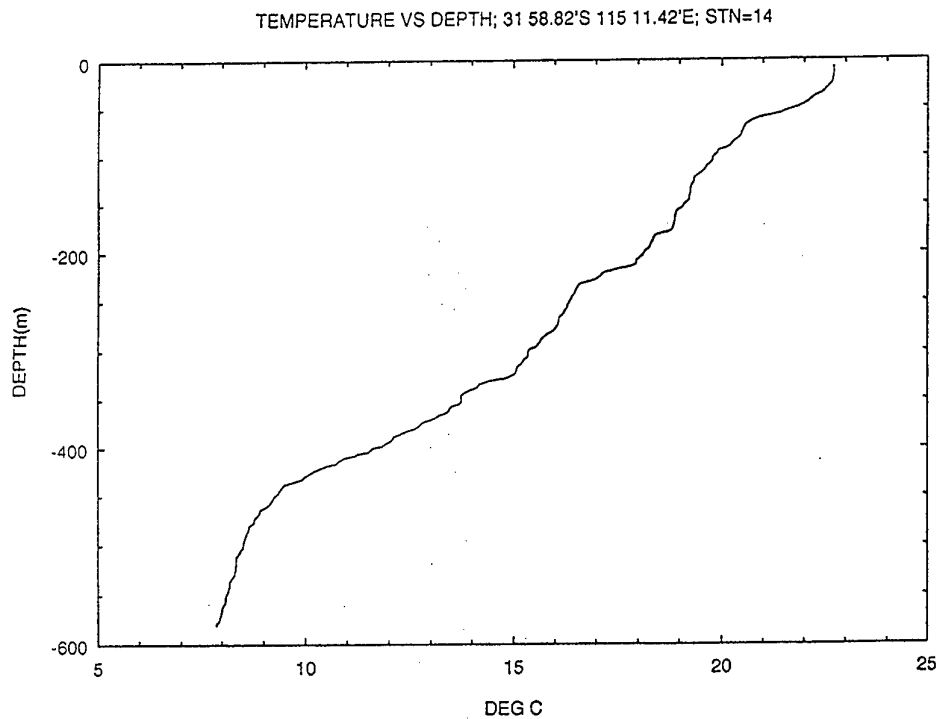
Fig 5.1 Temperature as a function of depth at 31°58.82'S, 115°11.42'E in October 1985. Data supplied by CSIRO Marine Laboratories, Hobart.

TEMPERATURE GRADIENT VS DEPTH; 31 58.82'S 115 11.42'E; stn=14
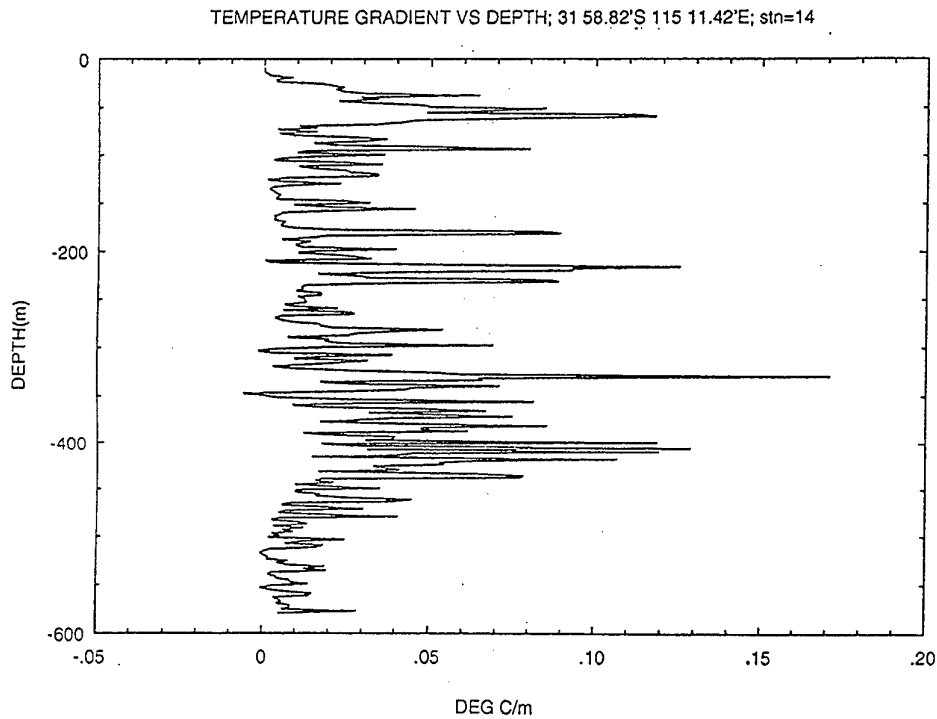
Fig 5.2 Temperature gradient as a function of depth derived from the temperature profile of Fig 5.1. Depth increment is 2 m.

2 km depth (see *Gregg et al 1973*). The Cox numbers near the Perth location indicate microstructure activity similar to the central North Pacific region.

The histogram of temperature gradient in the 0-580 m interval indicates a large skewness; see Fig 5.3. According to *Gould (1971)* this non-normally distributed temperature gradient can be caused by step like structure, consisting of sheets and layers. To show that a step-like temperature variation could account for these results *Hayes et al (1975)* used a simple model. They assumed that the temperature profile consists of layers of nearly homogenous water of thickness D separated by sheets of sharp gradients of thickness d << D. If a mixing process occurs randomly in the vertical where the layer thickness changes according to the Poisson probability law, then the probability distribution for the temperature gradient ($P(T_z)$) will be a gamma distribution,

$$P(T_z) = k(T_z^{\alpha-1} e^{-T_z/\beta})$$

where $P(T_z) > 0$ for $T_z > 0$ and $= 0$ for $T_z < 0$, and k is chosen such that $\int_{-\infty}^{\infty} P(T_z) dT_z = 1$. Here $\alpha = \mu\Delta$, $\beta = \underline{T_z}/\mu\Delta$, where μ is the mean rate of occurrence of sheets per unit length, Δ is the separation used to evaluate the temperature gradient, and $\underline{T_z}$ is the mean temperature gradient. For a given Δ, the mean and observed variance of the observed temperature gradients can be obtained. Since they are equal to $\beta\alpha$ and $\beta^2\alpha$, the gamma distribution can be evaluated. This gamma distribution is shown in Fig 5.3, along with the histogram of the temperature gradients. The agreement between the two appears satisfactory. The mean thickness of the layer evaluated using this model is 2.25 m. The value of the mean thickness in the North Western Atlantic was 1.65 m *(see Joyce and Desaubies 1976)*. In the central North Pacific values of 2.1 m and 4.7 m were obtained in the high and low temperature gradients respectively *(Gregg et al 1973)*.

5.3 Acoustic Fluctuations

The relation between sound speed variations and temperature-salinity variations can be written as

$$\delta c/c = a. \, \delta T + b. \, \delta S \quad \textit{(Dashen et al 1979)},$$

where $a = 3.19 \times 10^{-3}$ (°C)$^{-1}$, $b = 0.96 \times 10^{-3}$ (practical salinity units)$^{-1}$, T is the temperature in degrees C, and S the salinity. Since the salinity variation is less than one-tenth of the temperature variation, we ignore the second term. *Joyce and Desaubies (1976)* obtained the variance of the temperature jumps between two consecutive layers in the North Western Atlantic as 5×10^{-5} °C^2. The sound speed fluctuation corresponding to this is $<(\delta c/c)^2> = 5.1 \times 10^{-10}$. Since the average layer thickness for the CSIRO data is close to the pressure series difference, the variance of the temperature difference will be a good approximation to the variance of the temperature jumps between the layers. Using the temperature difference variance for the temperature profile shown in Fig 5.1, we obtained for the mean square sound speed fluctuation $<(\delta c/c)^2>$ a value of 3.1×10^{-8}.

HISTOGRAM OF TEMPERATURE GRADIENT AND GAMMA PDF
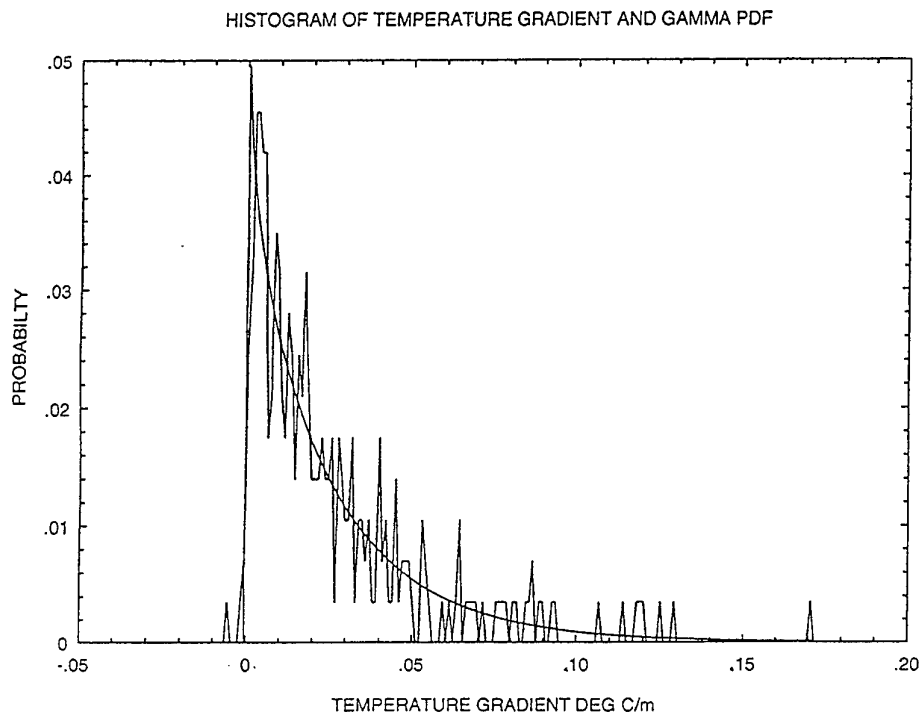
Fig 5.3 Histogram of temperature gradient and gamma probability density function (pdf) derived from Fig 5.2. μ=0.44m^{-1}, Δ=2 m, $\underline{T}_z$=0.026C, where μ is the mean rate of occurrence of sheets per unit length, Δ is the separation used to evaluate the temperature gradient, and $\underline{T}_z$ is the mean temperature gradient.

For the upper 700 m at the central North Pacific location the values varied from 1.2×10^{-8} to 4.0×10^{-8}.

Theoretical estimates of acoustic intensity and phase fluctuations at a horizontal range require values of parameters such as the frequency of sound, mean square sound speed fluctuation, and vertical and horizontal correlation lengths (*Unni and Kauffman 1981; Thuraisingham 1994*). With the available data it is not possible to estimate the horizontal correlation length at the Perth site. However this correlation length is in general about 50 times larger than the vertical correlation length, and the acoustic fluctuations are not very sensitive to the exact value. At the North Western Atlantic site a value of 74 m was estimated by *Unni and Kauffman (1981)*. Assuming a similar value for the Perth site, estimates for acoustic fluctuations were obtained for the two frequencies 2 and 5 kHz at a range of 200 m. At 2 kHz the root mean square intensity and phase fluctuations at the receiver are respectively 1.03 dB and 0.18 radian, while at 5 kHz they are 2.6 dB and 0.51 radian. Such a variation over an array would degrade its performance.

6. Wind, Waves and Rain

Wind, waves, and rain are important to the site survey as sources of surface generated noise. A knowledge of statistics of these parameters can allow noise to be forecast. Wind generated noise is the prevailing noise against which the signals must be detected. Winds and waves will also affect general sea conditions and vessel handling.

6.1 Winds

In winter the winds are predominantly from the west (westerly wind), bringing rain and a flow over the survey site that has a large and uniform fetch. In these situations, the anemometer at Rottnest Island, at the site shown in Fig 6.1, measures wind characteristic of the wind at our survey site. A wind buoy was deployed near the survey site and a comparison with the Rottnest anemometer is made in section 8. Wind buoys, it is claimed by *Ezraty (1991)*, can achieve precisions of 0.8 m.s^{-1} for speed and 5° for direction. The speed and direction of the Rottnest winds as well as their gustiness is shown in Fig 6.2a and 6.2b.

During summer there is commonly an easterly wind which flows off shore and then over the sea (a land breeze). For such winds, it is generally believed that the wind speed (at 10 m height) increases with fetch, i.e. with distance off shore. *Dobson et al (1989)* placed the increase at 30% at a fetch of 50 km. Sea breeze near Perth is discussed by *Gentilli (1971)* and the offshore gradient of the sea-breeze complicates the use of Rottnest wind statistics in summer. Such a set of statistics is shown in Fig. 6.3. Of note is the small number of "calm" days, especially during the summer months.

6.2 Waves

The wave climate has been measured at 32° 12'S, 115° 32'E where the water depth is 37 m. The probability of exceedence for significant wave height at various return periods is reproduced in Fig. 6.4 from the Cape Peron Ocean Outlet Feasibility Study by Binnie and Partners, Perth, 1981. Because of their exposed locations, the wave field should not be strongly influenced by topography at this location or at the survey site, and the wave climates at these sites might be related, after allowances for shoaling effects. The triangles in Fig. 6.4 are calculated from 20 years of hindcast data which provides a good statistical base. The vertical axis in Fig 6.4 is significant wave height, a statistical measure of the crest to trough height. From probability of exceedence one can calculate how often one expects 6-hourly averages of the significant wave height to exceed a particular value. It can be shown from Fig. 6.4 that a 10 year return period implies a significant wave height of 5 m for a six-hourly average. In contrast with the long term statistics at the Cape Peron site, Fig 6.5 shows the significant wave height, significant wave period and zero crossing period at location B (Fig 2.1) for a period in
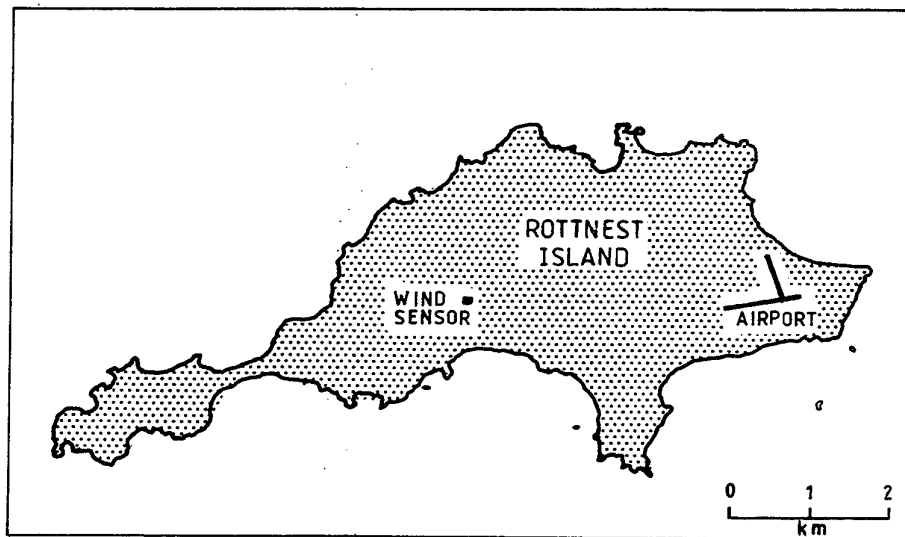
Fig 6.1 The site of the Rottnest Island wind anomemeter.

August 1992. Both time-series and spectral methods of calculating these statistics have been used. Five metres significant wave height was exceeded for longer than 5 hours on four occasions from 5 to 16 August 1992. The lengths of time exceeded were approximately 1 day, 5 hours, 2 days, and 1 day. An analysis of five years of waverider data for a nearby site (32°11'38"S, 115°32'22"E in 40 m depth) by Riedel and Trajer (1978) found a maximum wave height of 8.5 m, and extreme significant wave height of 5.1 m. Riedel and Trajer (1978) calculated from exceedence plots that 6.5 m significant wave height could be expected to occur for one day's duration in 10 years. For 6-hourly averages the value would be higher. The 10 year return period for a six-hourly average at site B can be expected to have a minimum value of 6.5 m, and could be guessed at as 9 m or higher.

6.3 Rain

The Perth area experiences the most rain in the winter season as shown in Fig 6.6. The number of rain free days can be deduced from Fig. 6.7 as 240 days a year. For the site survey, the rain rate was recorded by 5 cm radar and used in the assessment of the acoustic measurements. A time series of the rain rate is shown in Fig 6.8.
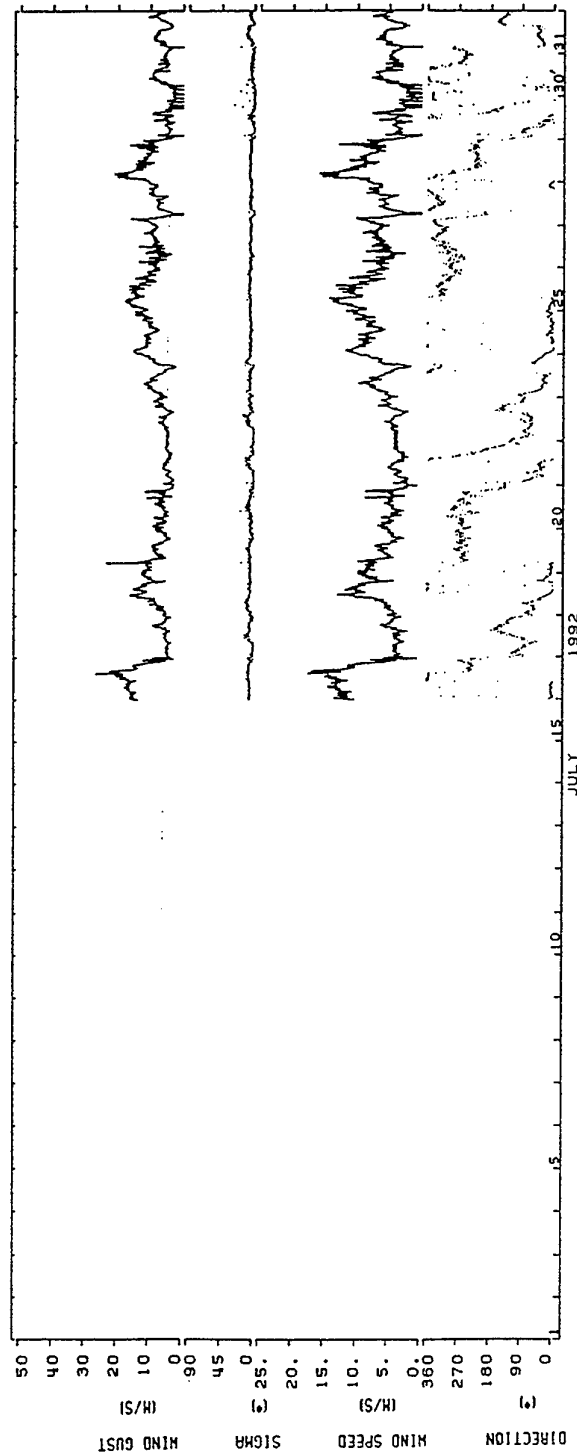
Fig 6.2a Wind speed, direction, standard deviation of direction and three second average wind gust data at the Rottnest site 16-31 July 1992.
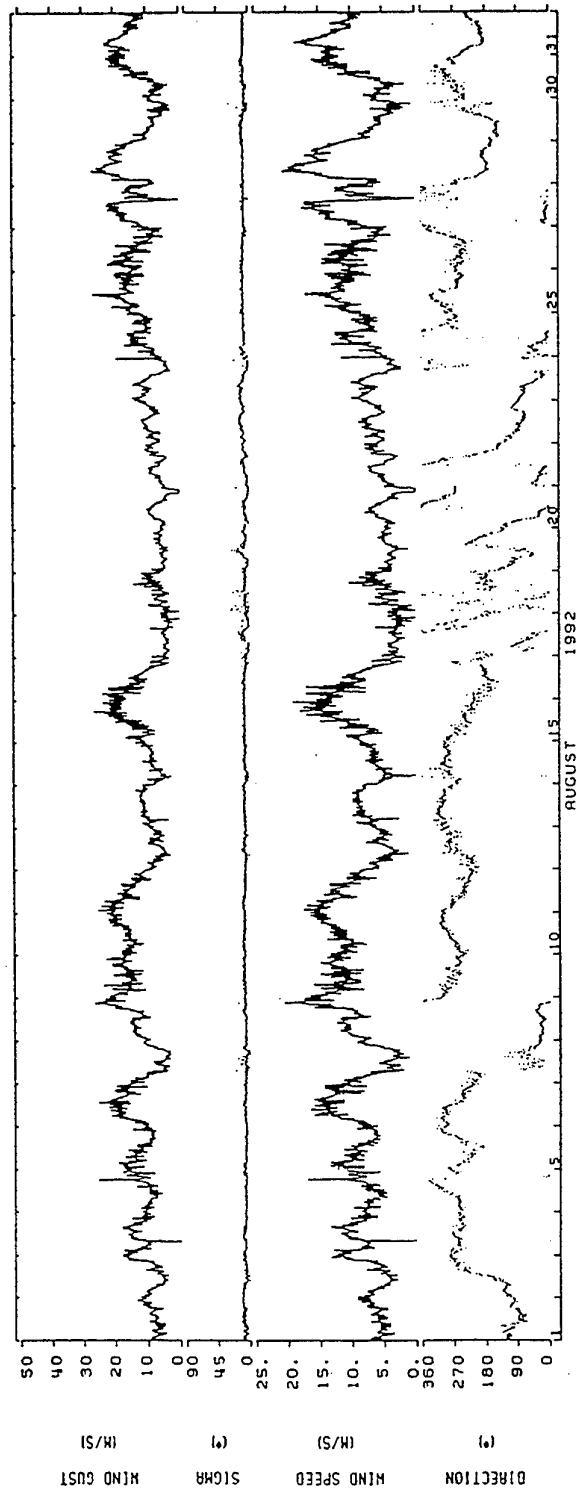
Fig 6.2b Wind speed, direction, standard deviation of direction and three second average wind
gust data at the Rottnest site 1-31 August 1992.
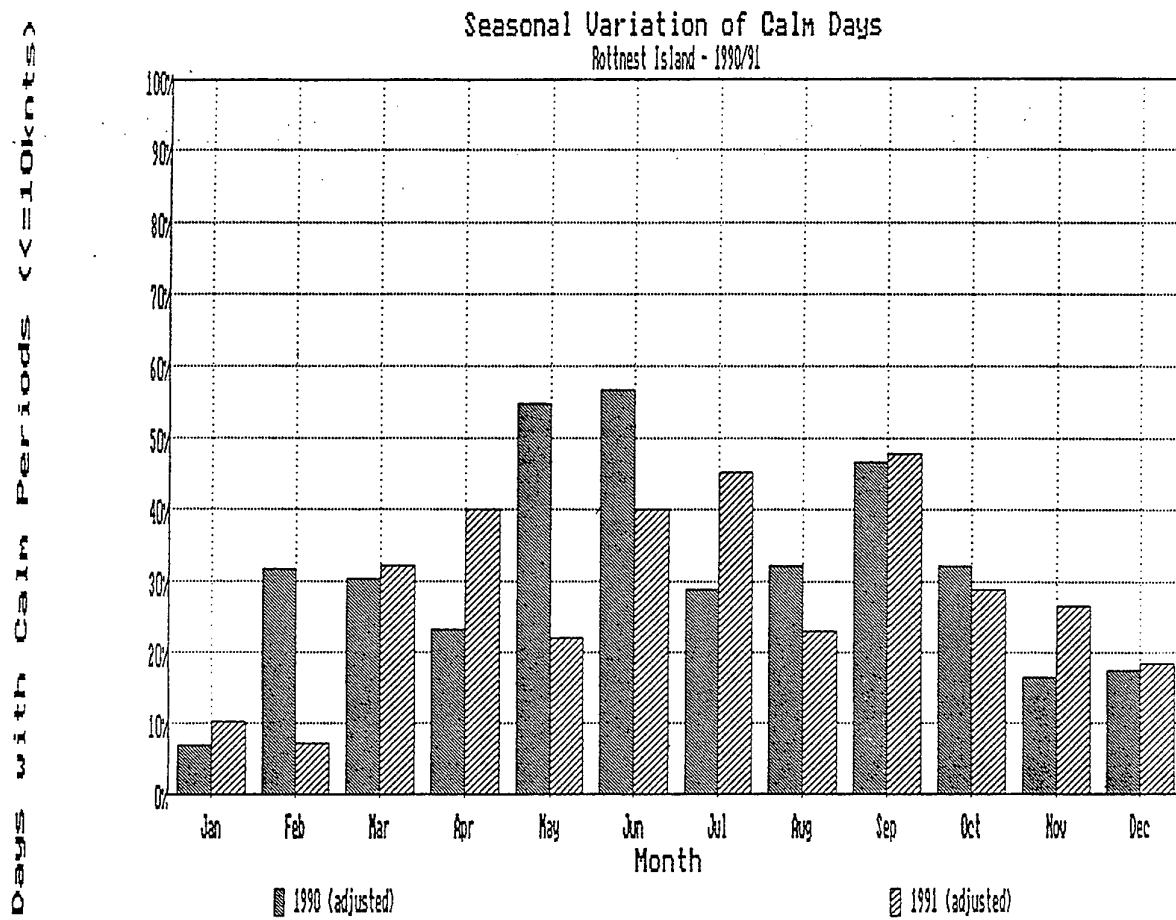
Fig 6.3   *Wind statistics for days with calm periods of more than 6 hours for Rottnest Island*
           1990-1991.
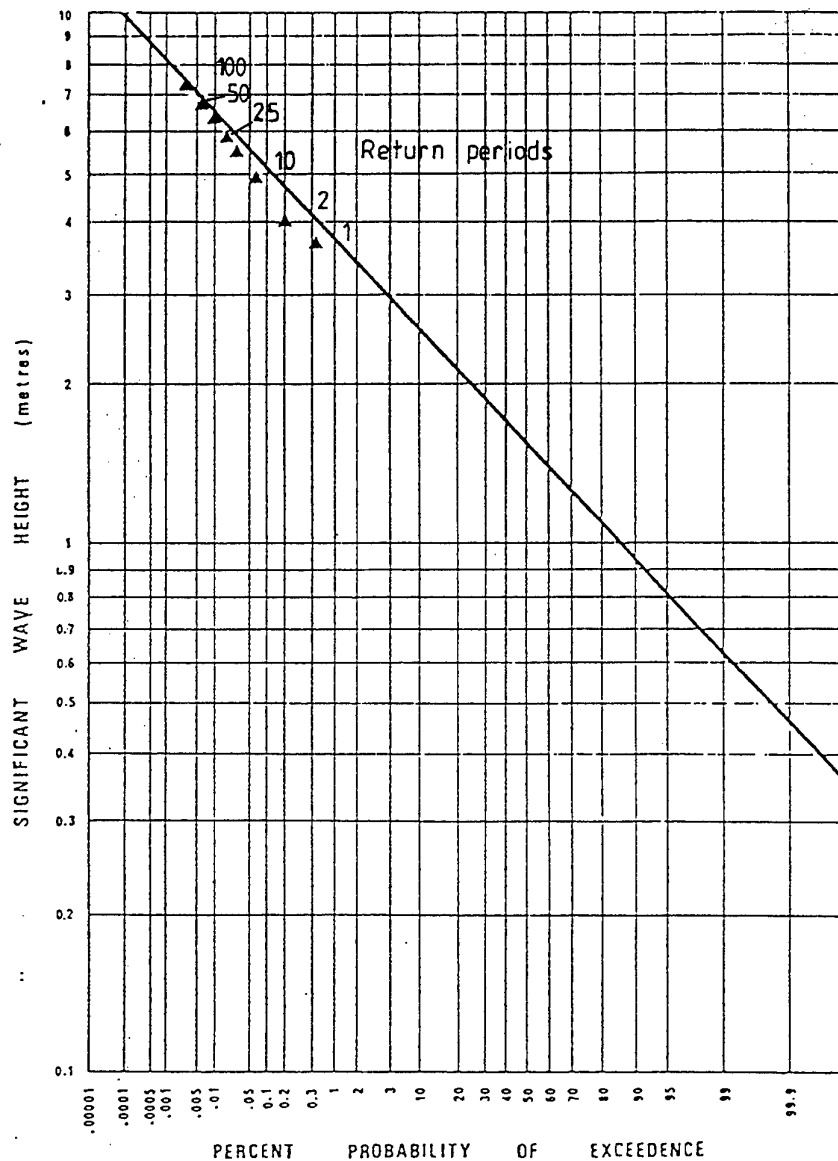
Fig 6.4   Significant wave height climate at 32°12'S, 115°32'E, water depth of 37 m. The solid line shows extreme significant wave heights determined from five years (1971 to 1975) of Commonwealth Department of Works waverider data. Triangles show 20 years (1962-1981) of hindcast data using Fremantle Port Authority wind records. Numbers with the triangles show expected return period in years. Figure supplied by Steedman Science and Engineering.
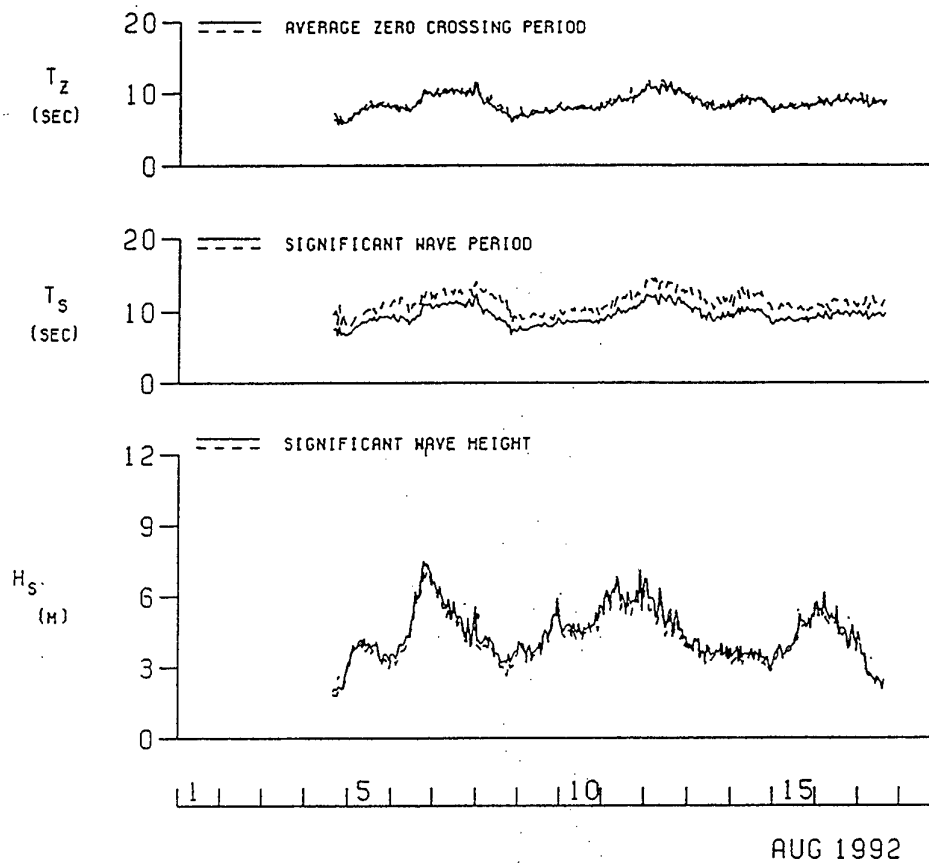
Fig 6.5 *Wave statistics at location B calculated by two methods. The broken line represents "wave-by-wave" time-series analysis while the solid line represents estimates from the spectra.*
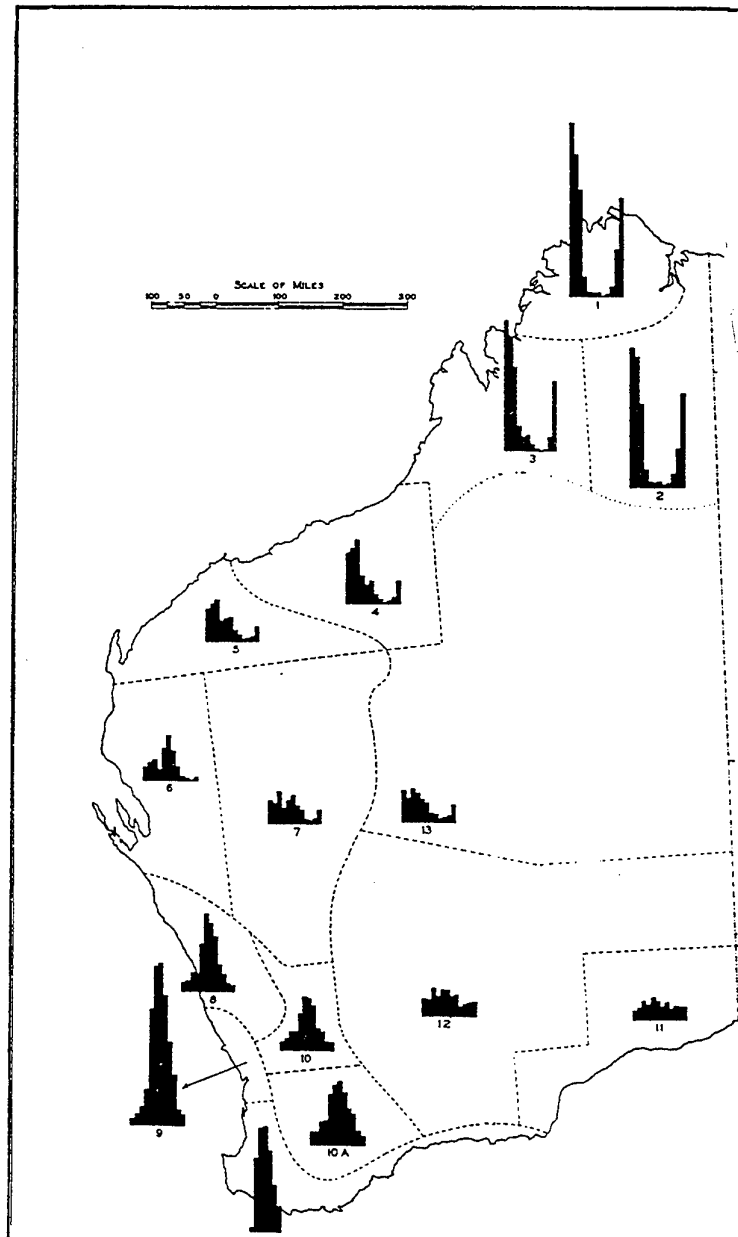
Fig 6.6   *Average rainfall each month of the year (after Gentilli 1971). The maximum value for the Perth region is 17 mm.*
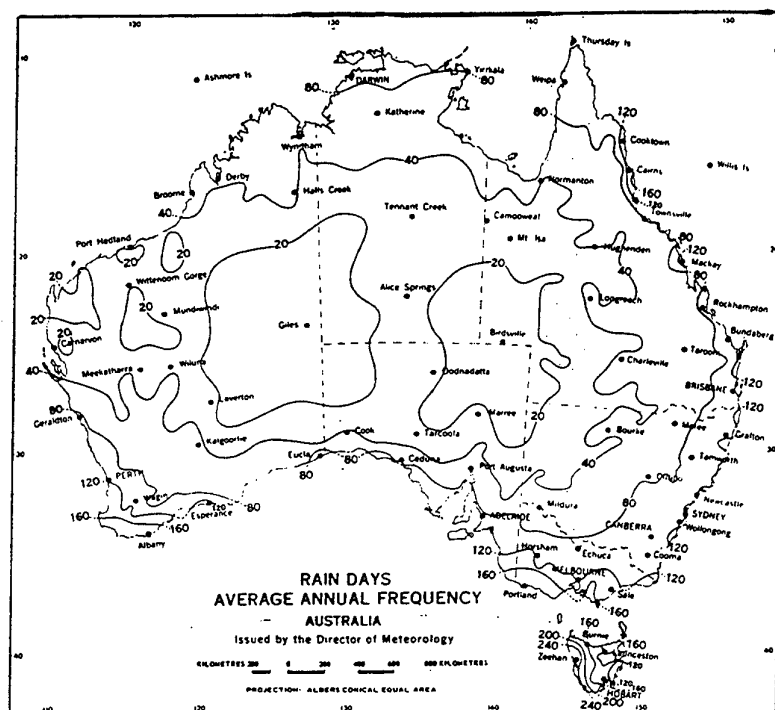
Fig 6.7 Average number of days with rainfall of 0.2 mm or more for Australia.

Rainfall for 10km Radius About Site.
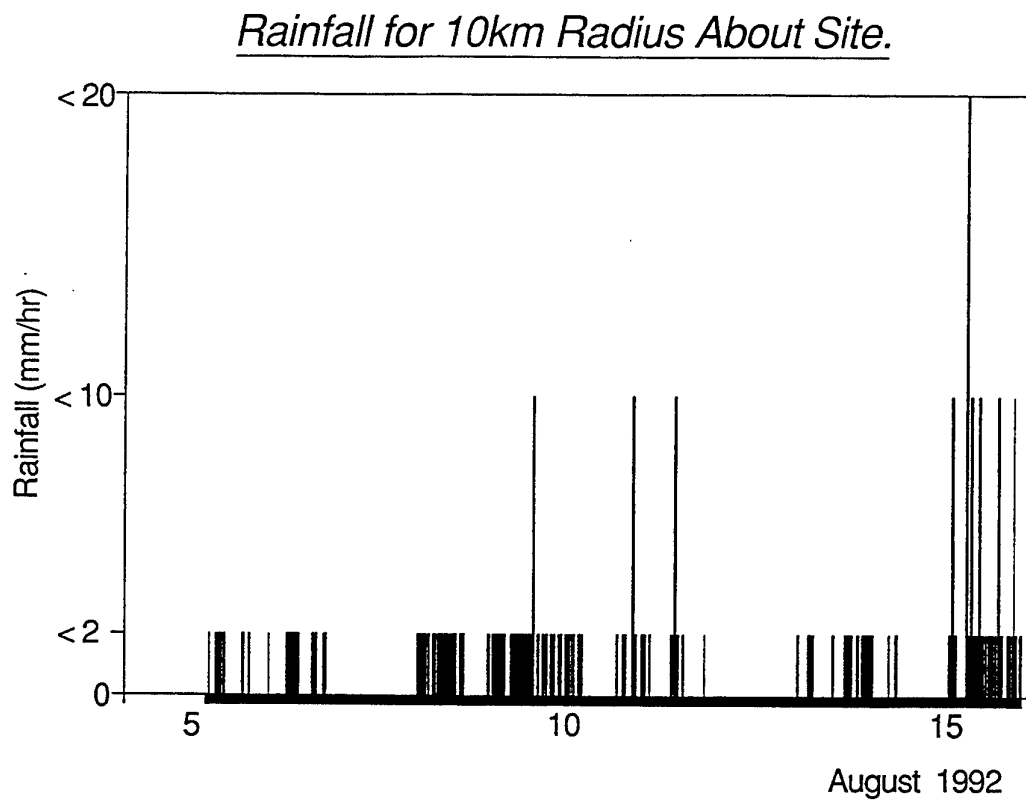
Fig 6.8 Rainfall rate over the site estimated from the Perth 5 cm radar.

7. Ambient Sea Noise

7.1 Introduction

Regardless of the circulation at the survey site, **the principal factor determining its suitability for an acoustic noise range is the ambient noise,** since this is the background against which acoustic signals must be measured. The ambient noise of the ocean, often referred to as "sea noise", is the general background noise from all sources, except those associated with the vessel or recording system making the measurements. It is a very complex phenomenon since it depends not only on the sound generation by the many different sources, but also on how the sound propagates to the receiver. It is common for ambient noise to vary over a range of about 20 dB as a result of varying weather conditions, shipping densities or biological activity, and this variation may be temporal, seasonal or geographical. The full range of variation of ambient noise, however is more than 30 dB. An approximate indication of the effect of this on system performance is that a variation of 20 dB would cause a variation of a factor of 10 in the distance to which a source would be detectable, while a variation of 30 dB corresponds to a factor of about 30 in distance.

The very properties of the ocean which make sound the most effective means of transmitting information also result in high ambient noise levels. In water sound propagates to distances two orders of magnitude greater than in air for the same absorption attenuation. As a result, the contribution of distant sources to ambient noise in water is much more significant than it is in air. For example, ships at distances of some miles may be clearly audible while those at ranges of hundreds of miles may contribute to the ambient noise in favorable propagation conditions. The extent to which distant sources may contribute depends on their source levels, propagation conditions, and the level of contributions from closer sources. However, in general, the ambient noise results from sources over a wide area.

The ambient noise field depends on the contributions from many different sources, and any contribution depends on the characteristics of the source and the way in which the sound it generates propagates to the receiver. Because there are many different types of source, and propagation conditions vary significantly, the noise field is very complex. It is these properties that make the noise so difficult to predict.

The main components of ambient noise in the ocean are:-

a. Sea surface noise: the noise of wind and wave action at the surface, usually referred to as "wind dependent noise", and rain noise

b. the noise of shipping, the contribution from distant shipping being distinguished by the term "traffic noise"; and

c. biological noise - the noise of fish, whales and invertebrates.

At frequencies below 100 Hz both wind dependent and traffic noise may be significant, sometimes one dominating, sometimes the other. Traffic noise is rarely significant above about 200 Hz and wind dependent noise is usually dominant. Biological noise is more intermittent than the other two and may occur in any frequency range. These components are reviewed in more detail in the appropriate sections.

7.2 Prediction of Ambient Noise

Because the various components are relatively independent, each varying significantly in space and time, spot measurements of ambient noise are no more than snap shots, and have little value in predicting the noise. The only effective method is to establish the relative contributions of the components and their individual behaviour. This requires a series of controlled measurements which allows the behaviour of the individual components to be analysed and interpreted and related to other parameters for which statistics are available, such as wind speed. Noise predictions can then be made by combining the components.

7.3 Measurements

Measurements were made with hydrophones on the bottom to avoid the problem of "flow noise" contaminating the recordings. Flow noise is caused by pressure fluctuations in turbulence in the vicinity of the hydrophones, which are sensed in the same way as acoustic pressures. Vortex shedding by flow about any cylindrical cross section is a particular problem. Fairings were fitted to all vulnerable components and the recording systems separated from the moorings by long lines lying on the bottom and thus subject to minimum water motion.

Samples of noise were recorded on tape at hourly intervals from 5 to 15 August 1992, and analysed after recovery. A meteorological buoy was moored at the site to provide measurements of wind speed and rain rate.

The recordings of ambient noise were analysed in 1/3 octave bands and converted to spectrum level (the value in a 1 Hz band).

8. Noise from Sea Surface Motion and Distant Shipping

This comprises the noise generated by various processes due to wind and wave action in the vicinity of the sea surface, and the noise generated by rain. Wind generated noise is the prevailing noise against which the signals must be detected. At low wind speeds, it gives the noise floor - the minimum background noise and best system performance. As a function of wind speed, it gives the range of wind speeds over which the system can be used. Thus from known wind speed statistics we can determine the proportion of the year that the system would be usable. **This is the crucial question that determines if the system will be viable.**

8.1 Noise from Wind and Wave Action

8.1.1 Review

The noise from wind and wave action is the prevailing noise in the ocean and was first described as a function of sea state by Knudsen, Alford and Emling (1944, 1948). Numerous studies since then have refined our knowledge of this component of ambient noise, but there still remains a significant uncertainty in the prediction of the noise. There are a number of different source mechanisms associated with wind and wave action, and these vary with limited interdependence. The resulting noise field depends on the strengths of the sources, their distributions and the prevailing propagation conditions. It varies, therefore, not only with weather conditions but also with position.

From many studies in waters near north America, Wenz (1962) found that noise from wind and wave action was mainly evident at frequencies above about 100 Hz, showing a broad peak at about 500 Hz. This work did not show the significance of surface generated noise below 100 Hz because it was obscured by the high levels of traffic noise in the waters where the measurements were made. In spite of much evidence of high levels of surface generated noise at frequencies below 100 Hz, especially in areas of low traffic noise like those around Australia and New Zealand, some prediction methods still limit surface generated noise to frequencies above 100 Hz.

The many complicated processes involved in the generation, breaking and decay of sea surface waves and their interaction with the wind result in a number of noise generation mechanisms which contribute to different parts of the noise spectrum. The term "wind dependent noise" is used because it has been found that the noise is more directly related to wind speed than to wave height or sea state. Although there are rule of thumb relationships between wind speed, wave height and sea state, these are average relationships and apply only to conditions of a steady wind over a fully developed area. For example, if the wind were to start blowing over a calm sea, small

scale capillary waves would appear almost immediately, but it may take many hours for the large scale gravity waves to develop to the full height corresponding to the wind speed, and these would persist well beyond the cessation of the wind. Experiments under these conditions have generally shown that the noise varies with the wind speed rather than the wave height and, as we shall see, an analysis of the mechanisms of noise generation indicates that it is the direct action of the wind that causes the noise.

Empirical evidence shows that there are two main components of wind dependent noise: the component identified by Wenz with a broad spectral peak at 1000 Hz, and a component that decreases with frequency and dominates from about 10 Hz to 200 Hz. In addition there is a component which is directly related to surface wave motion and dominant from less than 0.2 Hz to about 10 Hz.

Although it has been known for many years that the component with the broad spectral peak at about 1000 Hz is the result of wave breaking, it is only recently that the main source has become evident. In studies of wave breaking in water flowing through a laboratory tank, Banner and Cato (1988) found that the significant source was the oscillation of the air bubbles created by air entrainment as the wave breaks. Other studies have confirmed and extended this work. The significance of this knowledge is that it provides the information about the source characteristics needed to match to propagation models to predict the noise field. Volumetric oscillation of an air bubble in water is effectively a simple or monopole source of sound. If the bubble is close to the sea surface, the influence of its surface image substantially affects the sound radiation pattern and for depths significantly less than a wave length, the radiation from the bubble and its surface image may be modelled as a dipole with its axis of maximum radiation downwards.

There have been many measurements of this wind noise component and the dependence of the noise on frequency and wind speed has been fairly well established. However, there are other factors which affect the noise and actual noise levels at a particular wind speed may vary with the depth of receiver and also from one location to another. The actual noise level received at some depth depends not only on the noise generated but also on how it propagates to the receiver, so different propagation conditions from one location to another are likely to result in different noise levels. Some locations are as much as 10 dB noisier than others. On average, the noise decreases with depth and near the bottom in a deep ocean basin may be as much as 20 dB lower than near the surface. Another cause of variation is the actual sea surface conditions which will affect the noise generation.

Seasonal variations in noise level of several decibels have been observed possibly due to changes in surface wave conditions (for example a seasonal variation in the prevailing wind direction may result in a different wind fetch), and to changes in propagation caused by changes in the temperature profile which affects the sound speed profile.

Between about 10 Hz and 100 Hz, there is another wind dependent noise component which decreases in level with increasing frequency. This component has some similarity in its spectra to that of traffic noise, and it is usually difficult to determine how much of the measured noise is traffic noise and how much is wind dependent noise. As a result, less is known about this component of wind dependent noise than about the other components. The mechanism of noise generation is thought to be oscillation of bubble clouds (Prosperetti 1988a,b; Carey and Browning 1988). As with the high frequency component, one might expect that actual sea surface conditions and the propagation conditions will affect the actual level of noise received at a particular wind speed.

The nature of the sources of wind dependent noise suggests that they would radiate as distributed dipoles with axis of maximum radiation close to vertical. This is consistent with observations of the noise field characteristics (Ferguson & Wyllie 1987).

The component of surface generated noise that is directly related to the wave motion has a pronounced peak in the spectrum at a frequency of 0.2 Hz or above, being twice the frequency of the peak in the wave height spectrum. The spectrum level falls at about 20 dB per octave above the spectral peak and even more sharply below the peak. This component is evident up to frequencies of a few hertz until it becomes masked by the mid frequency component. The mechanism responsible for this component is better understood than the others, and noise levels can be calculated theoretically (Brekovskikh 1966; Hughes 1976; Cato and Jones 1988; Cato 1991b).

8.1.2 Relationship between Noise and Wind Speed

Although there is a general correlation of noise as a function of wind speed (better than with any other environmental parameter), the relationship between noise and wind speed varies with location, and even at a fixed position there is significant variation about the mean for a particular wind speed. The reasons for this relate to variation in propagation conditions between locations, and variations in the interaction between wind and waves affecting the complex mechanisms of noise production. There are a number of different mechanisms of noise production. Different mechanisms predominate in different frequency bands so that the noise behaves differently at different frequencies.

At frequencies above about 200 Hz, noise dependence on wind speed is fairly well known, but there is still significant unexplained variation at any wind speed. The between site variation i.e., the variation in level at a particular wind speed between studies in different locations is about 10 dB at 1 kHz for winds between 10 and 20 knots, and 10 to 15 dB for winds below 10 knots. The variation in level at a particular wind speed at a particular location is in the range 5 to 10 dB.

Far less is known about wind dependent noise below 200 Hz. Data are limited because of the difficulty of isolating this from the noise of distant shipping which has similar spectral characteristics. Generally, it has not been possible to separate the contributions from wind and shipping in North Atlantic studies because of the high shipping

densities there. There have been a few studies near Australia and other places in low shipping areas which give some idea of noise dependence on wind speed, but there is considerable variation and thus uncertainty in estimating levels. Comparison of data from the different studies in different locations shows a spread of about 20 dB at a particular wind speed.

Although we made measurements of noise at various wind speeds in 100 m of water near the proposed URNR site in January 92, these were merely "snapshots" and far too small a sample to give other than a general idea of wind generated noise levels, the purpose being to obtain a quick, first order indication of the noise rather than to carry out detailed controlled measurements. The wind measurements were made from the vessel with an uncalibrated hand held anemometer, which does not allow more than a very rough comparison with the long term wind statistics.

Without the measurements reported here we would rate the uncertainty in knowledge as ± 10 dB at frequencies below about 200 Hz, and ± 5 dB above 200 Hz. This is the uncertainty with which the wind versus noise relationship could be predicted without further measurements to determine the usable period of range operation in terms of wind statistics.

8.1.3 Results of Measurements near the Site

Figures 8.1 to 8.5 show the measured noise as a function of wind speed for various 1/3 octave frequency bands. The wind speed data were obtained from the Bureau of Meteorology anemometer at Rottnest Island, about 30 miles to the north east, since the meteorological buoy data were limited to only two days of the noise recordings. Comparison between the wind speed at the site measured on the buoy and that measured at Rottnest Island is shown in Figs. 8.6 and 8.7. This shows a fair degree of correlation. Weather patterns suggest that correlation between the wind at the site and at Rottnest should be good in winter, but less so in summer when it is complicated by the effect of the sea breeze.

The noise data in Figs 8.1 to 8.5 were carefully selected to ensure that the samples were not contaminated by other noise components. This meant rejecting a substantial number of samples which included rain, ship noise, or biological noise. Traffic noise (see below), however, cannot be excluded and remains a part of these samples.

At high frequencies (500 Hz to 8kHz: Figs. 8.3 to 8.5), a clear correlation of noise with wind speed is evident, surprisingly good considering the wind data were obtained from Rottnest Is. rather than at the site. Also shown on these figures is the linear regression line calculated as the regression of noise level on logarithm of wind speed.

At lower frequencies, the effect of traffic noise is evident, providing a non-wind-dependent noise floor evident at the lower wind speeds. The traffic noise varies over a range of about 10 dB, so the correlation of noise with wind speed is significantly poorer than at the higher frequencies.

Fig. 8.8 shows some sample spectra of noise at different wind speeds.
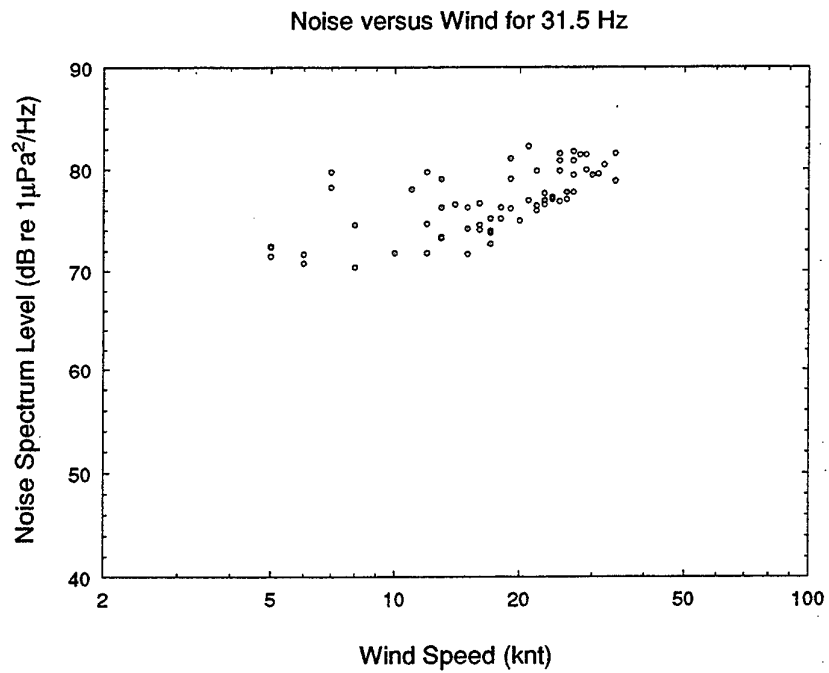
Fig 8.1 Noise versus Wind for 31.5 Hz.
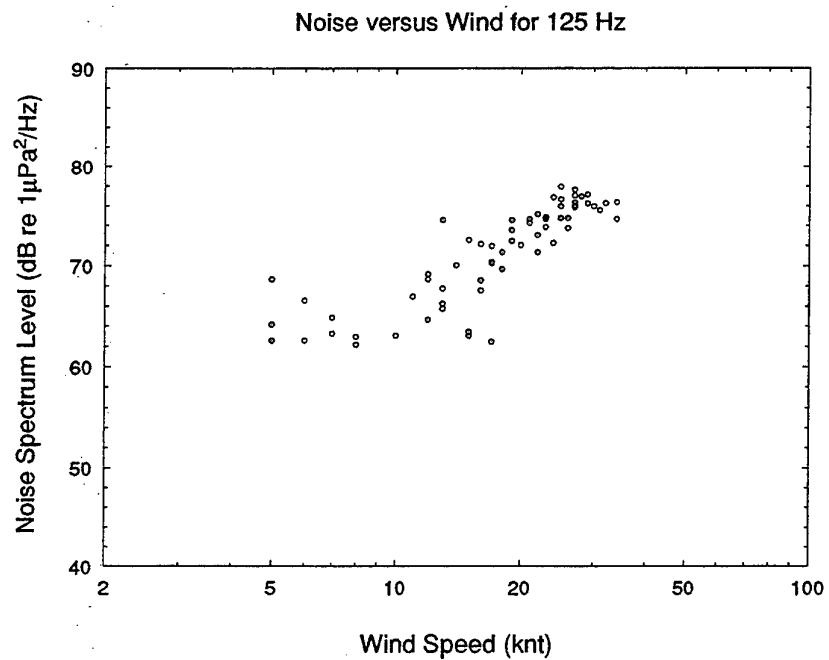
Fig 8.2 Noise versus Wind for 125 Hz.

Noise versus Wind for 500 Hz
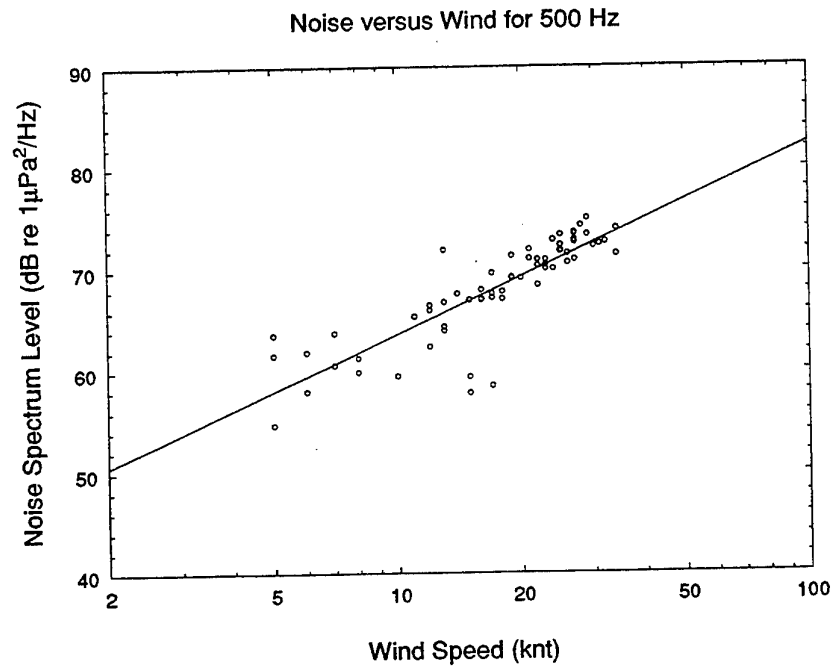
Fig 8.3 Noise versus Wind for 500 Hz.

Noise versus Wind for 1 kHz
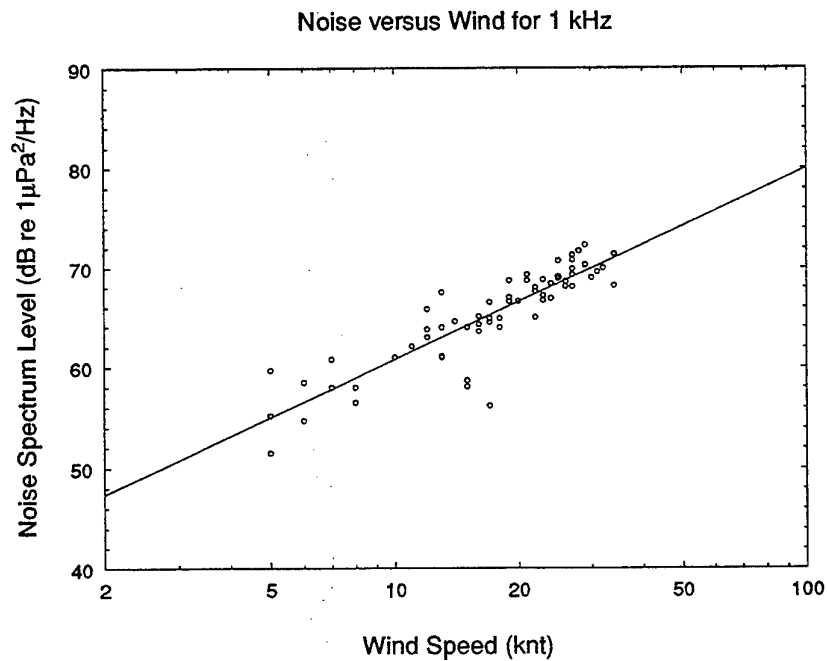
Fig 8.4 Noise versus Wind for 1 kHz.

Noise versus Wind for 8 kHz

Fig 8.5 Noise versus Wind for 8 kHz.
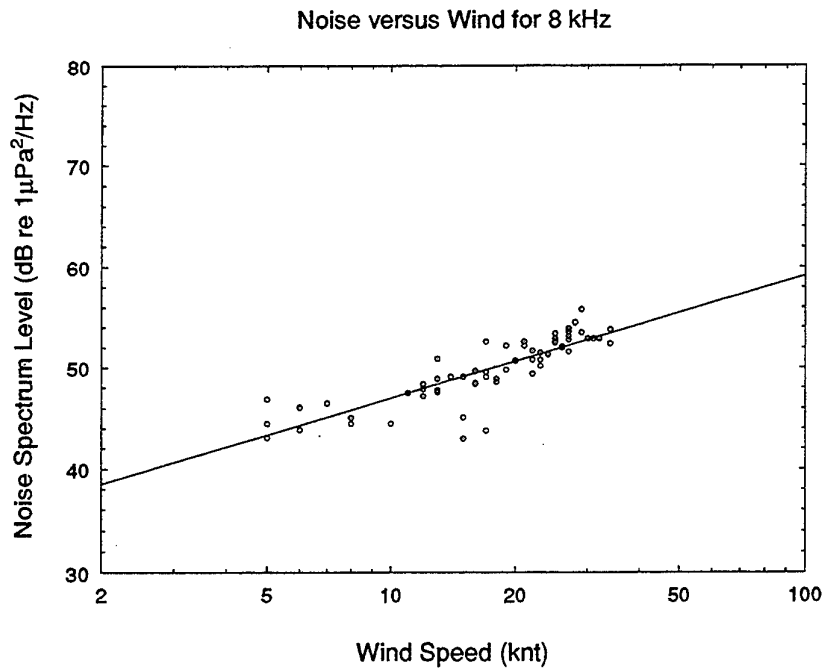
COMPARISON OF WIND SPEEDS AT SITE AND ROTTNEST IS.
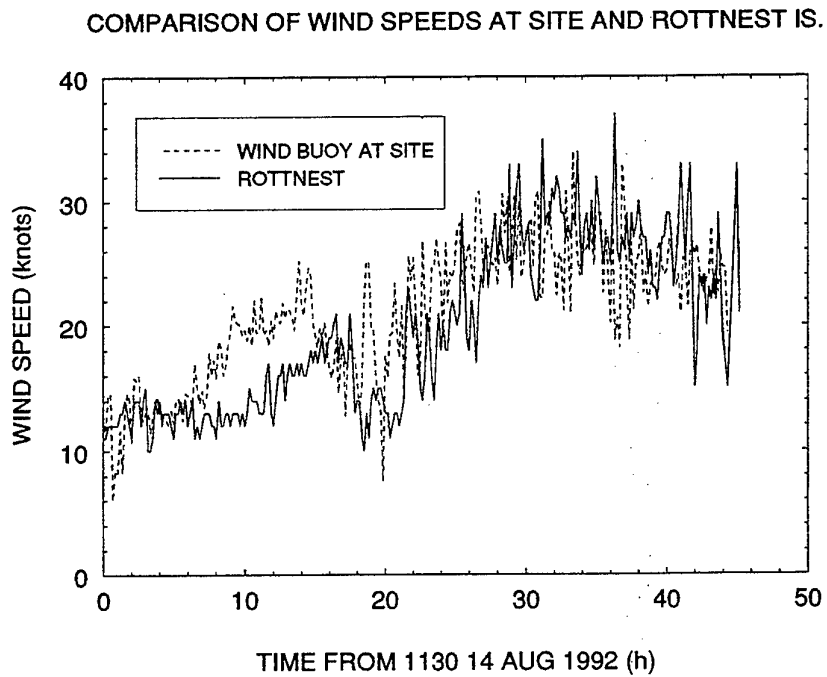
Fig 8.6 Time series comparison of Wind Speed at Site and Rottnest Is.

COMPARISION OF WIND SPEED AT SITE AND AT ROTTNEST IS.
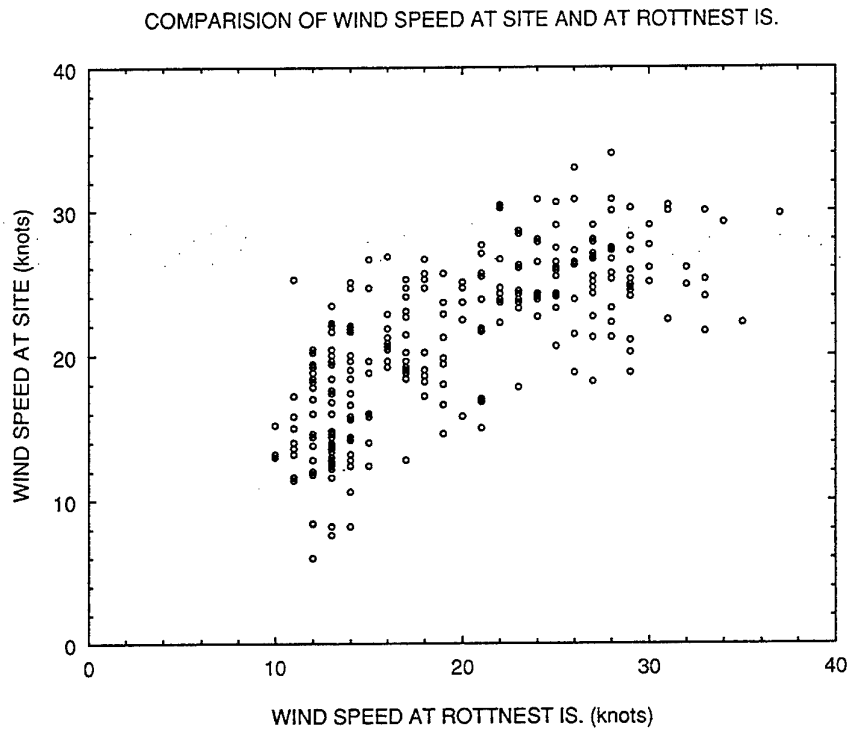
Fig 8.7 Scatter plot comparison of Wind Speed at Site and Rottnest Is.

Noise Spectrum Level at different wind speeds
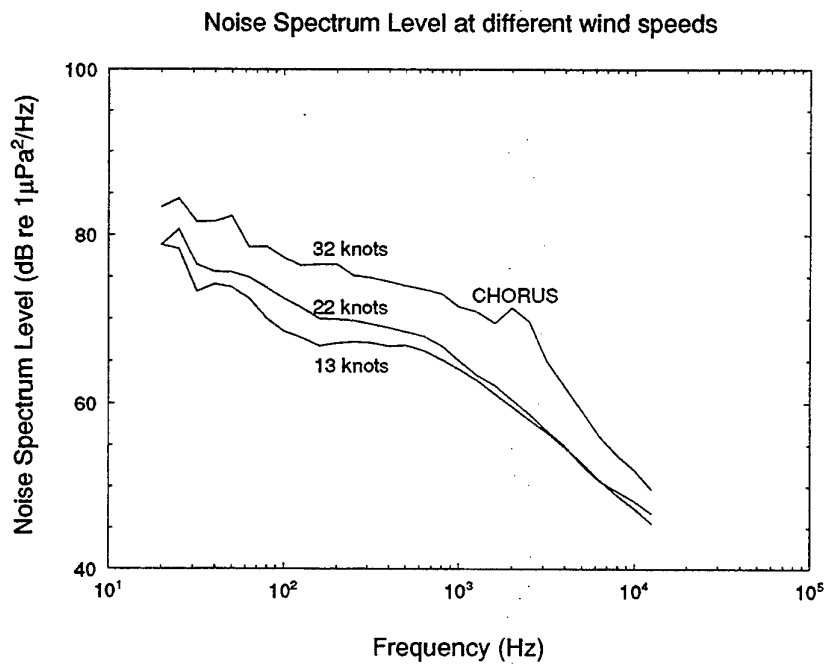
Fig 8.8 Noise Spectrum Level at different wind speeds.

8.2 Rain Noise

8.2.1 Review

It has been known for many years that rain causes high levels of ambient noise with a spectrum that is almost white in character. It is, however, only recently that the mechanics of sound production have been understood. The momentum of a rain drop as it strikes the sea surface may be sufficient to part the surface and allow a small parcel of air to be entrained as the surface closes behind it. The air is initially compressed but quickly expands to form a spherical bubble which expands and contracts in radial oscillation. The sound generated by this bubble oscillation is substantially more intense than the sound of the impact of the drop at the surface. The highest levels of rain noise are due to the oscillation of the entrained air bubbles. However, not all drops entrain air. Pumphrey and Crum (1989) showed that only drops in a certain range of diameters and impact velocities entrained air, and that this range of values varied according to the angle of impact which in turn depended on the wind speed. As a consequence, there is no simple relationship between rain noise level and precipitation rate.

As discussed above, sound radiation by air bubbles just below the sea surface may be expected to be dipole in character, with maximum radiation downwards. The generation of the much less intense sound by the impact of a rain drop on the sea surface may be expected to be dipole in character, the direction of the axis being in the direction of the drop momentum (Cato 1991a). As a consequence of the preferentially downward radiation, the noise of a rain storm can be expected to be fairly localised, the rain noise level decreasing significantly outside the area of rain.

8.2.2 Results of Measurements near the Site

Fig. 8.9 shows a sample measured spectrum of rain noise. There has been no detailed analysis of rain noise in this survey, since it is well known to produce high noise levels unsuitable for noise ranging. Measurements in other studies including some in Australian waters show that noise levels during the passage of a rain storm are likely to be as much as 10 dB higher than those shown in Fig 8.9.

Rain, 18:04 13 August 1992
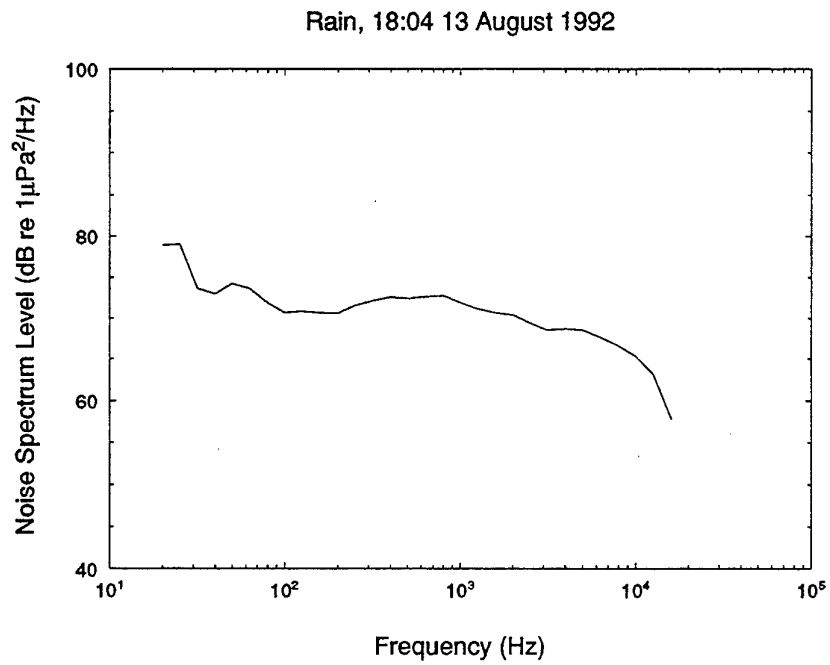
Fig 8.9 Acoustic Spectrum in the presence of Rain, 18:04 13 Aug 1992.

8.3 Traffic Noise

8.3.1 Review

Traffic noise was defined by Wenz (1962) as the combined effect of the noise of distant shipping where the noise from any one contributing ship would not be significant nor detectable by an omni-directional system. The noise of many ships combine to produce a nondescript background noise which has none of the distinguishing characteristics of noise from a single ship. The actual level of traffic noise depends on:-

a. the number and distribution of ships in the particular sea or ocean basin;

b. their source levels; and

c. the propagation conditions.

In deep ocean basins where propagation conditions are good, ships throughout the ocean basin may contribute. That is, if there are sufficient ships at a distance of, say, 300 miles, their combined effect may be a significant contribution to the ambient noise even though an individual's contribution may be negligible. This idea originated in the North Atlantic Ocean where there may be as many as 1000 ships underway at any time (Wenz 1962).

The deep water of the Indian Ocean provides good propagation conditions. The relatively small number of ships, however, means that the idea of traffic noise as the cumulative effect of the contribution of many ships is less applicable. Traffic noise in the Indian Ocean is thus likely to be quite variable since it depends on the disposition of a relatively small number of vessels. Lines from individual ships are more likely to be evident than in regions of high shipping densities. Most available measurements of deep water traffic noise in the Indian Ocean were taken around 20 years ago. These are summarised by Cato (1976) and more details are given in reports of the then RAN Research Laboratory by the same author. Since these measurements were made, there have been changes to both shipping distributions and the types of ships, due mainly to the development of mineral exports from Western Australian ports. The effect of such changes has been considered elsewhere (Cato 1984a,b). Although this would be expected to change the traffic noise levels, the change is not considered to be large compared to other uncertainties. This is mainly because traffic noise is relatively insensitive to the actual numbers of ships (for example, a doubling of the number of ships of the same ship type would increase the noise levels by only 3 dB).

Note that these comments apply only to "traffic noise" as defined above. Any ship close enough to be individually detectable would add to these noise values and close vessels would result in substantially higher noise levels, though of similar spectral shape.

8.3.2 Results of Measurements at the Site

Traffic noise levels were estimated from the measurements by examining the data used for the noise versus wind speed plots of Figs. 8.1 to 8.5, from which other noise contributions were eliminated as far as possible. The estimate was determined as the range of non-wind-dependent noise variation at low wind speeds. The resulting range of noise spectra are shown in the summary figure Fig. 8.10. The range of variation is a little less than 10 dB, comparable to that of the earlier measurements in deep water (Cato 1976). The mean level is about 2 dB different to these earlier measurements, which is insignificant in view of uncertainties involved in such estimates. It might be expected that the up-slope propagation required to reach a receiver at the site in water depth of 400 m could cause some reduction in noise levels compared to the deep water.

On the other hand, the presence of the port of Fremantle might be expected to result in higher noise levels than otherwise expected because of the concentration of shipping lanes in the area, and noise from shipping inshore of the site (where the shipping lanes are) could be somewhat enhanced by down-slope propagation.

Measurements in water depths of 100 m off Fremantle in January 1992 (Wyllie, Cato and Taylor 1992), however, showed that noise levels at low frequencies and low wind speeds (and thus attributable to traffic) are about 10 dB lower than those at the 400 m site. While these measurements were too few to provide other than a "snap-shot" of the noise (i.e. they are not significant statistically), they do suggest that traffic noise levels in 100 m depth are substantially lower than at the 400 m site or in deep water, in spite of the proximity of Fremantle to the shallow water site. This may be due to the poorer up-slope propagation to the 100 m water depth.

The above discussion refers to traffic noise as defined, and does not include the noise from ships that are individually detectable. Ships were audible as individual sources on a number of occasions resulting in much higher noise levels than obtained from traffic noise. An example is shown in the spectrum of Fig 8.11, which may be compared to the generally lower levels shown in Fig 8.8 caused by wind and chorus.
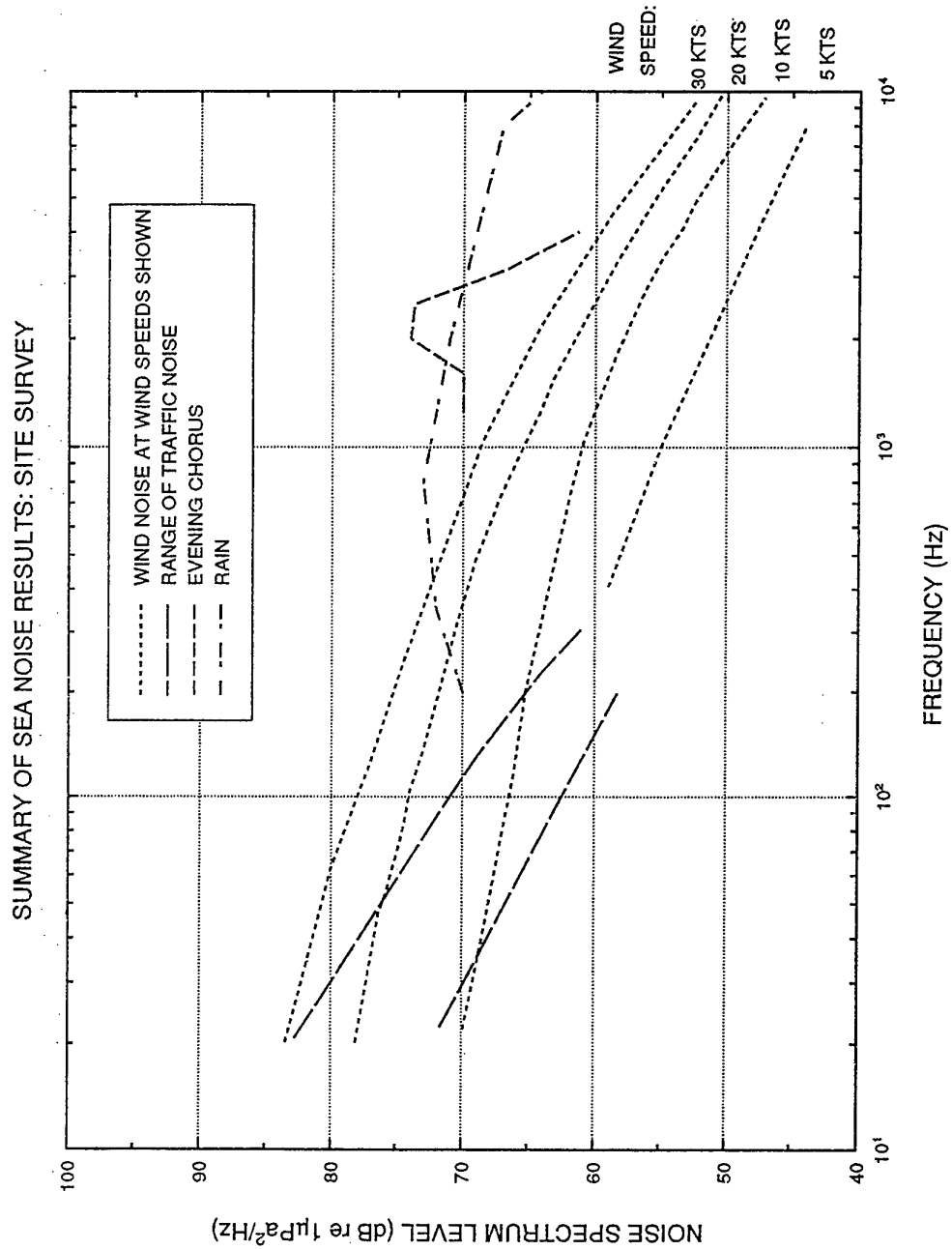
Fig 8.10   Range of traffic noise observed during measurements.

9. Biological Noise

While a wide range of animals produce sounds, not all are important in terms of the contribution to the ambient noise. The most significant contributions are (a) the choruses, which result when large numbers of animals are calling and (b) the intense transients of the higher source level calls. The choruses increase the general background noise levels while the transients are evident as individual signals.

9.1 Biological Choruses

The term biological chorus is used here to mean the continuous noise (averaging time ~1 s) produced when large numbers of individuals are producing sounds. So many sounds overlap that the noise level is far higher than that of an individual sound. In some choruses, the individual sounds may still be detectable, while in others they merge together. Choruses are common in Australian waters, causing levels to vary by more than 20 dB over periods of a few hours (more than 30 dB under some conditions). They occur frequently (usually daily), and contribute over a broad frequency band. Different choruses have different diurnal, seasonal, geographic and spectral characteristics.

A number of studies of ambient noise around Australia have shown the presence of choruses from which the general nature of their occurrence and spectral characteristics was determined (Wyllie 1971 ; Cato 1969, 1978a; Kelly, Kewley and Burgess 1985). Statistical analysis showed that choruses were widespread in waters near Australia, contributing in the frequency band from about 400 Hz to about 5 kHz. More recent work has found choruses with energy extending to frequencies as low as 50 Hz at levels up to 30 dB above the usual background (Cato 1992). Most choruses last for a few hours and the most consistent time of occurrence is just after sunset, although choruses have also been observed just before sunrise and around midday. Spectrally different choruses have often been observed at the same location, sometimes overlapping in their times of occurrence. The typical increase in noise level during a chorus is about 20 dB. There is some evidence of seasonal variation, but data are still too limited to draw general conclusions.

Most measurements have been made in the tropics either in shallow water, or in deep water within 6 km of shallow water. Choruses have, however, been observed in deep waters well distant from land and in latitudes comparable to those of the proposed site.

Choruses are produced by invertebrates, fish and whales. The best known chorus is that from snapping shrimp, but it occurs only in shallow water since the particular genera of shrimps responsible are found mainly in water depths of less than about 60 m.

Ship, 17:39 5 August 1992
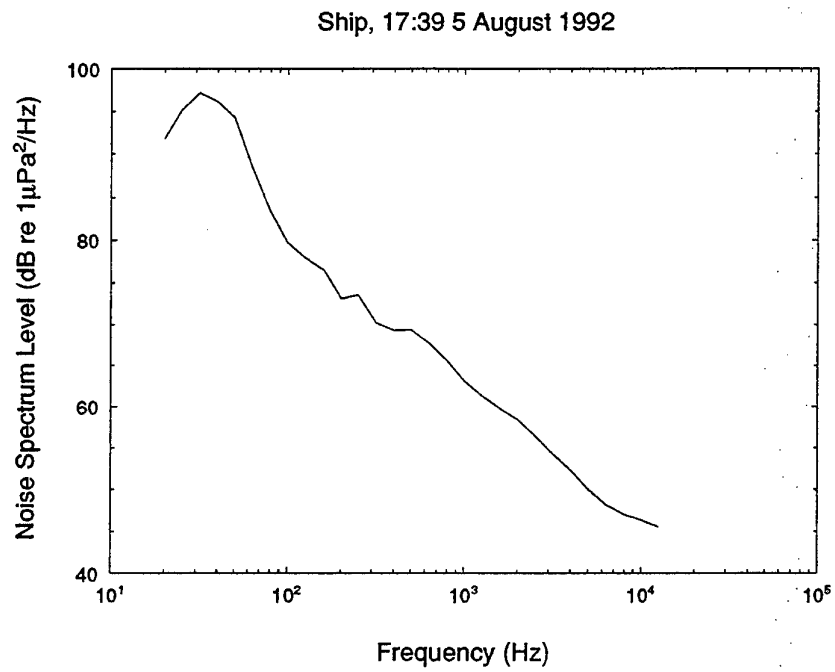
Fig 8.11   Acoustic Spectrum in the presence of a Ship, 17:39 5 Aug 1992.

The regularly occurring choruses with most energy in the frequency range 400 Hz to 5 kHz comprise large numbers of click sounds typical of stridulatory sounds of fish and invertebrates, usually with so many sounds overlapping that individual sounds are not distinguishable. These may be related to feeding or other diurnal behaviour of the animals. Choruses of this type have been observed off the New South Wales coast at similar latitudes to the site.

Regular choruses with most energy at frequencies between 50 Hz and 400 Hz have been studied in Australian tropical waters (McCauley 1989; Cato 1992). They comprise sounds typical of those produced by fish by muscular excitation of the swim bladder (Tavolga 1964). These are more variable in diurnal occurrence and may be quite seasonal, since sound production tends to be related to spawning. Choruses of this nature have been heard in the deep water of the Indian Ocean, though well north of the site (Cato 1978a; Kelly et al. 1985).

The diurnal, seasonal, and geographical variation of the choruses can be expected to depend on the behaviour of the animals in relation to sound production. Where sound is associated with feeding, perhaps incidental to it (such as fish scraping teeth on rocks, coral) choruses will, of course, be related to times and conditions of feeding, and so exhibit diurnal regularity. Sound used for communication during spawning can be expected to produce choruses with strong seasonal dependence. Seasonal dependence will also result from species migration, i.e., it will be determined by the time the animals pass through a particular area.

9.2 Sperm Whale Choruses

Some whales also produce choruses. The source strengths of their sounds are significantly higher than those of fish or invertebrates, so smaller numbers of individuals are needed to produce a substantial chorus. Although the popular conception is that whale numbers are very low, this is true only for a few species, and some of these have shown substantial recovery of stock numbers in the last 20 years. The most significant whale chorus is that from sperm whales. These are toothed whales, and in contrast to the other large whales which are all baleen whales, they often congregate in large schools like the smaller toothed whales (e.g. dolphins, killer whales). Schools of 10 to 50 sperm whales are common (Caldwell, Caldwell and Rice 1966) but there are reports of schools of thousands of individuals (Paterson 1986). Sperm whales generally keep to deep water. Significant numbers are to be expected in waters around Australia, as have been observed in the Tasman Sea (Paterson 1986).

Sperm whales produce intense clicking sounds which result in high level choruses with most energy between 1 and 5 kHz and maximum levels comparable to the other choruses. The significant difference between these choruses and those of fish and invertebrates is that they do not have the regularity of occurrence. Sperm whales choruses may persist for many hours at a time, even for days though with some waxing and waning. The occurrence of sperm whale choruses is more difficult to

predict than those of fish and invertebrates, because their behaviour is more complex and less predictable. These whales are nomadic and migrations patterns are ill defined. Their choruses are well known to sonar operators who refer to them as the "carpenter fish" since some consider that they sound like many carpenters hammering.

Sperm whales are known to congregate in the deep waters on the edge of the continental shelf around the south western corner of Australia (Bannister 1968). These were the whales taken off Albany during the final years of the whaling station which closed in 1978. It should be noted that in spite of whaling activities, sperm whales still exist in large numbers. The closure of the station at Albany was in response to community attitudes to whaling in general, not to any observed decline in the population. Sperm whale choruses have been observed in waters near Australia, including the tropical east Indian Ocean (Cato 1978a).

9.3 Humpback Whale Choruses

Humpback whale sounds were responsible for a persistent chorus observed near New Zealand in the late 1950's which had almost disappeared by 1961 as a result of the decrease in whale numbers through whaling (Kibblewhite, Denham and Barnes 1967). The significant recovery of humpback whale stocks in Australian waters has resulted in increasing chorus activity, though more often humpback whale sounds are audible as discrete transients rather than as continuous choruses.

9.4 Intense Biological Transients

The sounds of many whales are so intense that individual calls are audible for considerable distances, and thus detectable as signals rather than as part of the background noise. Some calls sound remarkably mechanical. These individual calls are transient in nature, having durations ranging from a fraction of a second to around 20 s, and in this respect contrast with the continuous sound of a chorus. The most intense sounds are those of the larger whales. Source levels have been estimated from measurements in the northern hemisphere to lie in the range 170-190 dB μ Pa^2 at 1 m (Winn, Perkins and Poulter 1971; Cummings and Thompson 1971; Thompson, Cummings and Ha 1986). Our measurements of received sound levels in Australian waters are consistent with these estimates. Such sounds would be audible for some tens of kilometres, depending on conditions. While these source level estimates are broadband, many of the sounds are harmonic, so have high narrow band levels.

Perhaps the most difficult whale sounds to categorise are those of the humpback whale, which produces a wide variety of sounds in a well structured pattern or song (Winn, Perkins and Poulter 1971; Payne and McVay 1971; Cato 1991c). Durations vary from about 0.1 to more than 4 s, and most of the energy lies in the range 100 Hz to 4 kHz. The rules of the song structure are complex. The characteristics of the sounds, the song structure, and even the rules themselves change with time. These whales migrate

Chorus, 19:53 6 August 1992
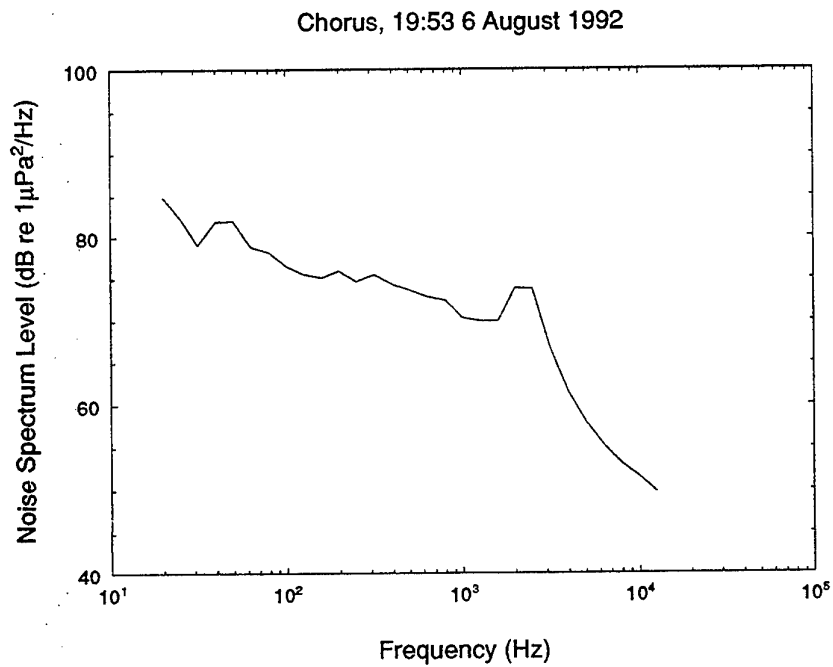
Fig 9.1 The Acoustic Spectrum during a Chorus, 19:53 6 August 1992.

Humpback, 16:53 9 August 1992
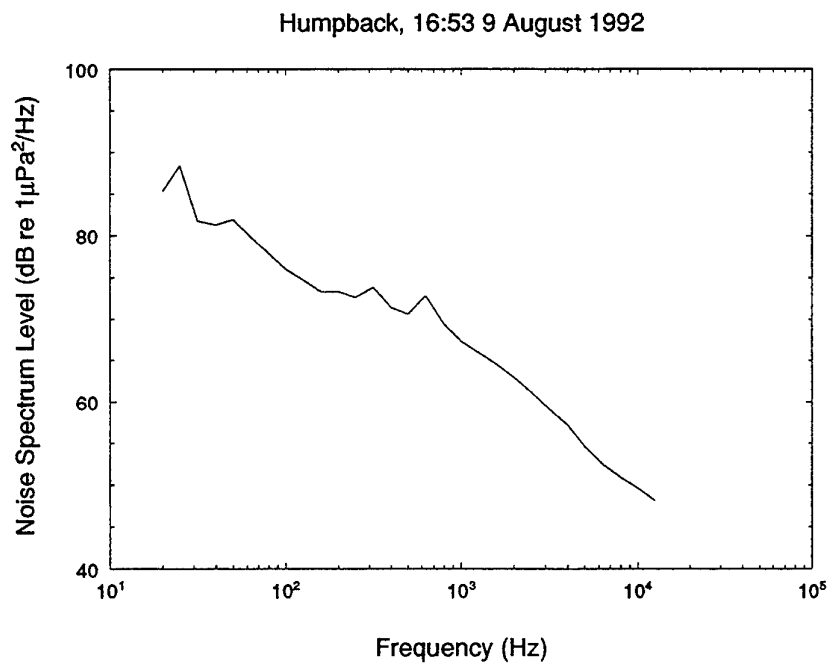
Fig 9.2 Acoustic Spectrum with Humpback whale sounds 16:53 9 August 1992.
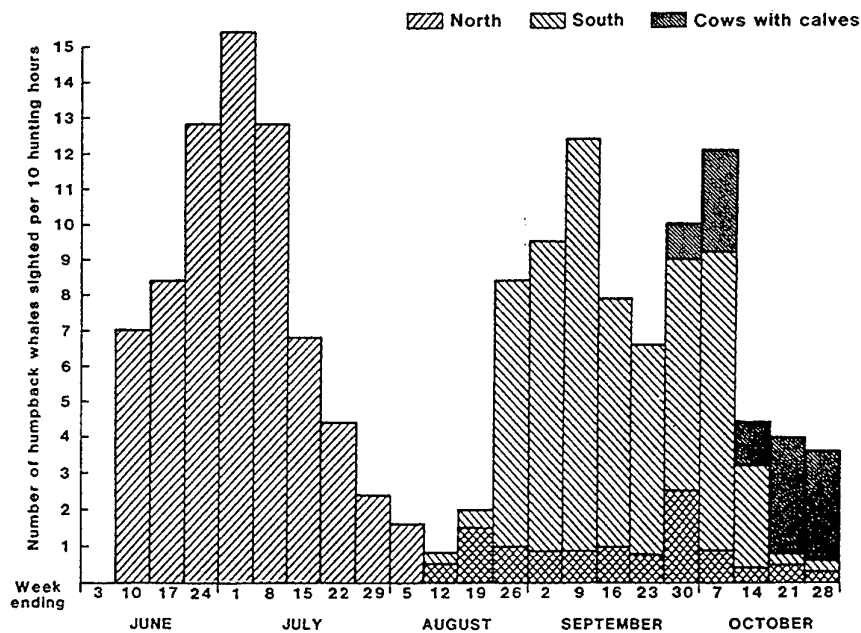
Fig 9.3 Number of Humpback whales seen in the vicinity of latitude 28°S on the east Australian coast per 10 hours of hunting during 1961 (from Chittleborough 1965).

Bioduck, 07:33 7 August 1992
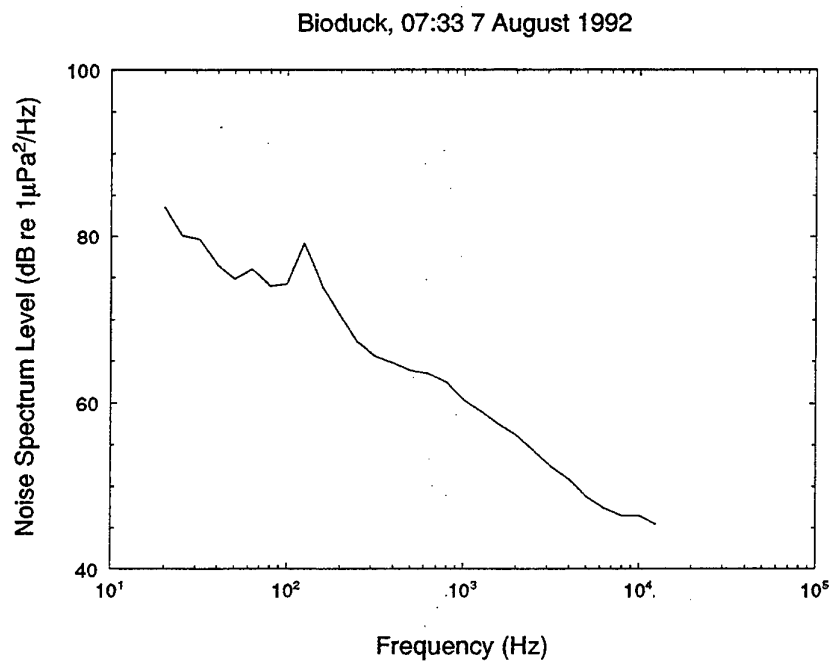
Fig 9.4 The Acoustic Spectrum with an Unidentified Sound ("bioduck"), 07:33 7 August, 1992.

along the east and west coastlines of Australia, and although numbers were depleted by whaling activities which ceased in the early 1960's, there has been a significant recovery since then. The rate of increase of around 10 % per year has been observed for at least the last 10 years off the east coast (Paterson and Paterson 1989) and off the west coast for several years. The current population off the west coast is about 3000.

9.5 Results of Measurements at the Site

A biological chorus similar to those observed in other waters around Australia was observed on all evenings, having a spectral peak at about 2.5 kHz, and most energy between 2 and 4 kHz. The duration of the chorus varied from 3 to 5 h, averaging 4 h. The time of occurrence varied somewhat over the period from 1800 to 0200 the next morning. An example of the chorus spectrum is shown in Fig. 9.1. It seems likely that this chorus would be a regular occurrence.

Humpback whales sounds were audible on 15 % of samples. An example of the contribution of spectral peaks to the noise spectrum is shown in Fig. 9.2. This whale would have been some kilometres distant, and substantially higher levels would be expected during the migrating season.

Humpbacks migrate in the vicinity of the site. Approximately 3000 whales pass north bound in June, July and the same whales pass south bound in September, October, though some are still passing by December. The population is increasing at a rate of about 10 % pa which implies that there will be about 6000 whales passing by about the year 2000. Based on recordings at similar latitudes (Cato 1991c) about 10 % of the whales passing will be singing and the sounds will be above the background for distances of about 10 km, and singing is likely to continue for some hours. While the times of migrations and the distribution with latitude have been well established (Chittleborough 1965; Dawbin 1966; Paterson and Paterson 1989; Bannister, Kirkwood and Wayte 1991), the distribution along an east-west line is not well known.

The time of the measurements in mid August is when few humpbacks would be expected at these latitudes. Almost all would be in the tropical breeding grounds at this time. Substantially higher and more frequent contributions to the sea noise from humpback whales can be expected in June, July and September, October, over a frequency band about 50 Hz to a few kilohertz. An idea of the rise and fall in numbers of humpbacks passing can be obtained from Fig 9.3. Although these observations (Chittleborough 1965) were made on the east coast, the timing is expected to be similar off the west coast. Thus humpback whales are likely to contribute significantly to the ambient noise in June, July and September, October as they pass during their migration. It is difficult to estimate the effect on the ambient noise, since our measurements were taken at a time when few whales would be expected to pass. The population size of 3000 suggests that, on average, 70 whales would pass this latitude per day during the two periods of six weeks when most of the stock passes. Of these, about 7 would be singing and the sounds of each would be audible for some hours at a

receiver within 10 km of their path. The unknown factor is the distribution of whales along an east west line from the coast which would determine what fraction of singers would be audible at the site. The fact that sounds from these whales were heared on 15 % of noise samples during these measurements when only a small percentage of the population would be passing suggests that their sounds are likely to be a major component of the ambient noise during the peak times of migration. Note that the population is expected to double by the year 2000, based on trends sustained over several years, and should continue to increase, since the population is still well less than the pre-whaling figures.

Sperm whales were audible on one occasion. As discussed above, these whales are nomadic with poorly defined migration patterns and occur in large schools. They produce sustantial choruses (for example, see Cato 1978a), and are known to inhabit the deep waters around the south west corner of Australia, often approaching the shelf. They may produce substantial choruses at the site at irregular times.

The unidentified sound known as the "bioduck" was audible in one sample, the spectrum being shown in Fig. 9.4. This is known to contribute significantly to the ambient noise in the frequency range 100 to 200 Hz.

10. Overview of Ambient Noise Results

10.1 Summary

The measurements have shown that the main components of ambient noise at the site are wind dependent noise, traffic noise, close shipping noise, rain noise, and biological noise from various sources. The contributions from these components (excluding close shipping and some biological components) is summarised in Fig. 10.1. Close shipping noise is excluded because it is so variable, and dependent on the distance and nature of the ship responsible. Some of the important biological components are not included because not enough information is available about their contribution (their main contribution occurring in seasons outside the period of measurement).

In Fig. 10.1 (presented earlier as Fig 8.10), averaged wind dependent noise spectra are shown for wind speeds of 5, 10, 20 and 30 knots. These were determined from plots of noise as a function of wind speed, as shown in Figs. 8.1 to 8.5, and the range of variability about the averages shown can be seen in these figures. At high frequencies and wind speeds, this variability is small. Some of the variability may be due to the difference between the local wind speed, which determines the noise, and the wind speed at Rottnest Is. which was used in the estimate. This may be more significant at lower wind speeds and this, with the effect of the intrusion of contributions from other sources, may account for the greater variability at low speeds. At lower frequencies the larger variability results from the contribution of traffic noise. Note that the wind dependent noise spectra are interpolated from values at frequencies of 31.5, 125, 500 Hz, 1 and 8 kHz (from Figs 8.1 to 8.5). The true shapes of the curves at other frequencies may depart significantly from those shown.

The traffic noise curves show the range of traffic noise levels determined from the plots of noise as a function of wind speed by estimating the non-wind-dependent component.

The evening chorus is an example taken from the highest levels of the spectra observed daily for about four hours between 1800 and 0200 the next day.

The rain noise spectrum is an example of one measure, but it should be noted that levels up to 10 dB higher than this could be expected as a heavy rain storm passes. Long term statistics show that it rains in Perth on 60 % of days in winter.
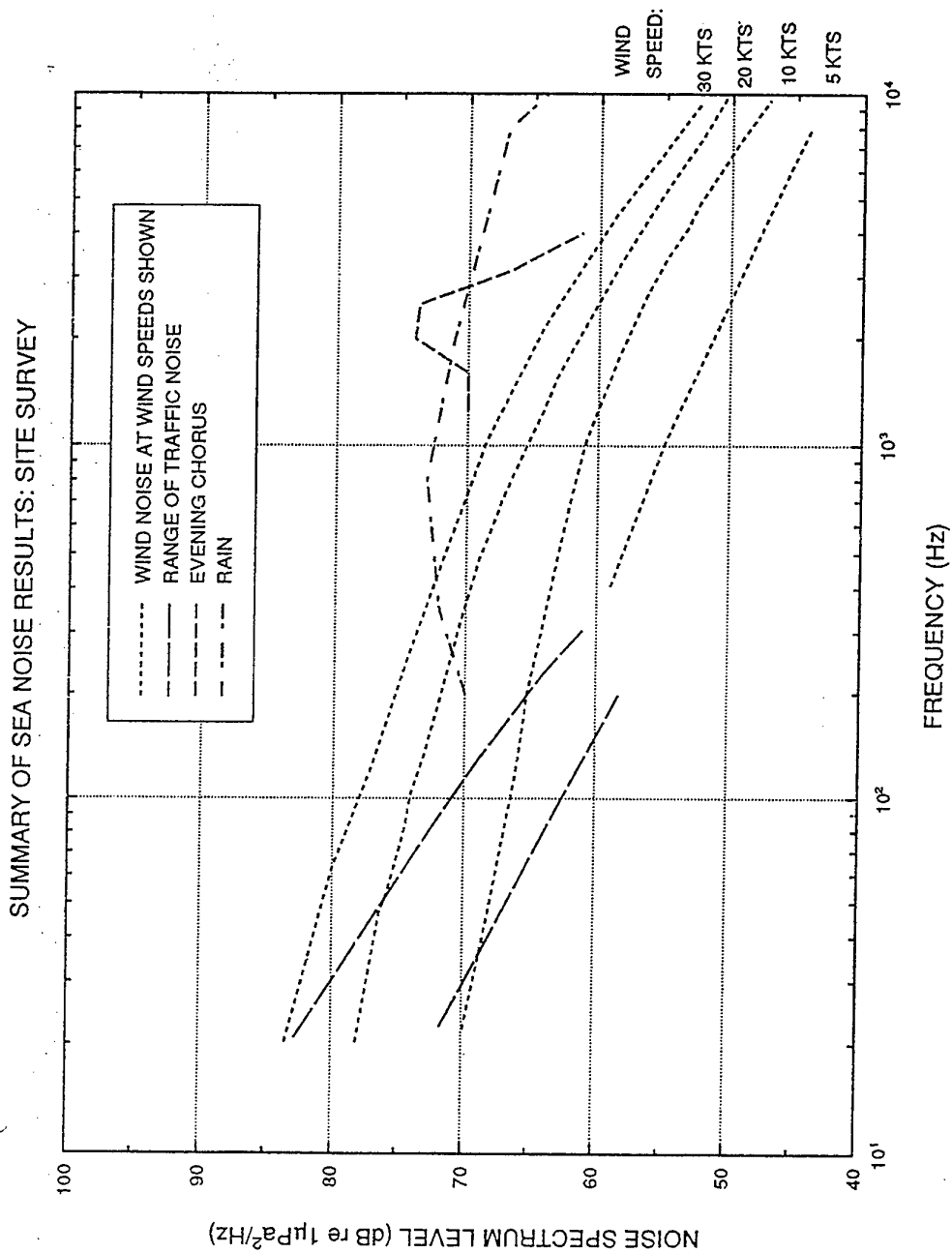
Fig 10.1 A summary of sea-noise results for the survey site. Wind noise curves were interpolated between frequencies of measurement (see Chapter 8).

10.2 Comparison with Earlier Results

Although the summarised results in Fig. 10.1 are within the range of values specified in the original prediction methods for Australian waters (Cato 1978a,b), there are indications of some consistent differences in the wind dependent noise curves. At low frequencies the values measured in the site survey are within the ± 6 dB uncertainty specified but are somewhat lower, the discrepancy increasing with decreasing frequency to about 5 dB lower at the lowest frequencies.

This is probably a real effect of the difference due to the receiver depth. The early predictions were obtained from measurements in a wide range of water depths with receiver depths of about 20 m. At such depths and frequencies, the receivers would have been in the near field of the dipole sources, and noise levels would be expected to be higher.

10.3 Additional Factors

Additional contributions to the ambient noise can be expected from sperm whale choruses which could be as high in level as the evening chorus shown in Fig 10.1 (depending on the distance to the whales). The contribution would be evident in part of the frequency range from about 1 to 10 kHz. Insufficient data about the behaviour of sperm shales makes it difficult to predict the likely occurrence of such choruses. In contrast to the evening chorus, this chorus may persist for hours or even days at a time.

Humpback whales are likely to contribute significantly to the ambient noise in June, July and September, October as they pass during their migration. For much of this period humpback whale sounds would be continuously audible.

Humpback whales produce a variety of sounds over various parts of the frequency range 50 Hz to a few kilohertz. Some are broadband, some pulsating and some narrow band.

10.4 Examples of Particular Features

Figures 10.2 to 10.12 show the noise level as a function of time in various frequency bands for each day during the period of measurements. Major peaks in these plots are labelled according to the sources responsible. Smaller peaks are not labelled. "Artefact" means an unidentified noise, apparently man made.

The substantial increase in noise levels due to the presence of a relatively close ship is quite evident (Fig 8.11). On average, 2 ships per day were detected, and 1.5 ships per day caused substantial increases in the ambient noise for an average of 5 h per day. Note that these results are from 1/3 octave band measurements: spectral lines may be

evident for a significantly greater proportion of the time. These results may, however, be somewhat higher than usual because there were naval exercises in the vicinity of the site during some of the period of measurement. Sonar pings are evident in some records.

Some examples of ambient noise spectra showing the various components are shown Figs 10.13 to 10.17. Figures 10.13 to 10.15 show noise for wind speeds of 11, 18, and 25 knots respectively. There is evidence of traffic noise dominance in Fig 10.13 for frequencies below 100 Hz. A peak in the noise spectrum at about 70 Hz due to a distant ship is shown in Fig 10.16. Figure 10.17 shows an example of the evening chorus.

Sea Noise 5 August 1992
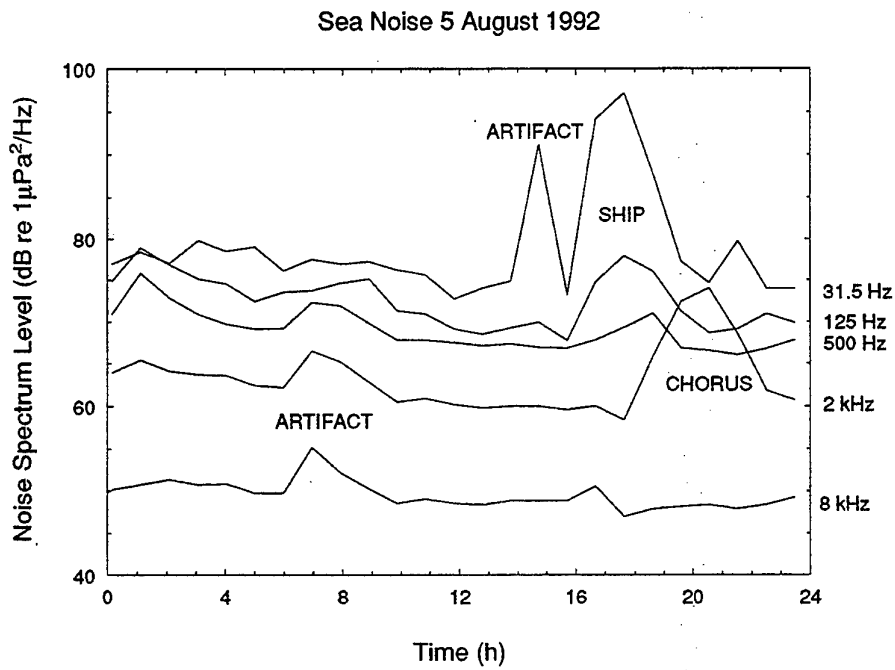
Fig 10.2   Sea noise as a function of time on 5 August, 1992.

Sea Noise 6 August 1992
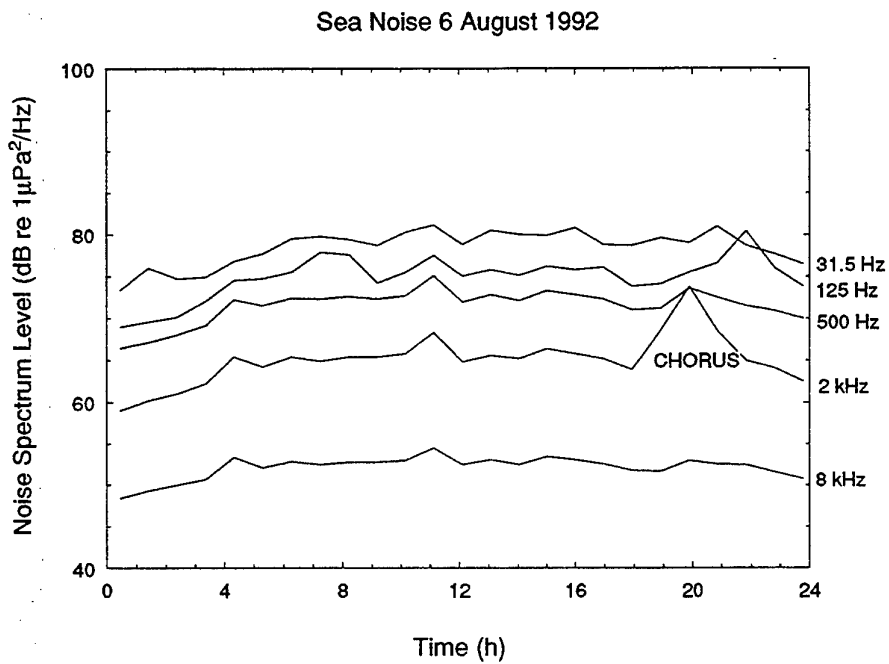
Fig 10.3   Sea noise as a function of time on 6 August, 1992.

Sea Noise 7 August 1992
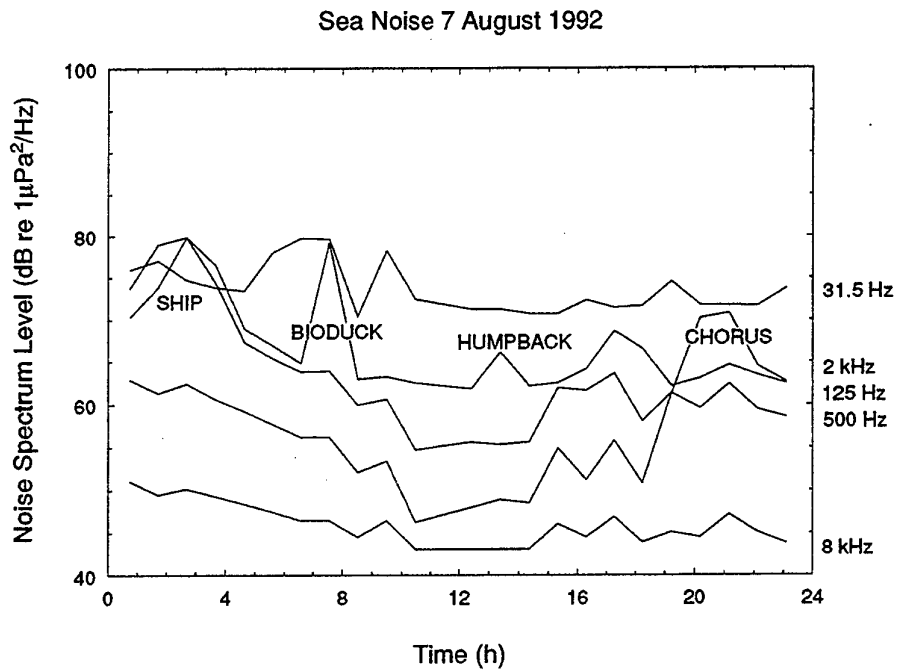
Fig 10.4   Sea noise as a function of time on 7 August, 1992.

Sea Noise 8 August 1992
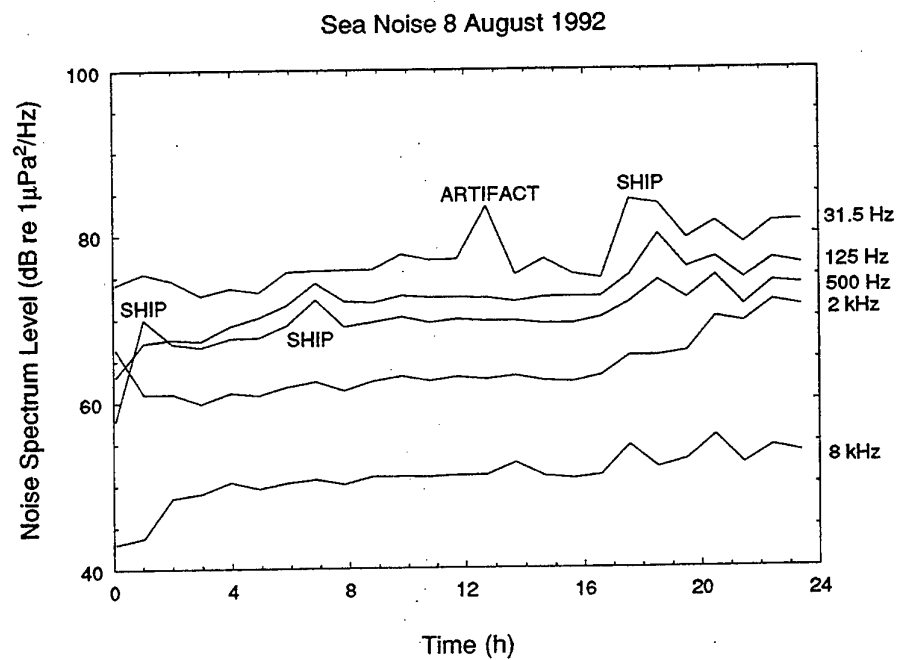
Fig 10.5   Sea noise as a function of time on 8 August, 1992.

Sea Noise 9 August 1992
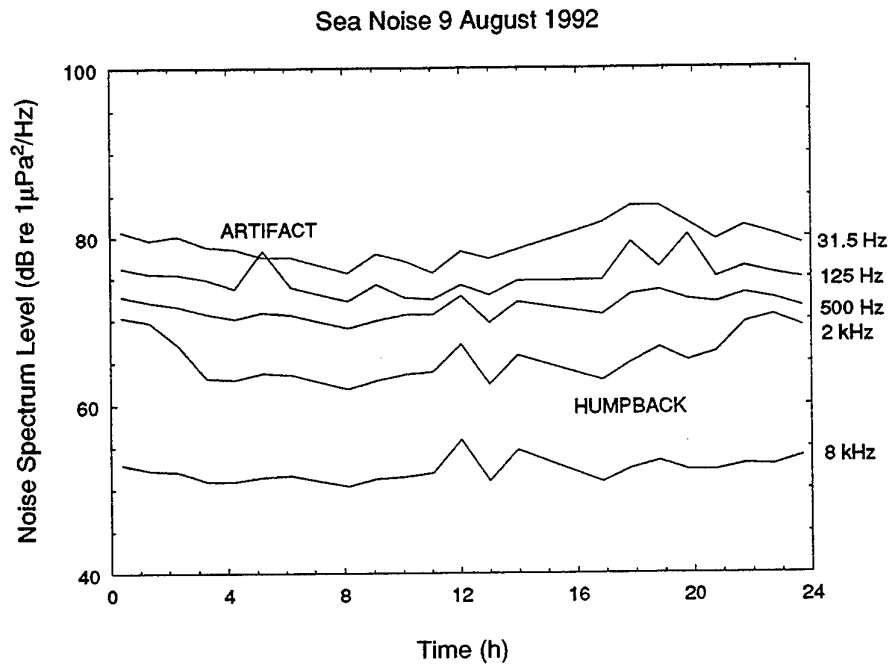
Fig 10.6   Sea noise as a function of time on 9 August, 1992.

Sea Noise 10 August 1992
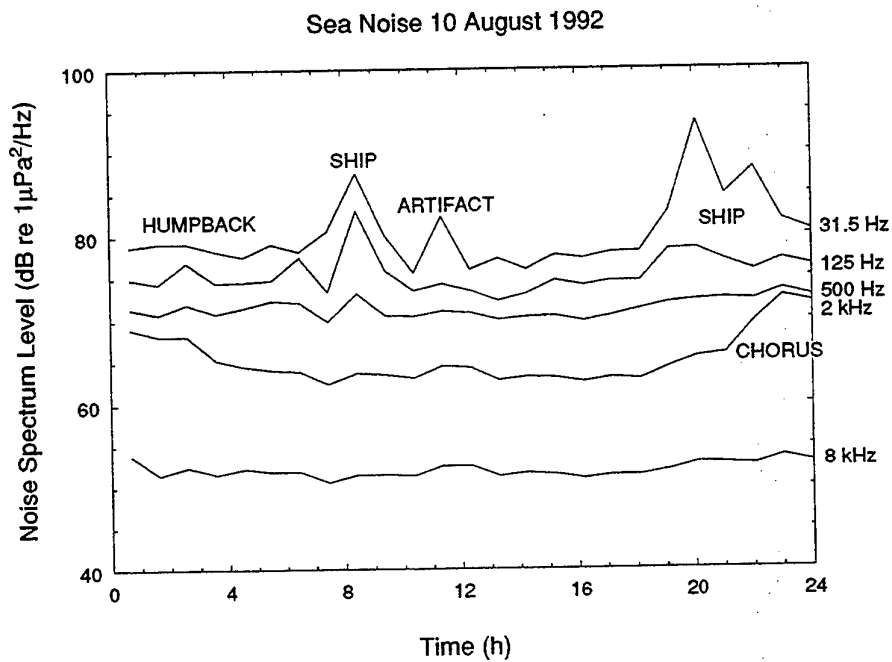
Fig 10.7   Sea noise as a function of time on 10 August, 1992.

Sea Noise 11 August 1992
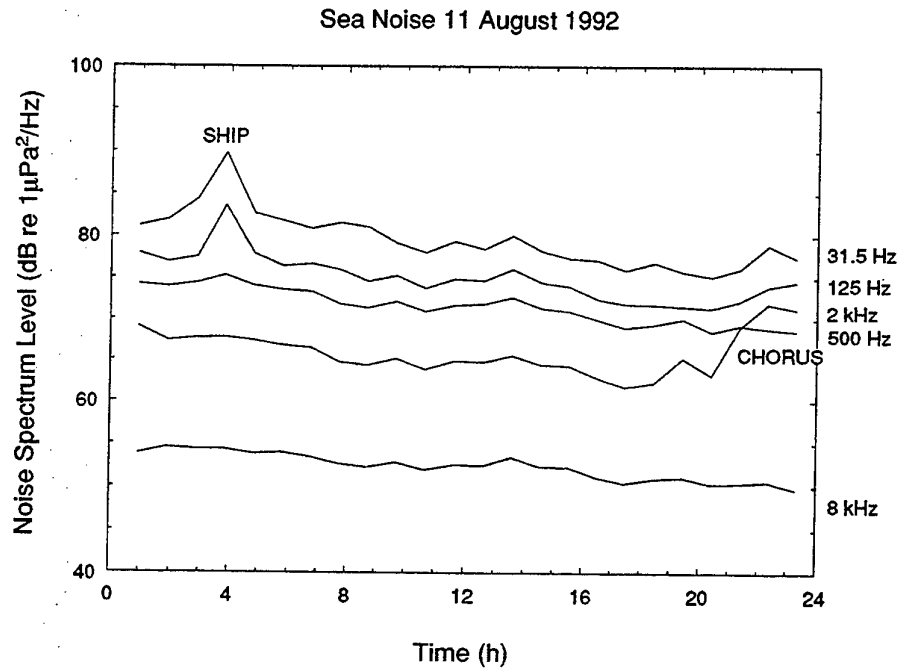
Fig 10.8   Sea noise as a function of time on 11 August, 1992.

Sea Noise 12 August 1992
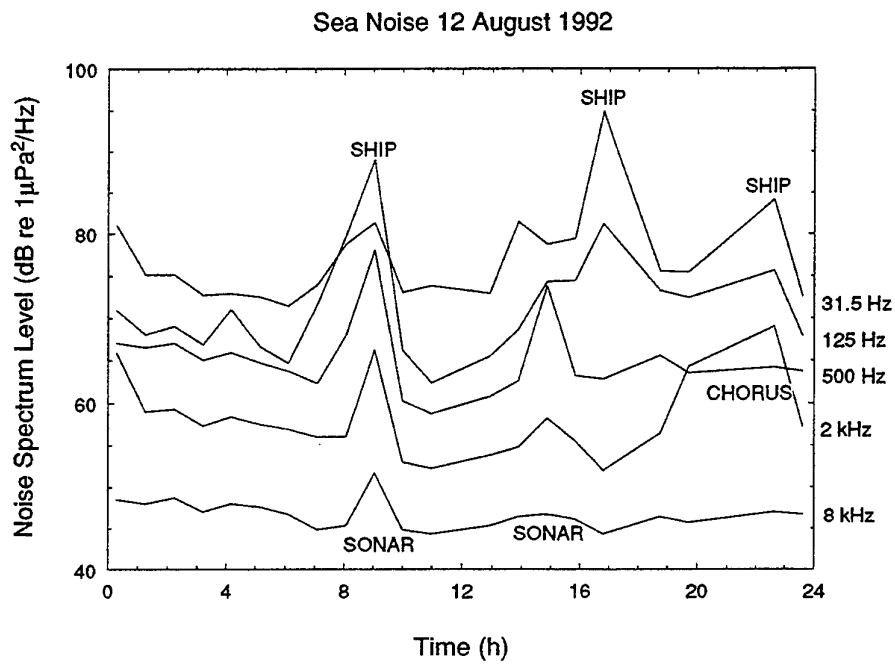
Fig 10.9   Sea noise as a function of time on 12 August, 1992.

Sea Noise 13 August 1992
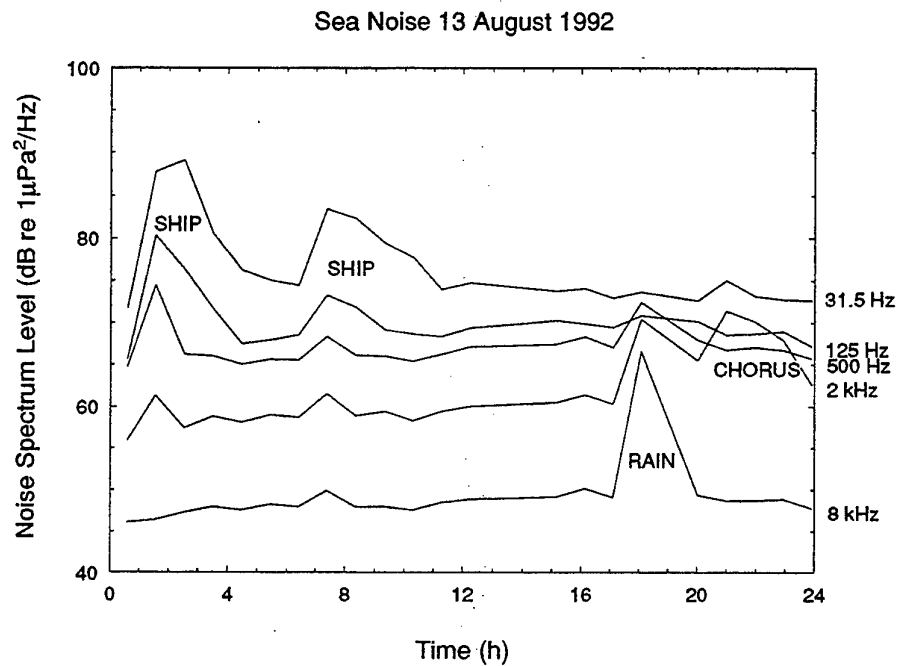
Fig 10.10   Sea noise as a function of time on 13 August, 1992.

Sea Noise 14 August 1992
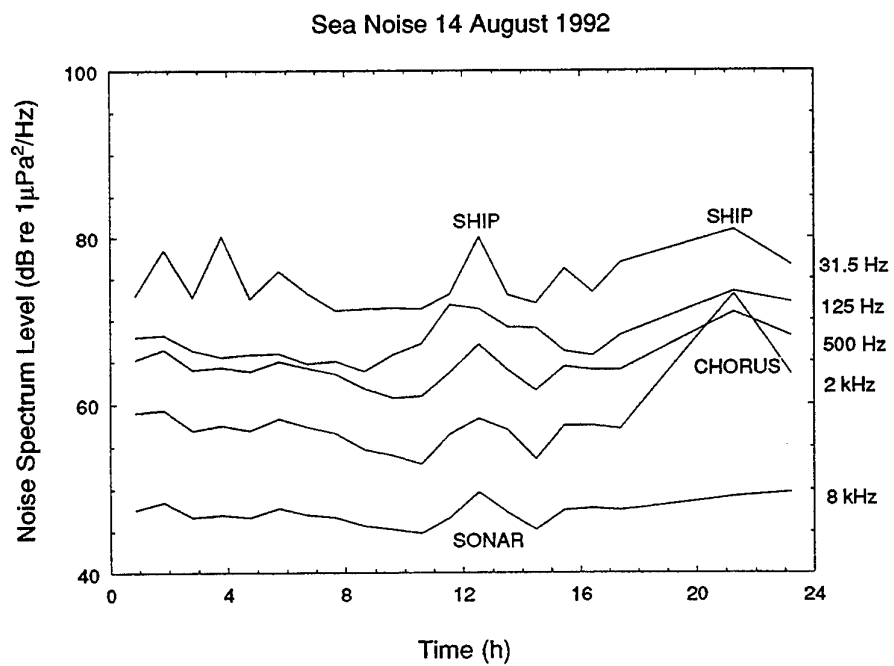
Fig 10.11   Sea noise as a function of time on 14 August, 1992.

Sea Noise 15 August 1992
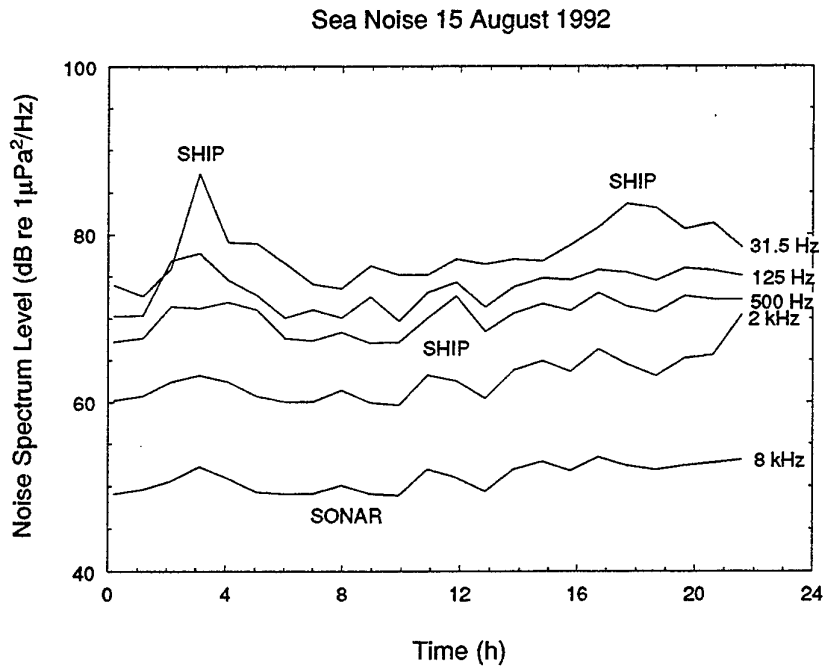
Fig 10.12   Sea noise as a function of time on 15 August, 1992.

11 knot wind, 05:36 7 August 1992
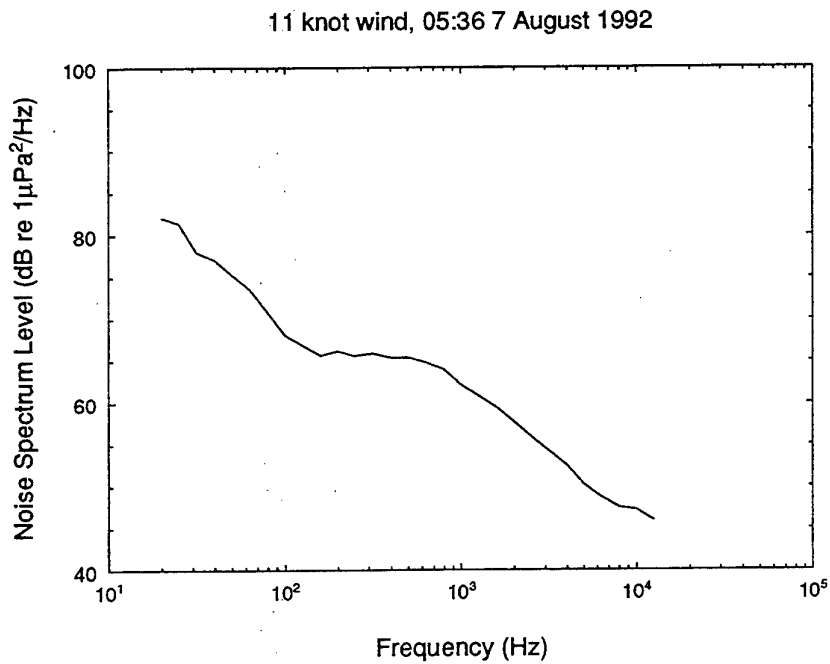
Fig 10.13   Noise spectrum level at 11 knot wind speed, 7 August 1992.

18 knot wind, 09:59 5 August 1992
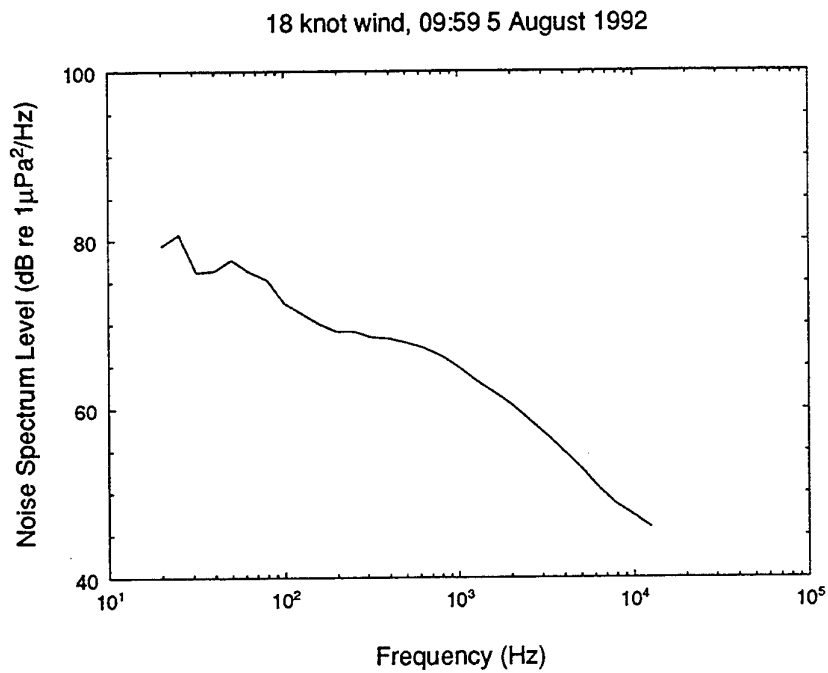
Fig 10.14 *Noise spectrum level at 18 knot wind speed, 5 August 1992.*

25 knot wind, 06:47 11 August 1992
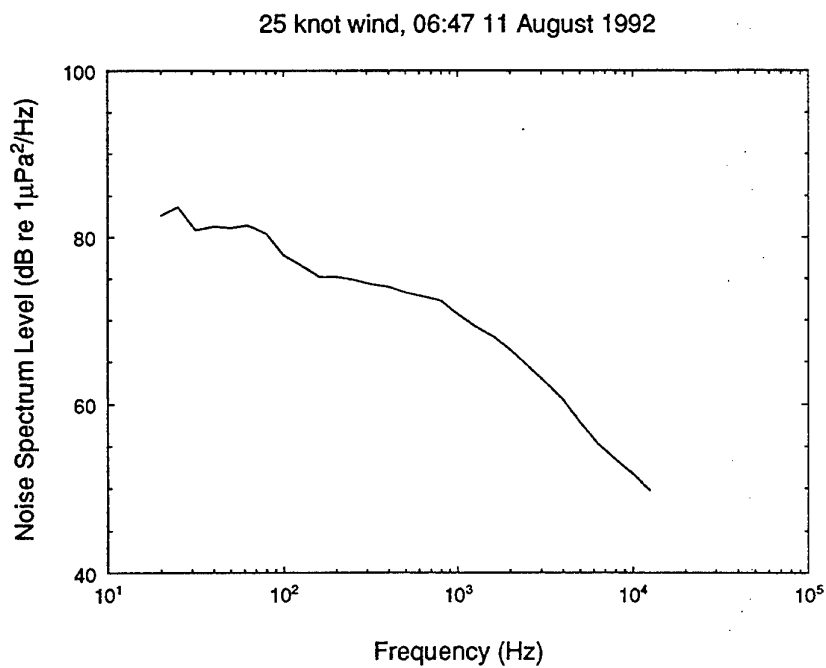
Fig 10.15 *Noise spectrum level at 25 knot wind speed, 11 August 1992.*

Distant Ship, 23:29 5 August 1992
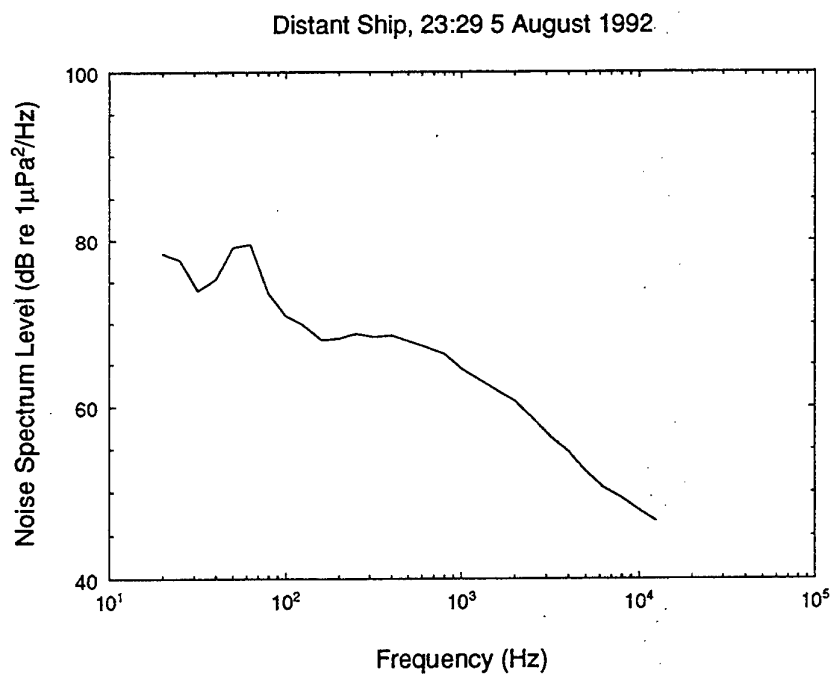
Fig 10.16 *Noise spectrum level showing a distant ship, 5 August 1992.*

Chorus with 12 knot wind, 20:34 5 August 1992
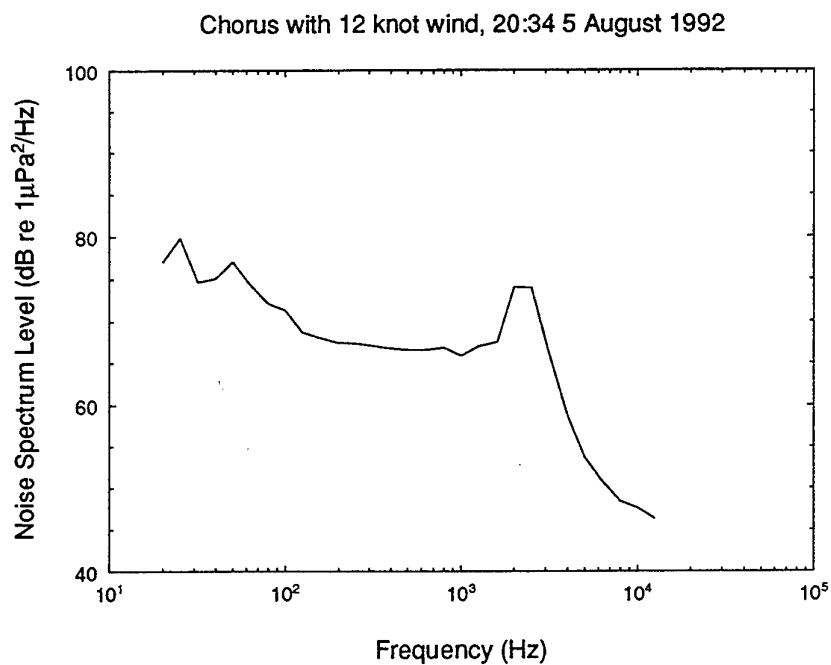
Fig 10.17 *Noise spectrum level with chorus and 12 knot wind, August 1992.*

11. Summary

The site at 32° 15'S, 115° 02'E examined in this report is a difficult one for designing and operating an acoustic range with the capacity to accurately determine the radiated noise level from quiet sources. The frequency of strong winds and large seas is high. Strong eddying currents and under-currents flow in this area and will cause problems with moored engineering structures. The 'view' into the Indian ocean ensures a high level of traffic noise. With about 6 shipping movements per day from the nearby port, there will be interference from other than the target vessel on a number of occasions. Migrating humpback whales are likely to cause significant acoustic interference by their intense sounds as they pass the site in June to July and September to October.

The design of a suitable acoustic range will have to take into account the high currents, the frequent rain, and the small periods when winds are low enough to provide a quiet environment. Temperature micro-structure is likely to cause degradation of received acoustic signal for some frequency bands.

12. Acknowledgments

References

ANDREWS J.C. (1977). Eddy structure and the West Australian Current. Deep-Sea Research, 24, 1133-1148.

ANDREWS J.C. (1979). Eddy structure and the West and East Australian Currents. Flinders Institute of Atmospheric and Marine Sciences, Flinders University of South Australia, Res. Rep. No. 30.

ANDREWS J.C. (1983). Ring structure in the poleward boundary current off Western Australia in summer. Aust. J. Mar. Freshw. Res. 34, 547-61.

AUSTRALIA PILOT (1972). North, north-west, and west coasts of Australia from the west entrance of Endeavour Strait to Cape Leeuwin. Volume 5, sixth edition. Hydrographic Office, Ministry of Defence, Taunton, Somerset, England.

BANNER M.L. and CATO D.H. (1988). "Physical mechanisms of noise generation by breaking waves - a laboratory study," in "Sea Surface Sound," edited by B.R. Kerman (Kluwer, Dordrecht).

BANNISTER J.L. (1968). "An aerial survey for sperm whales off the coast of Western Australia 1963-1965". Aust. J. Mar. Freshwar. Res., 19, 31-51.

BANNISTER J.L. , KIRKWOOD G.P. and WAYTE S.E. (1991). "Increase in humpback whales off Western Australia". Rep. Int. Whal. Commn. 41, 461-465.

BATCHLOR G.K. (1970). An Introduction to Fluid Dynamics (Cambridge University Press, Cambridge, 1970) Chap 3, pp 164-166.

BOLAND F.M, CHURCH J.A., FORBES A.M.G., GODFREY J.S., HUYER A., SMITH R.L. and WHITE N.J. (1988). Current-meter data from the Leeuwin Current Interdisciplinary Experiment. CSIRO Laboratories Report 198, 31pp.

BREKHOVSKIKH L.M. (1966). "Underwater sound waves generated by surface waves in the ocean," Izv. Atmos. Ocean Phys., 2, 582-587.

CALDWELL D.K., CALDWELL M.C. and RICE D.W. (1966). "Behaviour of the sperm whale, Physeter catodon L.," in Whales, Dolphins and Porpoises, edited by K.S. Norris (University of California, Berkeley, 1966), pp 667-717.

CAREY W.M. and BROWNING D. (1988). "Low frequency ocean ambient noise, measurements and theory," in Sea-Surface Sound: Natural Mechanisms of Surface Generated Noise in the Ocean, edited by B.R. Kerman (Kluwer, Dordrecht, 1988), pp 361-376.

CATO D.H. (1969). "Ambient Sea noise in the eastern Timor Sea". RANRL Tech Note 6/69.

CATO D.H. (1976). 'Ambient sea noise in waters near Australia', J. Acoust. Soc. Am., 60, 320-328.

CATO D.H. (1978a). "Marine biological choruses observed in tropical waters near Australia," J. Acoust. Soc Am., 64, 736-743.

CATO D.H. (1978b). "Review of ambient noise in the ocean: non biological sources. Bull. Aust. Acoust. Soc. 6: 31-36.

CATO D.H. (1983). "Theoretical and measured noise from water wave orbital motion", Proc. 11th Int. Congr. Acoust., Paris, July 1983 2, 449-452.

CATO D.H. (1984a). "Sea noise around Australia due to ship traffic". Proc. TTCP Sub Group G, Panel GTP-2 meeting Ottawa and Halifax, Oct 1984.

CATO D.H. (1984b). "Recording Humpback Whale sounds off Stradbroke Island. 285-290. In R.J. Coleman, J. Covacevich and P. Davie, (eds) 'Focus on Stradbroke'. (Boolarong Publications: Brisbane).

CATO D.H. (1991a). "Sound generation in the vicinity of the sea surface: source mechanisms and the coupling to the received sound field," J. Acoust. Soc. Am., 89, 1076-1095.

CATO D.H. (1991b). "Theoretical and measured underwater noise from surface wave orbital motion," J. Acoust. Soc. Am., 89, 1096-1112.

CATO D.H. (1991c). "Songs of humpback whales: the Australian perspective," Memoirs of the Queensland Museum, 30(2), 277-290.

CATO D.H. (1992). "The biological contribution to ambient noise in waters near Australia". Acoustics Australia, 20, 76-80.

CATO D.H. and JONES I.S.F. (1988). "Noise generated by motion of the sea surface - theory and measurement," in Sea Surface Sound: Natural Mechanisms of Surface Generated Noisei in the Ocean, edited by B.R. Kerman (Kluwer, Dordrecht, 1988), pp. 391-402.

CHITTLEBOROUGH R.G. (1965). "Dynamics of two populations of Humpback Whale, Megaptera novaeangliae (Borowski). Aust. J. Mar. Freshw. Res. 16, 33-128.

CRESSWELL G.R. (1977). The trapping of two drifting buoys by an ocean eddy. Deep-Sea Research, 24, 1203-1209.

CRESSWELL G.R. and D.J. VAUDREY (1977). Satellite-tracked buoy data report I: Western Australian releases 1975 and 1976. CSIRO Australia Division of Fisheries and Oceanography Report 86.

CRESSWELL G.R. and GOLDING, T.J. (1980). Observations of a south-flowing current in the southeastern Indian Ocean. Deep-Sea Res. 27A, 449-66.

CUMMINGS W.C. and THOMPSON P.O. (1971). "Underwater sounds from the blue whale, Balaenoptera musculus", J. Acoust. Soc. Am., 50, 1193-1198.

DASHEN R., MUNK W.H., WATSON K.M. and ZACHARIASEN F. (1979). "Sound transmission through a fluctuating ocean," edited by Flatte' S.M., Cambridge University press.

DAWBIN W.H. (1966). "The seasonal migratory cycle of the Humpback Whale. 145-170. In K.S. Norris (ed.) 'Whales, dolphins and porpoises'. (University of California Press: Berkeley).

DOBSON F.W., PERRIE W. and TOULANY B. (1989). "On the Deep-Water Fetch Laws for Wind-Generated Surface Gravity Waves". Atmos. Ocean, 27, P.210-236.

DONELAN M.A., HAMILTON J. and HUI W.H. (1985). "Directional spectra of wind generated waves," Philos. Trans. R. Soc. London Ser. A 315, 509-562.

EZRATY R.S. (1991). "Marine wind variability: illustration and comments". ed. R.C. Beal Directional Ocean Wave Spectra. John Hopkins Press.

FERGUSON B.G. and WYLLIE D.V. (1987). 'Comparison of observed and theoretical responses of a horizontal line array to wind-induced noise in the deep ocean', J. Acoust. Soc. Am., 82, 601-605.

GENTILLI, ed. (1971). "Climates of Australia and New Zealand". World Survey of Climatology. Vol.13. Elsevier, Amsterdam.

GODFREY J.S. and RIDGWAY K.R. (1985). The large-scale environment of the poleward-flowing Leeuwin Current, Western Australia: longshore steric height gradients, wind stress and geostrophic flow. J. Phys. Oceanogr., 15, 481-495.

GODFREY J.S., VAUDREY D.J. and HAHN S.D. (1986). Observations of the shelf-edge current south of Australia, winter 1982. J. Phys. Oceanogr., 16, 668-679.

GOLDING T.J. (1980). Currents off Western Australia. CSIRO Australia Division of Fisheries and Oceanography. Information Sheet, 16-2.

GOLDING T.J. and G. SYMONDS (1978). Some surface circulation features off Western Australia during 1973-1976. Australian Journal of Marine and Freshwater Research, 29, 187-191.

GOULD W.J., (1971). "Methods of measuring and the analysis of currents in coastal and oceanic waters," Ph. D. dissertation, U. College of North Wales, U.K.

GREGG M.C., COX C. and HACKER P.W. (1973). Vertical microstructure measurements in the central North Pacific. Journal of Physical Oceanography 3, 458-469.

HAMILTON L.J. (1984). Statistical features of the oceanographic area off south-western Australia with application to real-time analysis. Royal Australian Navy Research Laboratory Technical Note No. 4/84. Defence Science and Technology Organisation.

HAMILTON L.J. (1986). "Statistical Features of the oceanographic area off south-western Australia, obtained from bathy-thermograph data." Australian Journal of Marine and Freshwater Research, Vol.37, 421-436.

HAMON B.V. (1965). Geostrophic currents in the south-eastern Indian Ocean. Aust. J. Mar. Freshwater Res., 16, 255-271.

HAMON B.V. (1972). Geopotential topographies and currents off West Australia, 1965-69. CSIRO Division of Fisheries and Oceanography Technical Paper No. 32.

HAYES S.P., JOYCE T.M, and MILLARD JR. R.C. (1975). "*Measurements of vertical fine structure in the Sargasso sea,*" J. Geophy. Res., 80, 314-319.

HUGHES B. (1976). "Estimates of underwater sound (and infrasound) produced by nonlinearly interacting ocean waves," J. Acoust. Soc. Am. 60, 1032-1039.

JONES J.E. and JONES I.S.F. (1989) *Early Oceanographic Measurements off South-west Australia.* The Great Circle, 11, 27.

JOYCE T.M. and DESAUBIES Y.F. (1976). "*Discrimination between internal waves and temperatures finestructure,*" J. Phy. Oceanogr., 7, 22-32.

KELLY L.J., KEWLEY D.J. and BURGESS A.S. (1985). "A biological chorus in deep water northwest of Australia," J. Acoust. Soc. Am., 77, 508-511.

KIBBLEWHITE A.C. , DENHAM R.N. and BARNES D.J. (1967). "Unusual low-frequency signals observed in New Zealand waters," J. Acoust. Soc. Am., 41, 644-655.

KITANI K. (1977). The movements and physical characteristics of the water off Western Australia in November 1975. Bulletin of the Far Seas Fisheries Research Laboratory, 15, 13-19.

KNUDSEN V.O., ALFORD R.S. and EMLING J.W. (1944). "Survey of Underwater Sound, Report No.3, Ambient Noise," OSRD Report No.4333, Sec. No.6 1-NDRC-1848 (26 Sept. 1944) (unpublished).

KNUDSEN V.O., ALFORD R.S. and EMLING J.W. (1948). '*Underwater ambient noise*', J.Mar. Res., 7, 410-429.

LEGECKIS R. and CRESSWELL G.R. (1981). Satellite observations of sea surface temperature fronts off the coast of western and southern Australia. Deep-Sea Res. 28, 297.

McCAULEY R. (1989). "Aspects of marine biological sound production in northern Australia," James Cook University, Townsville.

OSBORN T. and COX C. (1972) *Oceanic fine structure.* Geophy. Fluid Dyn. 3, 321-345.

PATERSON R.A. (1986). "An analysis of four large accumulations of sperm whales observed in the modern whaling era," The Scientific Reports of the Whales Research Institution, 37, 167-172.

PATERSON R. and PATERSON P. (1989). "The status of the recovering stock of Humpback Whales *Megaptera novaeangliae* in east Australian waters. Biol. Conserv. 47, 33-48.

PAYNE R.S. and McVAY S. (1971). Songs of Humpback Whales. Science 173, 585-597.

PEARCE A.F. and CRESSWELL G.R. (1985). A Review of the Ocean Circulation off Western Australia. CSIRO Division of Oceanography Information Sheet, No. 16-3.

PEARCE A.F. (1991). "Eastern boundary currents of the souther hemisphere. In "The Leeuwin Current: an influence on the coastal climate and marine life of Westernn Australia". Eds. Pearce A.F. and Walker D.I. Journal of the Royal Society of Western Australia, 74. pp 35-46.

PEARCE A.F. and GRIFFITHS R.W. (1991). "The mesoscale structure of the Leeuwin Current: A comparison of laboratory models and satellite imagery". Journal of Geophysical Research, Vol.96, No.C9, 16739-16758.

PROSPERETTI A. (1988a). "Bubble-related ambient noise in the ocean," J. Acous. Soc. Am., 84, 1042-1054.

PROSPERETTI A. (1988b). "Bubble dynamics in ocean ambient noise," in Sea-Surface Sound: Natural Mechanisms of Surface Generated Noise in the Ocean, edited by B.R. Kerman (Kluwer, Dordrecht, 1988).

PUMPHREY H.C. and CRUM L.A. (1989). "Underwater sound produced by individual drop impacts and rainfall": J. Acoust. Soc. Am., 85, 1518-1526.

RIDGWAY K.R. (1982).Mean Temperature-Salinity relationships and shelf edge currents around Australia. Master of Applied Science Thesis, Warrnambool Institute of Advanced Education.

RIEDEL H.P. and TRAJER F.L. (1978). Analysis of five years of wave data, Cockburn Sound. Fourth Australian conference on coastal and ocean engineering. Adelaide, 8-10 November 1978. The Institution of Engineers Australia National Conference Publication No. 11, 143-147. (Barton A.C.T.)

SHEPARD F.P., MARSHALL N.F., McLOUGHLIN P.A. and SULLIVAN G.G. (1979).Currents in Submarine Canyons and other Seavalleys. Studies in Geology No.8. The American Association of Petroleum Geologists, Tulsa, Oklahoma, U.S.A.

SMITH R.L., HUYER A., GODFREY J.S. and CHURCH J.A. (1991). " The LeeuwinCurrent off Western Australia". Journal of Physical Oceanography, .21, No.2, 323-345.

TAVOLGA W.N. (1964). "Sonic characteristics and mechanisms in marine fishes," in *Marine Bio-Acoustics*, edited by W.N. Tavolga (Pergamon, New York, 1964), pp. 196-211.

THOMPSON R.O.R.Y. and CRESSWELL G.R. (1983). The Leeuwin Current and Undercurrent. Tropical Ocean-Atmosphere Newsletter, No. 19, 10-11.

THOMPSON P.O., CUMMINGS W.C. and HA S.J.(1986). "Sounds, source levels and associated behaviour of Humpback Whales, southeast Alaska. J. Acoust. Soc. Am., 80, 735-740.

THURAISINGHAM R.A. (1994). *"Models to estimate high frequency acoustic scattering due to thermal fine- and micro-structure of the ocean"*. Research Report DSTO-RR-0001. Aeronautical and Maritime Research Laboratory, D.S.T.O.

UNNI S. and KAUFMAN C. (1981). *"Acoustic fluctuations due to the temperature fine structure of the ocean,"* J. Acous. Soc. Am., 69, 676-680.

WEBSTER I., GOLDING T.J. and DYSON N. (1979). Hydrological features of the near shelf waters off Fremantle during 1974. CSIRO Australia Division of Fisheries and Oceanography Report 106.

WENZ G.M. (1962). 'Acoustic ambient noise in the ocean: spectra and sources', J. Acoust. Soc. Am., **34**, 1936-1956.

WINN H.E., PERKINS P.J. and POULTER T.C. (1971). Sounds of the humpback whale. Proc. 17th Annual Conference on Biological Sonar and Diving Mammals. Stanford Research Institute, Menlo Park, California.

WYLLIE D.V. (1971). "Sea noise measurements in the Coral, Solomon, and Bismarck Seas - 1970," Australian Weapons Research Establishment, Technical Memorandum 432 (WR&D) (unpublished). --

WYLLIE D.V. , CATO D.H. and TAYLOR S. (1992). "Measurement result summary Underway Radiated Noise Range (URNR)". DSTO 1992.

WYRTKI K. (1971). 'Oceanographic Atlas of the International Indian Ocean Expedition.' (National Science Foundation: Washington.)

WYRTKI K. (1973). Physical Oceanography Of The Indian Ocean. In "The Biology OF The Indian Ocean", Ed. Bernt Zertzchall. Springer Verlag Series: Ecological Studies No. 3, 18-36.

--

THIS PAGE INTENTIONALLY BLANK

Appendix A: URNR Site Survey Narrative

A.1 NARRATIVE

Prior to undertaking the present study of the proposed Underway Radiated Noise Range (URNR) site 50 km to the SW of Rottnest Island, Dr Cato of the Maritime Operations Division (MOD) had made a series of ambient noise measurements in January 1992 at a site to the east of the proposed site on the 200 metre isobath. In the next few months MOD assessed the environmental risks and advised the Submarine Project on the appropriate measurements to be made. MOD identified the currents as an important risk to the permanence and performance of the URNR, with lesser risks from ambient noise and water structure uncertainties. These measurements were carried out during the present study by MOD with the aid of a contractor, Steedman Science & Engineering, who in turn sub-contracted for the supply of ship support and satellite imagery.

The significant dates of events marking the beginning and end of measurements during the survey of the URNR site are set out in the table below. The table is followed by a short narrative with details for each line in the event table. Event times are for the West Australian time zone.

A.2 TABLE OF EVENTS

10 July, Contractor engaged for environmental measurements.
15 July, Sea surface temperature satellite images.
16 July, Wind measurements at Rottnest Island.
16 July, Deploy current meters at URNR site.
16 July, Deploy current meters off Dongara.
21 July, Deploy current meters at URNR site.
4 August, Deploy meteorology and waverider buoys, and ambient noise recorders at
    URNR site.
5 August, Rain measurements using weather radar.
7 August, Attempt repair of meteorology buoy at URNR site.
14 August, Repair of meteorology buoy at URNR site.
17 August, Recover and redeploy waverider buoy, and ambient noise recorders at URNR site.
18 August, Fly over URNR site and photograph wind waves.
18 August, Aerial search for meteorology buoy.
22 August, Deploy meteorology buoy at URNR site.
26 August, Movement of meteorology buoy from URNR site.
30 August, Recovery of current meters at URNR site.
1 September, Recovery of current meters off Dongara.
7 September, Recover and redeploy waverider buoy, and ambient noise recorder at URNR site.

11 September, Deploy Ambient noise recorder at URNR site.

15 July, Sea surface temperature satellite images.
Satellite images were obtained for the ocean area from Cape Inscription to Cape Leeuwin to determine the sea surface temperature structure and inferred surface currents. The first image was obtained on 15 July, and further images on cloud free days will continue until 11 September.

16 July, Wind measurements at Rottnest Island.
Wind data were obtained from the Rottnest Island weather station from 16 July, and will continue until 11 September.

16 July, Deploy current meters at URNR site.
Using the "Henrietta" an array of current meters was moored at depths of 50, 125, 200 and 250 metres at 32°27'16"S 114°56'53"E at 0100 hrs (chart depth 300 metres). A second current meter array was not deployed because the weather had deteriorated beyond the limited capability of the boat.

16 July, Deploy current meters off Dongara.
An array of current meters was moored at 29°32.60'S 114°09.45'E at 1005 hrs (chart depth 300 metres).

21 July, Deploy current meters at URNR site.
Using the "Saladin Sprint" an array of current meters was moored at depths of 125, 175, 200 and 350 metres at 32°16.98'S 115°01.71'E at 1100 hrs (chart depth 400 metres). A line of ten Submersible Data Logger (SDL) stations and surface salinity-temperature measurements was completed from six miles to the west of the current meter mooring site to near the 40 metre isobath to the east.

4 August, Deploy meteorology and waverider buoys, and ambient noise recorders at URNR site.
Using the "Tilbata Creek" the meteorology buoy was deployed at 32°19'38"S 114°59'39"E at 1320 hrs but the wind and rain sensors were broken during the launch operation. The waverider buoy was deployed at 32°19'57"S 114°59'47"E at 1550. The low frequency ambient noise recorder was deployed at 32°20'00"S 115°00'30"E at 1700. The high frequency ambient noise recorder was deployed at 32°20'46"S 115°00'28"E at 2015.

5 August, Rain measurements using weather radar.
Using the Bureau of Meteorology weather radar the location and density of rain in the region of the URNR site were recorded from 5 August, and will continue until 11 September. The radar is located on top of the Dumas Building in King's Park Road, West Perth, and has an effective range of about 200 km, which can be compared to the 85 km distance between the radar and the URNR site.

7 August, Attempt repair of meteorology buoy at URNR site.

Using the "Winifred" an attempt was made to go out to and repair the meteorology buoy. The changing weather conditions and a bearing failure on one of the boat's drive shafts caused the attempt to be abandoned.

14 August, Repair of meteorology buoy at URNR site.
Using the "Saladin Sprint" the wind and rain sensors were replaced on the meteorology buoy at 32°19'38"S 114°59'39"E.

17 August, Recover and redeploy waverider buoy, and ambient noise recorders at URNR site.
Using the "Tilbata Creek" the low frequency ambient noise recorder was recovered at 1500 hrs and the replacement recorder deployed at 32°19'34"S 115°00'55"E at 1730. The waverider buoy was recovered at 1540 and redeployed in same position at 1650 hrs. The high frequency ambient noise recorder was recovered at 2130 hrs and the replacement recorder was deployed at 32°20'25"S 114°58'24"E at 2258 hrs. On arrival at the URNR site earlier in the day at 1230 hrs the meteorology buoy could not be found, although the waverider buoy at the other end of the same mooring was still in place. After all work at the site was finished a search lasting three hours was undertaken before returning to Fremantle.

18 August, Fly over URNR site and photograph wind waves.
Using an aircraft, wind waves at the URNR site were photographed.

18 August, Aerial search for meteorology buoy.
Using another aircraft Steedman's staff carried out a search for the missing meteorology buoy towards the south as far as 33°20' but without success. The buoy was found on 1 September washed up on a beach near Mandura to the ESE of the mooring site.

22 August, Deploy meteorology buoy at URNR site.
Using the "Tilbata Creek" a replacement meteorology buoy was moored at 32°19'38"S 114°59'39"E.

26 August, Movement of meteorology buoy from URNR site.
Radio transmissions from the replacement meteorology buoy indicated that it had moved 4 miles from its moored position. By the 29 August radio transmissions had ceased, and it was found at Brun's Beach to the NE of the mooring site on 22 September.

30 August, Recovery of current meters at URNR site.
Using the "Tilbata Creek" the array of current meters at 32°16.98'S 115°01.71'E was recovered by 1150 hrs. During the afternoon a search was made for the current meter mooring at 32°27'16"S 114°56'53"E without sighting the marker buoys, and subsequent acoustic signals to the acoustic release did not result in the sub-surface buoy coming to the surface. Further work was abandoned due to deteriorating weather.

1 September, Recovery of current meters off Dongara.
Using the "Deja Vu" the array of current meters at 29°32.60'S 114°09.45'E was recovered by 0923 hrs.

8 September, Recover and redeploy waverider buoy, and ambient noise recorder at URNR site.
The "Tilbata Creek" was used to recover the low frequency ambient noise recorder and to deploy the replacement. The high frequency recorder (deployed 17 Aug) was not recovered. Recorder, near 32°20'S 115°00'E.

11 September, Deploy ambient noise earlier at URNR site.
The "Tama" was used to deploy the high frequency ambient noise recorder at 32° 20.61'S 115° 00.09' E which will be recovered on about 24 September.

DISTRIBUTION LIST

Site Survey for an Ocean Engineering Project West of Perth for July to September 1992
Ian S.F. Jones, D.H. Cato, L.J. Hamilton and B.D. Scott

AUSTRALIA

1. DEFENCE ORGANISATION

a. Task Sponsor SPD

b. S&T Program
Chief Defence Scientist ⎤
FAS Science Policy ⎬ shared copy
AS Science Industry and External Relations ⎪
AS Science Corporate Management ⎦
Counsellor Defence Science, London (Doc Data Sheet)
Counsellor Defence Science, Washington (Doc Data Sheet)
Scientific Adviser to MRDC Thailand (Doc Data Sheet)
Director General Scientific Advisers and Trials/Scientific Adviser Policy and
    Command (shared copy)
Navy Scientific Adviser
Scientific Adviser - Army (Doc Data Sheet and distribution list only)
Air Force Scientific Adviser
Director Trials

Aeronautical and Maritime Research Laboratory
Director
Chief of Maritime Operations Division
Research Leader (Dr. A. Theobald)
Task Manager: I.S.F. Jones (Task Manager) (2 copies)
Authors: D.H. Cato (2 copies)
          L.J. Hamilton (2 copies)
          B.D. Scott (2 copies)
South Australia
    A. Jones
    A. Larsson
    R. Macleod
    S. Taylor
Sydney
    M.J. Bell
    B. Ferguson
    M.V. Hall
    P.J. Mulhearn
    S. Tavener
    R. Thuraisingham
Melbourne
    P. Lewis
Western Australia
    C. Davis

Electronics and Surveillance Research Laboratory
Director

DSTO Library
Library Fishermens Bend
Library Maribyrnong
Library DSTOS (2 copies)
Australian Archives
Library, MOD, Pyrmont (2 copies)

c. **Forces Executive**
Director General Force Development (Sea)
Director General Force Development (Land) (Doc Data Sheet only)
Director General Force Development (Air) (Doc Data Sheet only)

d. **Navy**
SO (Science), Director of Naval Warfare, Maritime Headquarters Annex, Garden Island, NSW 2000 (Doc Data Sheet only)
ASSTASS, APW2-1-OA2, Anzac Park West, Canberra
Australian Construction Facility, PO Box 551, Port Adelaide SA 5015
Applied Oceanography Section, AJMWC, RAN Air Station, Nowra Naval PO, NSW 2450.
CO, HMAS Stirling, Rockingham WA
COMAUSMINFOR, HMAS Waterhen, Waverton, NSW 2060
DASD, APW2-4-01, PO Box E33, Queen Victoria Tce, Canberra 2600.
DAUW, Dept Of Defence A-3-15 Canberra, ACT 2600
DGFD(Sea) , Dept Of Defence B-4-03 Canberra, ACT 2600
DOM, Maritime Headquarters, Wylde St, Potts Point, NSW 2011
DSMPW, Russell Offices, Dept Of Defence, A-3-09 Canberra ACT 2600
ITTM, New Submarine Project, PO Box 551, Port Adelaide SA 5015
SO (Science), DNW, MHQ Annex, Garden Island NSW 2000
SPD, APQ1-5-14, PO Box E33, Queen Victoria Terrace, Canberra ACT 2600
Hydrographer RAN, Locked Bag 8801, South Coast Mail Centre, NSW 2521
MRA, MHQ Annex, Wylde St, Potts Point NSW 2011
Naval Weather and Oceanographic Centre, Nowra Naval PO, NSW 2450.
OIC RANRAU, MHQ Annex West, HMAS Stirling, Garden Island WA
Operations Staff Officer, Hydrographic Office, Locked Bag 8801, South Coast Mail Centre, NSW 2521
LCDR D. Plummer RAN, HMAS Stirling, Rockingham WA
LCDR P. Campbell RAN, c/- Computer Sciences Company, Level 5 CSC Bldg, 53 Nicholson St, St Leonards NSW 2065

e. **Army**
ABCA Office, G-1-34, Russell Offices, Canberra   (4 copies)
SO (Science), HQ 1 Division, Milpo, Enoggera, Qld 4057

f. **Air Force**
No compulsory distribution

g. **S&I Program**
Defence Intelligence Organisation
Library, Defence Signals Directorate (Doc Data Sheet only)

h. **Acquisition and Logistics Program**
No compulsory distribution

i. **B&M Program (libraries)**
OIC TRS, Defence Central Library
Officer in Charge, Document Exchange Centre (DEC), 1 copy
*US Defence Technical Information Center, 2 copies
*UK Defence Research Information Centre, 2 copies
*Canada Defence Scientific Information Service, 1 copy
*NZ Defence Information Centre, 1 copy
National Library of Australia, 1 copy

2. **UNIVERSITIES AND COLLEGES**

Deakin University, Serials Section (M list), Deakin University Library, Geelong, 3217
Senior Librarian, Hargrave Library, Monash University
Flinders University
    Library
    Flinders Institute for Atmospheric and Marine Sciences
Australian Defence Force Academy
    Library
    Dept of Geography and Oceanography
    Head of Aerospace and Mechanical Engineering
Centre for Water Research,
    University of Western Australia, Nedlands WA 6150
Centre for Water Research,
    School of Environmental Science, Murdoch University, WA 6150
Coastal Studies Unit, Dept of Geography, University of Sydney, NSW 2006
Centre for Marine Sciences and Technology, Curtin University Of Technology,
    PO Box U1987, Perth WA 6001
Ocean Sciences Institute, 108 Darlington Road, H34 University of Sydney 2006
Remote Sensing Applications Centre,
    Dept Of Land Administration, 184 St Georges Tce, Perth WA 6000
M. Gunaratnam, University of Sydney, NSW 2006

3. **OTHER ORGANISATIONS**

NASA (Canberra)
AGPS
AIMS (Australian Institute of Marine Science), PMB 3, Townsville MC, QLD 4810
AODC (Australian Oceanographic Data Centre), Level 2, Maritime Headquarters
    Annex, Wylde Street, Potts Point 2011
CSIRO
    Library CSIRO Division Of Oceanography, GPO Box 1538, Hobart TAS 7001
A. Pearce, PO Box 20, North Beach WA 6020
Environmental Protection Authority, Environment House, 1 Mount St, Perth WA 6000
IOS (Institute of Oceanographic Sciences), Brook Rd, Wormley, Godalming, Surrey
    GU8 5UB England
WNI Science and Engineering, 31 Bishop St., Jolimont Perth, WA 6014
VIMS (Victorian Institute of Marine Sciences), 23 St. Andrews Place, East Melbourne
    VIC 3002

OUTSIDE AUSTRALIA

4. **ABSTRACTING AND INFORMATION ORGANISATIONS**
   INSPEC: Acquisitions Section Institution of Electrical Engineers
   Library, Chemical Abstracts Reference Service
   Engineering Societies Library, US
   American Society for Metals
   Documents Librarian, The Center for Research Libraries, US

5. **INFORMATION EXCHANGE AGREEMENT PARTNERS**
   Acquisitions Unit, Science Reference and Information Service, UK
   Library - Exchange Desk, National Institute of Standards and Technology, US

SPARES (30 copies)

Total number of copies: 135

DEFENCE SCIENCE AND TECHNOLOGY ORGANISATION DOCUMENT CONTROL DATA		1. PRIVACY MARKING/CAVEAT (OF DOCUMENT)

2. TITLE Site Survey for an Ocean Engineering Project West of Perth for July to September 1992	3. SECURITY CLASSIFICATION (FOR UNCLASSIFIED REPORTS THAT ARE LIMITED RELEASE USE (L) NEXT TO DOCUMENT CLASSIFICATION) Document (U) Title (U) Abstract (U)

4. AUTHOR(S) Ian S.F. Jones, D.H. Cato, L.J. Hamilton and B.D. Scott	5. CORPORATE AUTHOR Aeronautical and Maritime Research Laboratory PO Box 4331 Melbourne Vic 3001

6a. DSTO NUMBER DSTO-TR-0459	6b. AR NUMBER AR-009-949	6c. TYPE OF REPORT Technical Report	7. DOCUMENT DATE November 1996

8. FILE NUMBER G6 4/8-4702	9. TASK NUMBER NAV 92/254	10. TASK SPONSOR SPD	11. NO. OF PAGES 124	12. NO. OF REFERENCES 83

13. DOWNGRADING/DELIMITING INSTRUCTIONS N/A	14. RELEASE AUTHORITY Chief, Maritime Operations Division

15. SECONDARY RELEASE STATEMENT OF THIS DOCUMENT

Approved for public release

OVERSEAS ENQUIRIES OUTSIDE STATED LIMITATIONS SHOULD BE REFERRED THROUGH DOCUMENT EXCHANGE CENTRE, DIS NETWORK OFFICE, DEPT OF DEFENCE, CAMPBELL PARK OFFICES, CANBERRA ACT 2600

16. DELIBERATE ANNOUNCEMENT

No limitations

17. CASUAL ANNOUNCEMENT	Yes

18. DEFTEST DESCRIPTORS

Acoustic ranges, hydrophone arrays, surveys, noise

19. ABSTRACT
Oceanic environmental surveys were made by DSTO off Perth, Western Australia over July to September 1992 to assess site suitability for an Underwater Radiated Noise Range for the Royal Australian Navy. Acoustic ranges are required to measure the noise radiated from ships and submarines. Salient factors for range design and performance include ambient noise, currents, topography and nature of the seafloor, water properties, wave, wind, and weather conditions. Measurements of these parameters indicate that the waters off Perth for bottom depths of 400 m are a difficult regime in which to construct and operate an acoustic range. High currents with strong vertical and horizontal shear were experienced, with directions varying through the water column, and with surface and bottom flows sometimes in opposite directions. Temperature micro-structure caused by meeting of warm, low salinity northern Leeuwin Current waters with cool, high salinity southern waters is predicted to cause fluctuations in intensity of acoustic signals. Ambient noise is significantly affected by rain, migrating whales, and shipping. Significant wave heights over 7 m were measured in August 1992. The environmental results are of general interest, and are presented for use by the wider scientific community.